SYNTHESIS OF CERAGENIN-LOADED HYDROGEL AND INVESTIGATION OF ITS DRUG RELEASE CHARACTERISTICS

Nawal Y A ALJAYYOUSI

T.C.
BURSA ULUDAĞ UNIVERSITY
GRADUATE SCHOOL OF NATURAL AND APPLIED SCIENCES

SYNTHESIS OF CERAGENIN-LOADED HYDROGEL AND INVESTIGATION OF ITS DRUG RELEASE CHARACTERISTICS

Nawal Y A ALJAYYOUSI
0009-0002-3324-8718

Prof. Dr. Bilgen OSMAN
(Supervisor)

MSc THESIS
DEPARTMENT OF CHEMISTRY

BURSA – 2023

THESIS APPROVAL

This thesis titled "SYNTHESIS OF CERAGENIN-LOADED HYDROGEL AND INVESTIGATION OF ITS DRUG RELEASE CHARACTERISTICS" and prepared by Nawal Y A ALJAYYOUSI has been accepted as a **MSc THESIS** in Bursa Uludağ University Graduate School of Natural and Applied Sciences, Department of Chemistry following a unanimous vote of the jury below.

Supervisor : Prof. Dr. Bilgen OSMAN

Head :	Prof. Dr. Bilgen OSMAN 0000-0001-8406-149X Bursa Uludağ University, Faculty of Arts and Science, Department of Chemistry	Signature
Member:	Prof. Dr. Asım OLGUN 0000-0002-0657-334X Bursa Uludağ University, Faculty of Arts and Science, Department of Chemistry	Signature
Member:	Assoc. Prof. Dr. Emel TAMAHKAR IRMAK 0000-0002-5913-8333 Bursa Technical University, Department of Bioengineering	Signature

I approve the above result

Prof. Dr. Hüseyin Aksel EREN
Institute Director
../../….

I declare that this thesis has been written in accordance with the following thesis writing rules of the U.U Graduate School of Natural and Applied Sciences;

- All the information and documents in the thesis are based on academic rules,
- audio, visual and written information and results are in accordance with scientific code of ethics,
- in the case that the works of others are used, I have provided attribution in accordance with the scientific norms,
- I have included all attributed sources as references,
- I have not tampered with the data used,
- and that I do not present any part of this thesis as another thesis work at this university or any other university.

…/…/……

Nawal Y A ALJAYYOUSI

TEZ YAYINLANMA
FİKRİ MÜLKİYET HAKLARI BEYANI

Enstitü tarafından onaylanan lisansüstü tezin/raporun tamamını veya herhangi bir kısmını, basılı (kâğıt) ve elektronik formatta arşivleme ve aşağıda verilen koşullarla kullanıma açma izni Bursa Uludağ Üniversitesi'ne aittir. Bu izinle Üniversiteye verilen kullanım hakları dışındaki tüm fikri mülkiyet hakları ile tezin tamamının ya da bir bölümünün gelecekteki çalışmalarda (makale, kitap, lisans ve patent vb.) kullanım hakları tarafımıza ait olacaktır. Tezde yer alan telif hakkı bulunan ve sahiplerinden yazılı izin alınarak kullanılması zorunlu metinlerin yazılı izin alınarak kullandığını ve istenildiğinde suretlerini Üniversiteye teslim etmeyi taahhüt ederiz.

Yükseköğretim Kurulu tarafından yayınlanan "**Lisansüstü Tezlerin Elektronik Ortamda Toplanması, Düzenlenmesi ve Erişime Açılmasına İlişkin Yönerge**" kapsamında, yönerge tarafından belirtilen kısıtlamalar olmadığı takdirde tezin YÖK Ulusal Tez Merkezi / B.U.Ü. Kütüphanesi Açık Erişim Sistemi ve üye olunan diğer veri tabanlarının (Proquest veri tabanı gibi) erişimine açılması uygundur.

Danışman Adı-Soyadı Tarih	Öğrencinin Adı-Soyadı Tarih
İmza Bu bölüme kişinin kendi el yazısı ile okudum anladım yazmalı ve imzalanmalıdır.	İmza Bu bölüme kişinin kendi el yazısı ile okudum anladım yazmalı ve imzalanmalıdır.

ÖZET

Yüksek Lisans Tezi

SERAGENİN YÜKLÜ HİDROJEL SENTEZİ VE İLAÇ SALIM ÖZELLİKLERİNİN ARAŞTIRILMASI

Nawal Y A ALJAYYOUSI

Bursa Uludağ Üniversitesi
Fen Bilimleri Enstitüsü
Kimya Anabilim Dalı

Danışman: Prof. Dr. Bilgen OSMAN

Bu çalışmada, liyofilizasyon yöntemiyle seragenin yüklü polivinil alkol (PVA)/aljinat (SA)/jelatin (G) (PAG) hidrojel hazırlandı. Seragenin olarak CSA-44 kullanıldı. Hazırlanan hidrojel (PAG-CSA), glutaraldehit (GA) ile kimyasal olarak çapraz bağlandı. Hidrojel bileşimindeki PVA, SA ve G oranı; farklı GA miktarlarında ve çapraz bağlanma sürelerinde hazırlanan 7 farklı PAG hidrojel üzerinde yapılan optimizasyon çalışmaları ile belirlendi. PVA:SA:G oranı 2:1:3 olarak belirlendi ve seragenin yüklü liyofilize PAG-CSA hidrojel % 0,125 (v/v) GA oranında 20 dakika çapraz bağlama ile hazırlandı. PAG ve PAG-CSA hidrojeller Fourier Dönüşümü kızılötesi spektroskopisi (FTIR), taramalı elektron mikroskobu (SEM) ve civa porozimetrisi ile karakterize edildi. PAG ve PAG-CSA hidrojellerin şişme (%), hidrolitik ve enzimatik bozunma (%), dehidrasyon (%), su buharı geçirgenliği, hava geçirgenliği, gerilme mukavemeti, temas açısı ve kalınlığı belirlendi. Hidrojelden CSA-44 salım çalışmaları yapıldı ve verilerin kinetik modellere uygunluğu araştırıldı.

PAG-CSA hidrojelin şişme oranı %780,48 ± 14,80 olarak belirlendi. Hidrojel bir ay sonunda sırasıyla %61,17 ± 9,3 ve %48,16 ± 4,29 degredasyon oranları ile hidrolitik ve enzimatik degredasyona karşı direnç gösterdi. PAG-CSA'nın hava geçirgenlik değeri 50,7 ± 1,69 l/m^2/s, su buharı geçirgenliği değeri ise 905,41 ± 35,38 g/m^2/gün olarak belirlendi. Gerilme mukavemeti 9,14 ± 2,39 kPa olup CSA-44 ilavesi ile esneklik azaldı. PAG-CSA hidrojelin temas açısı değeri ölçülemedi. Bu sonuç hidrojele CSA dahil edildikten ıslanabilirliğin arttığını gösterdi. Dehidrasyon testi sonuçları hidrojelin 37 ^oC'de 3 saat içinde kuruduğunu ve dehidrasyon oranını koruyarak su tutma özelliği ile maserasyonu önleme arasında bir denge sağladığını gösterdi. CSA-44 salımı Fickian olmayan Korsmeyer-Peppas salım model (n=0,61) ile açıklandı. İlaç salım çalışmaları CSA-44'ün 8 saat içinde % 23 oranında patlama salımı ile salındığını ve 7 gün sonra (%29) dengeye ulaştığını gösterdi. Elde edilen sonuçlara göre PAG-CSA hidrojeli yanık yaraları için antibakteriyel bir yara örtüsü olarak kullanılma potansiyeline sahiptir.

Anahtar Kelimeler: Hidrojel, seragenin, katyonik steroid antibiyotik, yanık yara örtüsü, ilaç salımı
2015, vii + 114 sayfa.

ABSTRACT

MSc Thesis

SYNTHESIS OF CERAGENIN-LOADED HYDROGEL AND INVESTIGATION OF ITS DRUG RELEASE CHARACTERISTICS

Nawal Y A ALJAYYOUSI

Bursa Uludağ University
Graduate School of Natural and Applied Sciences
Department of Chemistry

Supervisor: Prof. Dr. Bilgen OSMAN

In this study, ceragenin-loaded polyvinyl alcohol (PVA)/alginate (SA)/gelatin (G) (PAG) hydrogel was prepared by lyophilization. CSA-44 was used as ceragenin. The resulting hydrogel (PAG-CSA) was chemically cross-linked with glutaraldehyde (GA). The amount of PVA, SA, and G was determined after optimization studies preparing seven different PAG hydrogel compositions at different GA amounts and cross-linking times. The PVA:SA: G ratio was determined at 2:1:3 and used to prepare ceragenin-loaded lyophilized PAG-CSA hydrogel cross-linking with 0.125% GA for 20 min. The PAG and PAG-CSA hydrogels were characterized by Fourier Transform infrared spectroscopy (FTIR), scanning electron microscopy (SEM), and mercury porosimetry. Swelling (%), hydrolytic and enzymatic degradation (%), dehydration (%), water vapor transmission rate (WVTR), air permeability, tensile strength, water contact angle (WCA), and thickness of the PAG and PAG-CSA hydrogel were determined. The CSA-44 release studies were conducted, and the fitness of the data to the kinetic models was investigated.

The PAG-CSA had a swelling ratio of 780.48% ± 14.80 and maintained resistance towards hydrolytic and enzymatic degradation, which appeared to be 61.17% ± 9.3 and 48.16% ± 4.29, respectively, after a month. The air permeability value of PAG-CSA was 50.7 ± 1.69 $l/m^2/s$, while the WVTR value was 905.41 ± 35.38 $g/m^2/d$. Tensile strength was 9.14 ± 2.39 kPa, indicating decreased flexibility attributed to cross-linking. WCA was not measured after CSA incorporation, demonstrating the hydrophilicity of the PAG-CSA hydrogel. The dehydration test showed that the hydrogel dries out within 3 hours at 37 oC, indicating the ability to keep a balance between water retention and preventing maceration by maintaining a reasonable dehydration rate. The CSA-44 release followed the non-fickian Korsmeyer-Peppas release model (n=0.6103). The drug release studies showed a burst release of 23% CSA-44 within 8 hours, reaching equilibrium after 7 days (29%). The PAG-CSA hydrogel has a high potential to be used as an antibacterial wound dressing material for burn wounds.

Key words: Hydrogel, ceragenin, cationic steroid antibiotic, burn wound dressing, drug release**2023, vii + 114 pages.**

PREFACE AND/OR ACKNOWLEGDEMENT

I would like to express my heartfelt appreciation to Prof. Dr. Bilgen OSMAN, my supervisor, for her invaluable guidance and support throughout my master's degree. Without her great knowledge, patience and help, my academic pursuits would have remained unfulfilled. She was consistently eager to impart all her theoretical and practical knowledge to me, and never hesitated to provide guidance whenever I needed it.

I would like to extend my sincere gratitude to Assoc. Prof. Dr. Emel TAMAHKAR IRMAK, my committee member, for her unwavering patience and eagerness to share her knowledge with me. She went above and beyond by readily answering all my questions and providing invaluable guidance throughout my academic journey.

I would like to extend my sincere appreciation to Prof. Dr. Elif TÜMAY ÖZER for her unwavering determination in finding solutions to the various challenges I faced during my work. Her persistence was crucial in overcoming these obstacles and completing my project successfully.

I owe my deepest gratitude to Dr. Anas AL ALI for introducing me to the chemistry field and being a great support through every step of my academic journey. I would also love to thank every teacher who encouraged me to pursue my academic career.

I am indebted to my teacher Asst. Prof. Monireh YÜCEL, and colleagues Azize ÇERÇİ, Melike KÜÇÜK and Merve İlkay ALTUNTUĞ CESUR for supporting me all the way long. Without their help and compassion, I would have never been able to pursue my journey nor write this thesis the way I did.

This thesis would have remained a dream had it not been for my lovely family, my first teacher my grandfather Abdelhalim ALJAYYOUSI, my first supporter my father Dr. Yazid ALJAYYOUSI, my loving mother, Liliya ALJAYYOUSI and my siblings Dana, Jumana and Murad ALJAYYOUSI and all of my other family members to whom I owe a great amount of gratitude and appreciation. They have always been there to support me through all the ups and downs and encouraged me to pursue my dream.

I am deeply grateful to all my friends and loved ones who stood by me, supported me, and helped me through difficult times, especially when I felt overwhelmed and hopeless. I am also grateful for the family who never made me feel homesick and who considered me one of their own children Mehmet and Leyla ÇERÇİ.

Finally, I want to thank Prof. Dr. Paul B. SAVAGE for providing us with CSA-44, Prof. Çağla BOZKURT GÜZEL for establishing this communication and Prof. Dr. Esra KARACA and her team for providing us with their laboratory facilities. Finally, I want to thank Bursa Uludağ University Scientific Research Projects Unit, which supported my thesis through project number FOA-2022-1097.

Nawal Y A ALJAYYOUSI
…/…/…….

CONTENTS

Page

SYMBOLS and ABBREVIATIONS

Symbols	Definition
A_R	Cross-sectional area
M_t	The amount of drug released in time
Q_O	Initial drug amount in the solution
Q_t	Drug amount that is dissolved in a specific time
F	Break force
M	The water content of the hydrogel
TS	Tensile strength
n	n value in korsmeyer peppas

Abbreviation	Definition
AMPs	Antimicrobial peptides
AMPS	2-acrylamido-2-methylpropane
CA	Cellulose acetate
CHI	Chondroitin
CMC	Carboxymethyl cellulose
CMCS	Carboxymethyl Chitosan
CMGG	Carboxymethyl guar gum
DHBA	2,3-dihydroxybenzoic acid
ECM	Extracellular matrix
EDA	Ethylenediamine
EDX	Energy dispersive X-ray
EGF	Epidermal growth factor
ESBL	Extended spectrum beta-lactamase
GMs	Gelatin microspheres
HNTs	Halloysite Nanotubes
HPLC	High performance liquid chromatography
MA	Methacrylamide
MBC	Minimum bactericidal concentration
MFC	Minimum fungicidal concentration
MIC	Minimal inhibitory concentration
MRSA	Methicillin-resistant Staphylococcus aureus
OAlg	Oxidized Alginate
PAG	Polyvinyl alcohol/Sodium alginate/Gelatin
PAG-CSA	(Polyvinyl alcohol/Sodium alginate/Gelatin)-CSA 44
PEGDA	Poly(ethylene glycol) diacrylate
PEI	Polyethyleneimine
PHEA	Poly(2-hydroxyethylacrylate)
PSSA-MA	Poly(styrene sulfonic acid-co-maleic acid)
PWD	Platform wound device
SF	Silk fibroin
TBSA	Total body surface area affected (% TBSA)
UV	Ultraviolet
VEGF	Vascular endothelial growth factor
ZN	Zein

FIGURES

TABLES

1. INTRODUCTION

Wounds occur when the function and normal anatomical structure of the skin are disrupted, and that can be caused by thermal, physical, mechanical, or electrical shock (Boateng et al., 2008). Wounds can be sorted into seven categories according to duration, depth, complexity, cause, contamination, type of injury, and the color of contaminated tissue (Dubay and Franz, 2003; Katz et al., 1991; Li et al., 2007). If left untreated nor managed, wounds can cause significant medical issues such as infections due to bacterial colonization, sepsis, the need for limb amputations, and can even be life-threatening. Proper wound management is essential for optimal healing and prevention of complications. According to World Health Organization (WHO) burn wounds are one of the most causes of disability, where each year 27 million require professional treatment and 7 million of those need hospitalisation (WHO, 2014). While autologous skin grafting is the standard treatment for burn wounds it might not be always possible due to the lack of a suitable skin donor, improper physiological condition of the patient for the surgery and other reasons. The importance of preparing burn wound dressings came from these reasons (Dhaliwal et al., 2018).

Burns are defined as disruption of the skin that is caused by extreme heat, chemicals, electricity, or friction. Third-degree burns, or named as full-thickness burns, are one of burn wound types. This type specifically can destroy all three layers of the skin (epidermis, dermis and hypodermis) which provokes immediate cell death and the destruction of matrix.

In the ancient times there were several methods that were used to treat wounds and decrease infections. These methods included dressing a wound with resin and honey after washing it with water and milk, or even using vinegar or wine to clean wounds (Daunton et al., 2012). It was only until the late 20th century when occlusive dressings were introduced to protect the wound and to keep it moisturized. The first cotton gauze was produced in 1891 while the effect of moist chamber was only described in 1948 by Oscar Gilje. The initial contemporary wound dressing was created in the mid-1980s. It was feasible with this dressing to maintain a moist environment and absorb exudates of the wound. After this, a great development in wound dressings production occurred. Different

types of wound dressings were synthesized for different wound types such as hydrogels, nanofibers, alginates, films, and foams (Rezvani Ghomi et al., 2019).

Hydrogels have distinguishing properties that made them excellent candidates for wound dressings. They have high water retention ability which helps to create a moist environment for the wound. Hydrogels are also known to facilitate gas exchange for the wound site as they are highly porous materials. Hydrogels are usually synthesized of biodegradable and biocompatible materials that do not provoke an immune system response. They are non-adhesive materials which eliminates the need of continuous change of the dressing, and they are capable of absorbing wound exudates. Hydrogels are important in burn wounds especially as they have a cooling effect due to their water retention ability. In burn wounds, these substances aid in the decomposition of necrotic tissue by using the body's natural immune cells and enzymes that break down proteins. This process reduces the likelihood of scarring and infection in the affected area (Dhaliwal and Lopez, 2018).

Wounds in general are susceptible to infections as the most popular types of infections are skin and soft tissue infections. These infections can be mild or even life threatening. Even though our immune system gets activated in case of a wound and tries to eliminate pathogens, it sometimes fails, and infection occurs. *P. aeruginosa* is a common bacteria that is found in burn injuries which is also associated with high morbidity (Savage,2020). Due to this, it is crucial to develop wound dressings with antibacterial effect. A lot of antibacterial agents (e.g antibiotics, nanoparticles, natural products, antibacterial peptides, etc.) are being incorporated into wound dressing to prevent bacterial infection from both gram-positive and gram-negative bacteria. Antimicrobial peptides (AMPs) are molecules that are produced in animal and plant tissues as a first line of defense. They have a broad antibacterial spectrum as they connect to the bacterial membrane that causes it to interrupt the bacterial activity, in addition to antifungal, antiviral and antiparasitic activity (Li et al., 2018;). Zhou et al. (2011) prepared a hydrogel from ε-poly-L-lysine-graft-methacrylamide which is an AMP and photopolymerized it, this hydrogel showed to be a good antibacterial coating for implants and some medical devices. Despite the great potential of AMPs in fighting wound infections without gaining bacterial resistance towards it, the production expenses, their susceptibility to degradation by bacterial

proteases, hemolysis and tissue toxicity made their applications limited. However, Ding et al. (2004) and Savage et al. (2002) synthesized non peptide mimics of AMPs that are called ceragenins. Ceragenins, or as also also called, cationic steroid antibiotics (CSAs), can be classified into two groups: squalamine mimics and polymyxin mimics. Ceragenins are easy and cheaper to synthesize, they are stable and are not susceptible to bacterial proteases as they are not peptide based, and they also have a similar broad antibacterial spectrum as AMPs because they mimic the amphiphilic structure of them (Hashemi et al., 2018). Ceragenins exhibit antibacterial, antifungal, antibiofilm, sporicidal, antiviral, and anti-parasite properties. Savage (2020) assessed the effect of CSA-44 on *P. aeruginosa* in a porcine second degree burn wound model. Results showed that with 0.05% of aqueous CSA-44 there was a 99.6% reduction of bacterial counts which provides us with the applicability of ceragenins to fight burn wounds infections.

In this study we have used three biocompatible polymers (PVA, SA and G) to synthesize a hydrogel for burn wound dressing application. These three polymers combined were mentioned in literature in three places. Satish et al. (2018) designed an alginate/gelatin/polyvinyl alcohol hydrogel by lyophilization and incorporated it with triiodothyronine hormone for chronic wound tissue regeneration. Kuo et al. (2019), PVA, SA, and Gel were bound to methacrylic anhydride (MA) and photo-cross-linked to prepare PVAMA-SAMA-GelMA hydrogels for the purpose of pancreatic differentiation of the induced pluripotent stem cells (iPS) cells. The last is a freeze-thawed G/ PVA hydrogel that was prepared by Marrella et al. 2018 and incorporated with alginate micro-particles as a porogens to be used as a substitute for meniscus cartilage. In our study we used these three polymers in different ratios and concentrations of these found in literature to prepare our hydrogel and incorporated it with CSA-44 as an antibacterial which was proved to reduce bacteria infection in burn wounds. A hydrogel with this polymeric combination accompanied with CSA-44 was not prepared in the literature and was not characterized before.

2. THEORETICAL BASICS and LITERATURE REVIEW

2.1. Hydrogels

Hydrogels are polymeric networks that are hydrophilic and have a porous, three-dimensional structure, with the capability to absorb water ranging from ten to a thousand times their own weight (Cho et al., 2018; González-Henríquez et al., 2017). They are usually synthesized from hydrophilic monomers; however, hydrophobic polymers can sometimes modify the hydrogel's properties for specific uses. Their properties or solubilities in water can also be adjusted using different cross-linking methods (Ahmet, 2015; Peppas et al., 2006) (Figure 2.1).

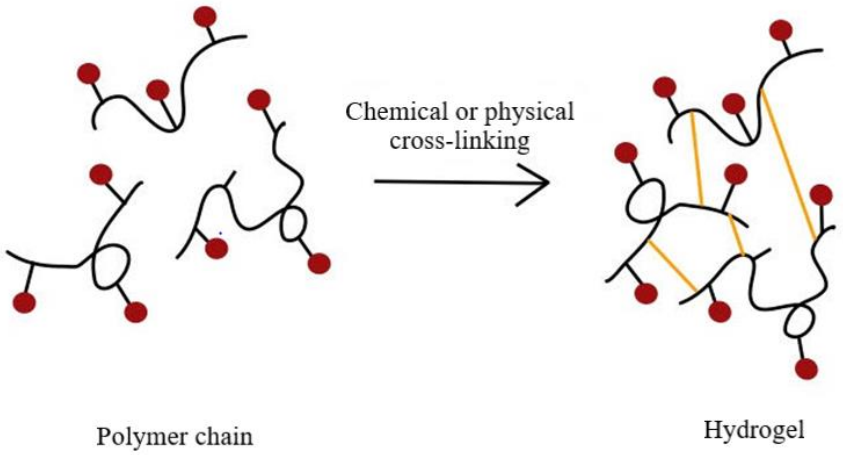

Figure 2.1. Preparation of a hydrogel.

Hydrogels have distinguishing properties that make them popular in different types of applications. They have exquisite moisture retention and donation properties and can be easily removed as they are non-adhesive. In addition, hydrogels can be loaded with different healing agents and antimicrobial agents, which can be released at a controlled rate (Gupta et al., 2019). Moreover, hydrogels have a high gas permeability, are biodegradable, and have enhanced biocompatibility (Li et al., 2018).

Throughout the years, hydrogels have been used as joint and dental implants and as a coating for urinary catheters. Cao et al. (2019) developed a chitosan (CS) based biocompatible and thermosensitive hydrogel used for lubricating and sealing in dental implant systems, exhibiting a significant antibacterial effect and biocompatibility. Hydrogels have also been used to carry different antimicrobial agents for a systematic drug release which helped to overcome bacterial resistance (Li et al., 2018). Figure 2.2 summarizes different compositions of antibacterial hydrogels and their applications.

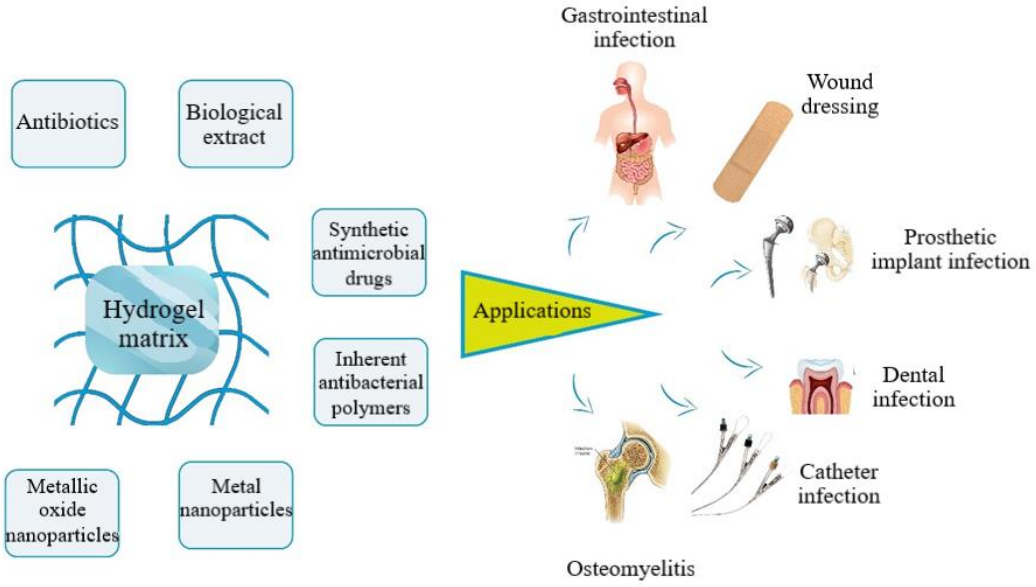

Figure 2.2. Compositions and applications of antibacterial hydrogels

Wichterle and Lim (1960) prepared the first synthesized hydrogel from cross-linked 1-hydroxyethyl methacrylate (HEMA). Due to its hydrophilicity, the develped hydrogel was used in various biomedical applications like drug delivery systems, osteoporosis, and neoplasm (Gibas and Janik, 2010). After that, Yannas et al. (1981) developed a hydrogel of a natural polymer for wound dressing applications. The increasing popularity of hydrogels has led to a revolution in wound dressing. Thanks to hydrogels, wound dressing shifted from passive dressings having minimal effect on wound healing to active ones. Winter (1962) developed the first polymeric wound dressing providing an optimal environment for wound healing. After that, chitin-based wound dressings appeared and

were preferred due to their antimicrobial activity. For a while, researchers believed that hydrogels have ideal properties to heal burn wounds because hydrogels control fluid loss, maintain the wound's bed moisture, and mimic the tissue structure. Unfortunately, due to the low mechanical stability of hydrogels in a swollen state, they are not ideal. To overcome this obstacle, hybrid or composite hydrogel membranes that consist of more than one polymer were developed. In addition, the stability of hydrogels were incerased by using chemical or physical cross-linking techniques (Kamoun et al., 2017).

Hydrogels are categorized in different ways. They are categorized into solid, semi-solid, and liquid forms, based on their physical state. Another method of classification, which is more prevalent, is based on the cross-linking technique. Hydrogels of both natural and synthetic polymers are classified to chemically and physically cross-linked hydrogels (Chung and Park, 2009; Sharma et al., 2014).

The importance of solid hydrogels lies in their capability of mimicking the properties and structure of most living tissues, which creates a suitable cellular microenvironment. Solid hydrogels are solid at room temperature due to their cross-linked structure. However, they can quickly swell in water and biological fluids. Many biological and inorganic materials were incorporated into this hydrogel type to fulfill the biomedical application in which it will be used (Jayaramudu et al., 2013). In a study by Hu et al. (2016), a UV cross-linked triclosan (TC) incorporated acryloyl chloride-modified hydrogel was developed. It was concluded that TC was released in a controllable way, which can help reduce the drug's side effects and cytotoxicity.

Semisolid hydrogels play a crucial role in medical applications that require prolonged and effective drug delivery due to their unique adhesive characteristics. Therefore, these hydrogels are named mucoadhesive and bio-adhesive hydrogels. The synthesis of those hydrogels includes a material of a biological nature and polymers of a high molecular weight (Varaprasad et al., 2017). Singh et al. (2014) developed a ciprofloxacin-loaded polyvinylpyrrolidone (PVP) and polysaccharide sterculia gum hydrogel for gastrointestinal tract drug delivery. The drug release exhibited a non-Fickian diffusion mechanism of 45% release of the drug in 24h in an acidic buffer.

Liquid hydrogels are liquid at room temperature. However, at specific temperatures, liquid hydrogels have an elastic phase. Liquid hydrogels are easily synthesized and adjusted. They stand out because of their ability to get easily incorporated with various organic and inorganic materials and their injectability without any surgical procedure (Varaprasad et al., 2017). Kakkar et al. (2016) developed a keratin-silica hydrogel as a wound dressing material. The novel hydrogel showed high biocompatibility with fibroblast cells.

Due to the widespread use of hydrogels in biomedical area and food industries, chemical cross-linking agents are not preferred; instead, physical cross-linking methods are used. Physical cross-linking is based on the physical interactions between the polymer chains of the hydrogel. Physically cross-linked hydrogels are synthesized in different ways: freeze-thawing, ionic interaction, stereo complex formation, H-bonding, and maturation (heat-induced aggregation) (Chung and Park, 2009; Slaughter et al., 2009). Freeze-thawing is based on continual freeze-thawing cycles that help to create microcrystals in the structure. This method enhances the porosity and elasticity of hydrogels compared to other methods. Marrella et al. 2018 prepared a G/ PVA hydrogel by the freeze-thawing method as a substitute for meniscus cartilage. It was incorporated with alginate micro-particles to function as a porogen. The resulting hydrogel was highly porous and elastic and reached a swelling ratio plateau after 48 hours. Stereocomplex formation is simple since the hydrogel is formed by dissolving each polymer in water and mixing these polymer solutions all together. This method's main restriction is that only a few specific polymer compositions can be used. The ionic interaction method is applied by adding multivalent ions of opposite charge to a polyelectrolyte solution that forms a cross-linked hydrogel. H-bonding cross-linking is achieved by replacing an ion in the hydrogel network with hydrogen, eventually leading to cross-linking of the hydrogel. The final method is maturation, in which heat causes aggregation and accumulation of components with an accurately ordered molecular dimension, consequently forming a hydrogel with enhanced mechanical properties and swelling ability (Varaprasad et al., 2017).

Chemically cross-linked hydrogels are prepared by covalently bonding hydrogel's polymer chains. This covalent bonding stabilizes the hydrogel and makes it insoluble in

solvents if the covalent bonds are not broken. Chemical cross-linking increases the mechanical stability of hydrogel networks, subsequently extending degradation time. Several ways of chemical cross-linking were mentioned in the literature: agents, grafting, radical polymerization, condensation reaction, enzymatic reaction, and high-energy radiation (Chung and Park, 2009; Slaughter et al., 2009). Chemical cross-linking is applied by using chemical agents such as GA to create covalent linkages through the reaction between functional groups. Lin et al. (2019) developed a hydrogel using different ratios of PVA, dextran, and CS, then cross-linked it using GA. The results showed that using higher GA concentration led to chitosan not being released. In contrast, lower concentrations enabled chitosan release, inhibiting the growth of both gram-positive and negative bacteria (*E. coli* and *S. aureus*). Meanwhile, grafting is associated with polymerizing a monomer on a main polymer chain and can be divided into two categories based on the type of activation: chemical grafting and radiation grafting. On the other hand, one of the most used methods for preparing hydrogels is radical polymerization which involves cross-linking low molecular weight monomers by successive addition of radical monomers. Radical polymerization leads to the formation of hydrogels quickly and efficiently, even under mild conditions. Condensation reactions usually involve hydrogels containing amine groups, hydroxyl groups, carboxylic acids, or their compounds. Nonetheless, enzymatic reactions involve enzyme catalyzing of linkages between polymers. Finally, in high-energy cross-linking, water-soluble polymers are derivatized with vinyl groups using radiation, such as gamma rays, which creates radicals on the polymer chains through homolytic scission (Varaprasad et al., 2017). Table 2.1 shows different types of physically and chemically cross-linked hydrogels and their applications (Varaprasad et al., 2017).

Table 2.1. Applications of some physically and chemically cross-linked hydrogels (Varaprasad et al., 2017)

Cross-linking method	Polymers	Applications
Freeze-thawing	PVA PVA/CS, PVA/starch, PVA/G	Therapeutic applications Tissue engineering
Ionic interaction	Cellulose microfibrils Chitosan	Drug delivery Antigen delivery
Stereocomplex formation	Dextran, poly(lactic acid) Poly(ethylene glycol)	Drug delivery Biomedical and pharmaceutical
H-bonding	Hyaluronic acid Cyclodextrin, polypseudorotaxane	Drug delivery Biomedical
Chemical grafting **Radiation grafting**	Chitosan-cellulose Poly(ε-caprolactone), Poly(ethylene glycol)	Agriculture and horticulture Tissue engineering
Maturation (heat-induced aggregation)	Alginate capsules Hyaluronic acid	Cartilage tissue Soft tissue engineering, cell scaffold.
Radical polymerization	Poly(ethylene glycol)methyl ether Methacrylate	Antifouling
Chemical cross-linking	Whey protein Poly(ethylene glycol)	- Biomedical
Enzymatic reaction	Poly(ethylene glycol) methacrylate Chitosan	Biocatalysis and tissue engineering Wound dressing and packaging
Condensation reaction	B-Cyclodextrin Cellulose nanofiber	Controlled delivery Advanced
High-energy radiation	Poly(oligo(propylene glycol) methacrylate)	Biomedical

2.2. Antibacterial hydrogels

Antibiotics have played a crucial role in improving the human life quality and have helped defeating many infections and diseases since their discovery. Nevertheless, many pathogens have gained multidrug resistance over time due to the continued and wrong consumption of antibiotics, which caused an increase in the mortality ratio. To conquer this issue, researchers have been developing antibacterial materials, which unfortunately, kill not just pathogens but also healthy cells. As the need for an effective biocompatible antibacterial material has risen, hydrogels have been researched as an ideal alternatives. Antibacterial hydrogels can be divided into three categories: inorganic antibacterial containing hydrogels, antibacterial agent-containing hydrogels, and hydrogels with inherent antibacterial capabilities (Li et al., 2018).

Inorganic antibacterial agent-incorporated hydrogels are primarily incorporated with metal ions or metal oxide nanoparticles. Those include silver, gold, zinc oxide, nickel oxide, and much more. However, the most prevalent inorganic antibacterial are silver nanoparticles. Those hydrogels can prolong the drug release time, which by decreases bacterial resistance chances (Li et al., 2018). Silver nanoparticles were incorporated into a SA hydrogel and cross-linked with Ca^{2+} or N, N-methylene bisacrylamide by Neibert et al. (2012). The developed hydrogels showed a prolonged inhibitory effect against *E. coli*, and silver was released in a sustained matter. Boonkaew et al. (2014) synthesized 2-acrylamido-2-methylpropane sulfonic acid sodium salt (AMPS-Na^{+}) hydrogel loaded with silver-nanoparticles (SNPs) as a burn wound dressing material. To synthesize SNP-infused hydrogel, silver nitrate was dissolved in an AMPS-Na+ solution and then subjected to gamma irradiation. Drug release studies showed a burst release of 60% of silver in the first 24 h. In the 24-72 h, burst release was followed by the cumulative release of silver 82.41% for 2.5 mM, 75.63% for 5 mM, and 78.56% for10 mM. The terminal release was relatively small but continuous for all hydrogels, which continued for 240 h. According to the pilot study, the 5 mM silver hydrogel was effective in preventing bacterial colonization of wounds and showed comparable results to commercial silver dressings. The hydrogels loaded with silver demonstrated potent inhibitory effects against *P. aeruginosa* and *MRSA*.

To overcome the obstacle of bacterial resistance mentioned before, there had to be a way to decrease the antibiotic dosage and increase the delivery time. Due to the hydrogels' porosity and similarity to the structure of living tissue, drugs can be selectively released at a specific site (Norowski and Bumbgadner, 2009; Montanari et al., 2014). Therefore, antibacterial agent-containing hydrogels have been developed. Roy et al. (2016) developed ciprofloxacin-loaded keratin hydrogels to help heal porcine skin's partial thickness thermal burn. For both *P. aeruginosa* and *S. aureus*, the levels of bacteria in the tissue remained under 10^4 cfu per gram during the first two weeks post injury. Wen et al. (2020) synthesized SA incorporated with G hydrogels loaded with the antibiotic tetracycline hydrochloride (TCH) to be used in wound dressing applications. The G/SA hydrogel exhibited a swelling ratio of 2190% after 24 h. This can be attributed to the abundance of carboxyl and hydroxyl groups in SA and G in addition to the amino groups of G. In contrast, TCH-loaded hydrogels showed slightly lower swelling ratios of 1780% to 1960% due to the decrease of the porosity of hydrogels after incorporating TCH. Hydrogels displayed a burst release behavior in the first hour due to the drug distribution on the surface of the hydrogel. The release had gradually increased since then to last for 12 h. Hydrogels can also be loaded with biological extracts from animals and plants, such as seaweed extract, curcumin, and much more. Naghshineh et al. (2019) designed three CS-based hydrogels, one containing SA in addition to CS, the other containing G, and the last containing collagen. Curcumin was incorporated into all three hydrogels. Antibacterial studies showed that all hydrogel composites exhibited an inhibitory effect on the bacteria; however, the highest impact was revealed by the CS/G/curcumin composite.

Hydrogels with inherent antibacterial activity consist of antibacterial components. They can be synthesized from antibacterial polymers, AMPs, or amphoteric ion hydrogels. Antibacterial polymers have specific functional groups in their structures that help to inhibit bacteria; not just that, but they are also biocompatible (Li et al., 2018). AMPs have a strong inhibitory effect against different types of pathogens. Bai et al. (2016) developed hydrogel by the gelation of self-assembling peptide A_9K_2 that showed remarkable selectivity, good biocompatibility, and inhibitory effect for gram-negative and gram-positive bacterial cells. This type of hydrogel has some disadvantages, including

cytotoxicity and hemolysis. However, compared to synthetic drugs, they still have the upper hand in antibacterial ability and biocompatibility (Forbes et al., 2013). Amphoteric ion hydrogels have a mechanism of action similar to AMPs as they create electrostatic interactions that lead to the binding of bacterial membranes and polymers, which lead to the destruction of the bacterial membrane and, subsequently, cell death (Liu et al., 2012).

2.3. Wound and wound healing

Comprising of three layers, namely epidermis, dermis, and hypodermis, the skin is recognized as the human body's largest organ (Ambekar and Kandasubramanian, 2019). The skin operates as a protective layer of the underlying tissues, such as bones, ligaments, muscles, and internal organs, from external chemical, biological, physical, and mechanical factors (Chua et al., 2016; Sundaramurthi et al., 2014). Skin also plays a significant role in regulating body temperature, immunological monitoring, reduction of dehydration rate, and vitamin D3 synthesis (Paul, 2015). Nevertheless, skin is vulnerable to cuts, burns, or diseases such as diabetes (Mühlstädt et al., 2012). Epidermis layer comprises melanocytes, keratinocytes, and Merkel and Langerhans cells that aid in sustaining the body temperature. Stratum corneum, stratum granlosum, stratum lucidum, stratum germinativum and stratum spinosum are the five layers into which the epidermis is subdivided. Epidermis can heal after a superficial injury by constantly shedding old epidermal cells and replacing them with new ones. Dermis is the layer that consists of connective tissue and contains hair follicles, sweat glands, sebaceous glands, apocrine glands, and lymphatic and blood vessels. Based on the depth of the epidermis, dermis can be divided into two regions, namely the papillary and reticular regions, and the primary function of epidermis is to shield the body from external stress. Hypodermis lies under the dermis. It comprises fibroblasts, macrophages, and adipocyte cells (Ambekar and Kandasubramanian, 2019). Figure 2.3 represents the layers of the skin.

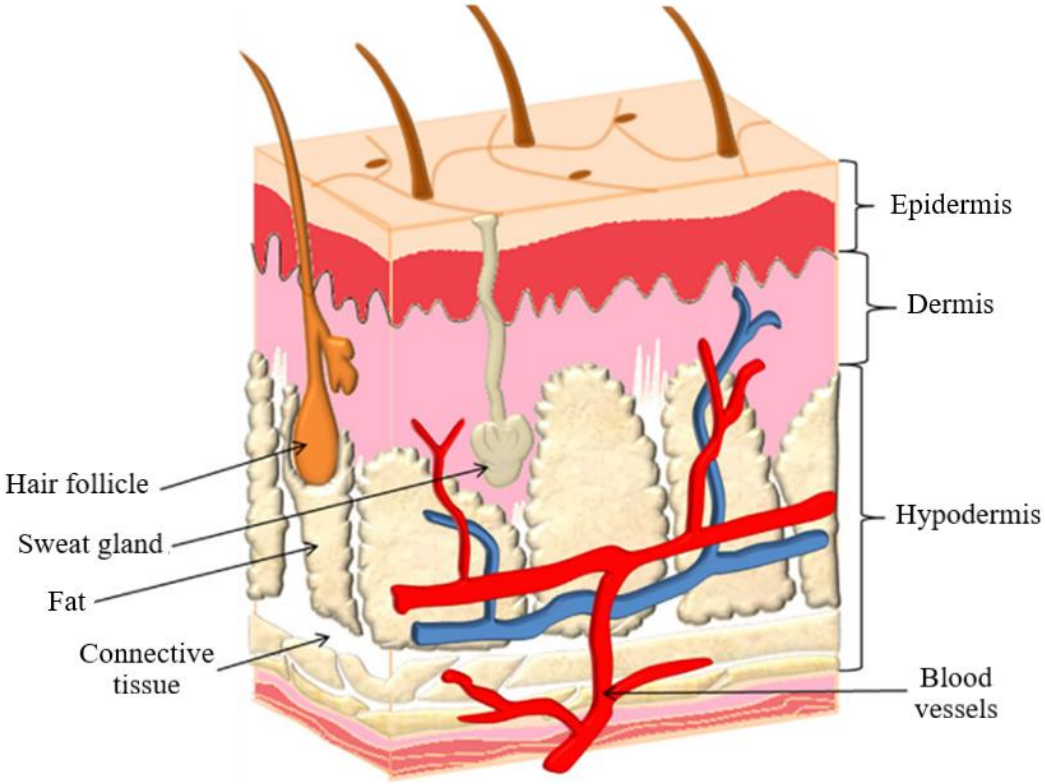

Figure 2.3. Layers of skin (Ambekar and Kandasubramanian, 2019)

When the usual anatomical structure and function of the skin are disturbed, it is referred to as a wound. This distruption may occur due to thermal, physical, mechanical, or electrical factors (Alonso, 1996; Boateng et al., 2008; Lazarus et al., 1994). Wounds are classified into seven categories according to duration, depth, complexity, cause, contamination, type of injury, and the color of contaminated tissue (Dubay and Franz, 2003; Katz et al., 1991; Li et al., 2007). Based on healing time, wounds are categorized into acute and chronic wounds. While acute wounds heal quickly without needing external assistance, chronic wounds required longer time to heal. In addition, chronic wounds do not adhere to the usual sequence of stages involved in the healing process of a wound (Kim et al., 2003; Stojadinovic et al., 2005; Visavadia et al., 2008). Based on depth, wounds are classified as superficial, deep dermal, and full-thickness wounds. If the damaged layer is only the epidermis, then the wound is considered superficial. These wounds usually heal quickly (10 days) without leaving any marks (Debats et al., 2009; Subrahmanyam, 1998). A deep dermal wound usually heals through scar formation in 10-21 days (Chong et al., 2007; Marler et al., 1998). A full-thickness wound happens when the wound has extended to reach both of dermis as well as the hypodermis by default

needing a longer healing time (>21 days) (Debats et al., 2009; Roh et al., 2006). The wound can also be categorized as simple, complex, or complicated wound based on the complexity of the wound (Berk et al., 1992). The superficial wound is related to the loss in the dermal layer, while the complex wound is related to severe tissue loss. The complicated wound is the name of a complex infected wound (Kendrick et al., 1982; Sørensen et al., 2002). As for the cause of the wound, it can be sorted into three groups: traumatic, iatrogenic, and burn wounds. Traumatic wounds include abrasions, cuts, skin tears, and bites (Khan and Naqvi, 2006). Iatrogenic is an infected wound that is mainly caused by surgeries. Burn wound is caused by thermal shock on the skin. Unfortunately, burn wounds are prone to bacterial infection due to damage to macrophages and neutrophils (Rodriguez et al., 1997). Contamination wounds are divided to clean wounds, clean soiled wounds, contaminated wounds, and finally dirty wounds. A clean wound is free of infection but might get infected by bacteria on the skin's surface. A clean/contaminated wound refers to a wound on the respiratory or digestive tract that hasn't lost tissue fluid. A contaminated wound does not contain exudate, while a dirty wound does (Ambekar and Kandasubramanian, 2019). Wounds are classified into abrasion, ulceration, incision, laceration, and degloving according to the mode of injury. The abrasion wound comprises the epidermis subcutaneous layer, and blood leakage indicates this type of wound (Ambekar and Kandasubramanian, 2019). Ulceration wound includes wounds that take more than 6 months to heal because of different ulcer types. (Markova and Mostow, 2012). An incision is a wound that occurs due to surgery, and these types of wounds close within 6 hours (Dorsett-Martin, 2004). Laceration is a wound that occurs due to skin contact with a blunt object or heavy swimming (Atiye et al., 2009). Degloving occurs due to the skin rupture from the underlying fascia layer. In this case, the wound-healing process is complicated due to edema and bleeding of the underlying tissue (Hudson et al., 1992). Wounds can be classified based on the color of the contaminated tissue. Necrotic tissue is defined as black, infected tissue as green, drooping tissue as yellow, granulation tissue as red, and epithelial tissue as pink (Gizaw et al., 2018). Figure 2.4 summarizes the classification of wounds.

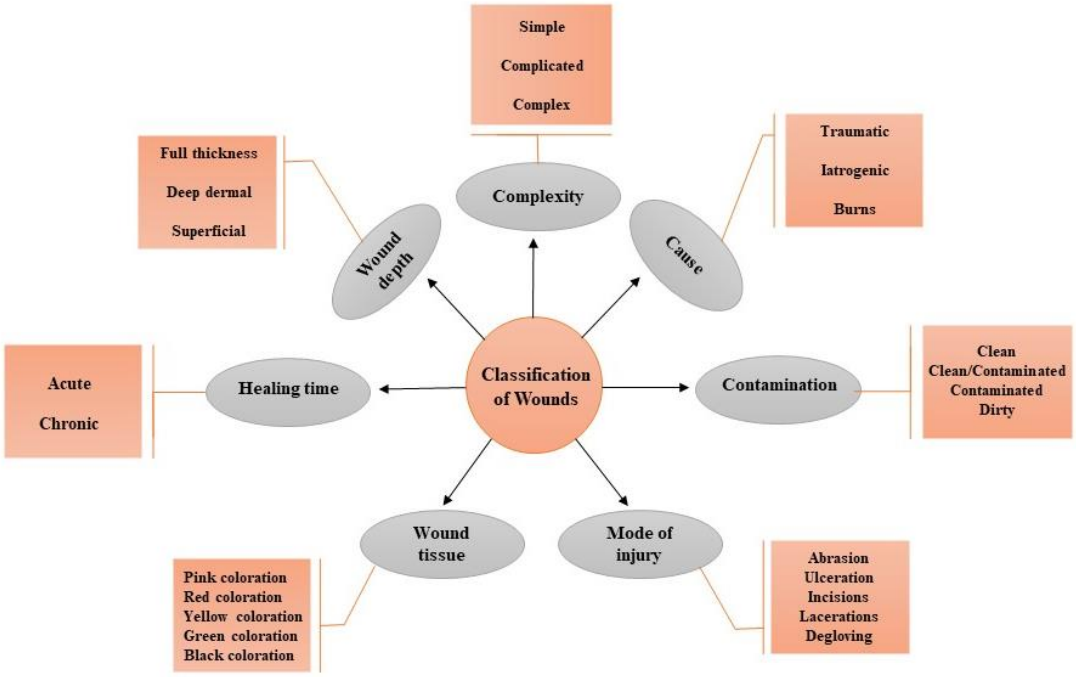

Figure 2.4. Classification of wounds

After the skin structure is ruptured, its functions and structure should be re-established quickly to ensure body homeostasis. After a skin injury, the wound-healing process starts to prevent the risk of bacterial contamination (Mühlstädt et al., 2012). Wound healing happens in four phases; hemostasis, inflammation, proliferation, and remodeling (Figure 2.5) (Ambekar and Kandasubramanian, 2019). In hemostasis, a fibrin clot forms preventing blood loss and microbial contamination through vasoconstriction (Thiruvoth et al., 2015). This step is the initial response to skin injury that occurs by accumulating platelets and inflammatory cells that bind to a structural protein like collagen in the extracellular matrix (ECM). Platelets can secrete various proteins to aid the next stages of wound healing and enhance the regeneration of platelets and growth factors (Ambekar and Kandasubramanian, 2019). The inflammatory phase commences nearly at the same time as hemostasis, and it includes the activation of neutrophil monocytes, macrophages, and lymphocytes that give a specific response to microbes (Thiruvoth et al., 2015). The inflammatory phase has observable signs because mast cells release enzymes and chemicals such as histamine, which dilates blood vessels and might cause redness, swelling, a sense of itchiness, or other signs (Bielefeld et al., 2013). During the migration

and proliferative phase, fibroblasts that move to the wound location transform into myofibroblasts. This process promotes ECM and the formation of new blood vessels by producing the components of extracellular matrix such as hyaluronic acid, fibronectin, proteoglycan, and collagen (Thiruvoth et al., 2015). Maturation or remodeling is the final stage of wound healing. All activated processes are terminated at this stage (Morgado et al., 2015). The last step starts 2 weeks after injury and persist for over than 1 year. Sweat glands and hair follicles cannot heal after severe wound damage. Endothelial cells, macrophages, and myofibroblasts leave the wound site, and the remainder undergo apoptosis. As the small arterioles merge into larger blood vessels, the metabolic activity involved in wound healing declines. Ultimately, the wound is mended through a combination of apoptosis, cell migration from the wound site, and the breakdown of the extracellular matrix by matrix metalloproteinase. (Ambekar and Kandasubramanian, 2019).

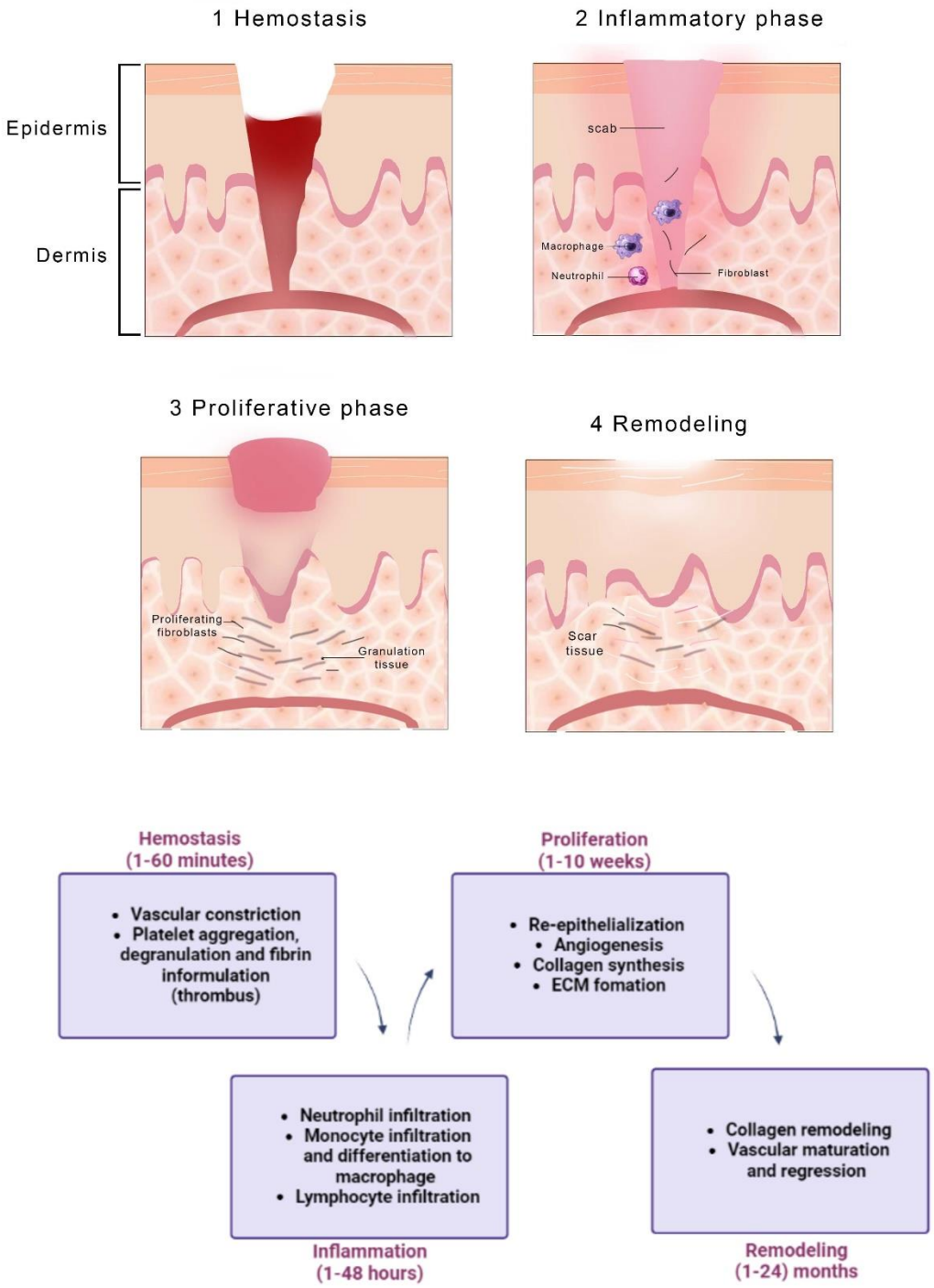

Figure 2.5. The stages of wound healing

2.4. Burn Wounds

The WHO defines a burn as an injury that affects the skin or other organic tissues and is predominantly caused by exposure to heat, chemicals, radiation, electricity, radioactivity, or friction. Burns are the most common soft tissue injuries, and sometimes they may result in death. They can also cause severe mental and emotional discomfort due to skin contractures and excessive scarring. Treating burns has always been a problematic medical obstacle (Oryan et al., 2017). Some critical functions of the skin are restricted by thermal injury. Surviving a severely burned patient needs immediate access to a burn care unit. Immediate burn response and constant treatment are designed to relieve systemic changes resulting from acute skin disruption. In burn wound treatment, tremendous attention is paid to preventing fluid loss, maintaining body temperature homeostasis in a constant normal range, relieving severe pain, and preventing infection (Church et al., 2006).

Two parameters classify burns, the percentage of total body surface area affected (TBSA%) and the burn depth. Knowing the burn type helps to determine the patient's nutritional needs and the strategy of treatment (Rnjak et al., 2011). Burns are classified as first, second, third, and fourth-degree burns depending on the depth of the burn (Figure 2.6). First-degree burns usually occur when only the epidermis is damaged (Hermans, 2005; Rnjak et al., 2011). Second-degree burns happen when the epidermis and part of the dermis are damaged. Second-degree burns are subdivided into superficial and deep dermal burns. Superficial second-degree burns have moist surface because of the plasma that leaks from the burned area, whereas scarring is less common in these burns. Pain is more severe in deep dermal burns. The burn may develop into a third-degree burn if infection develops (Evers et al., 2010). Third-degree burns occur when the epidermis, dermis, and hypodermis are wholly destroyed. Re-epithelialization in third-degree burns depends on the disruption of the dermis, the proportion of burned hair follicles and sweat glands, and the degree of infected areas (Evers et al., 2010). Fourth-degree burns are wounds where the burned area extends to reach underlying tissues such as tendons, muscles, and bones. These burns are painless since the nerve terminals are destroyed. Nevertheless, these burns are rare and often fatal (Hermans, 2005; Parrett et al., 2006).

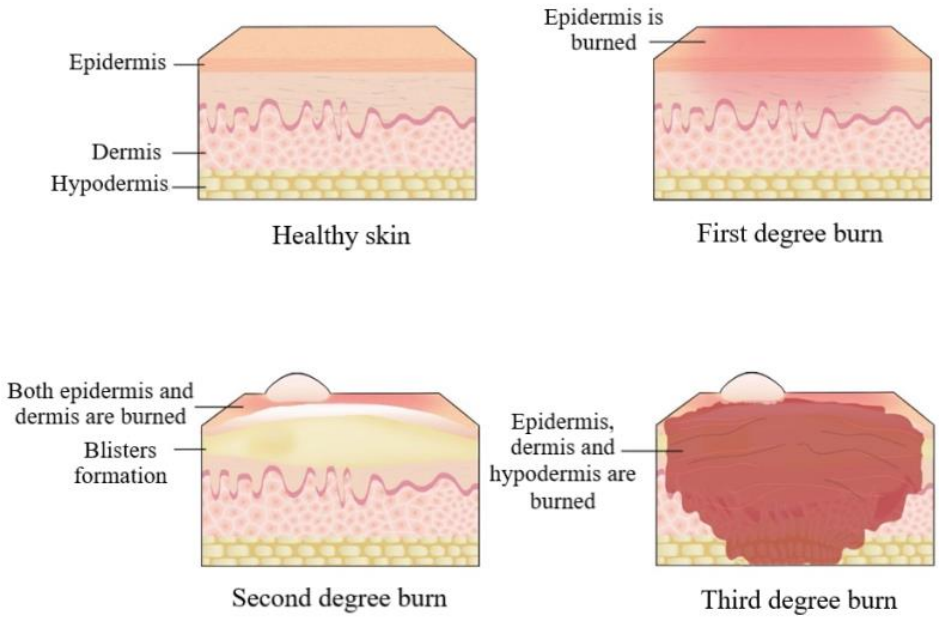

Figure 2.6. Types of burns based on the affected skin layer

Moderate treatment is usually sufficient for first-degree and superficial partial-thickness burns, which tend to heal with minimal scarring. In contrast, full-thickness and deep dermal partial burns tend to heal with scarring and frequently require prolonged scar management and multiple reconstructive surgeries. After a third-degree or deep burns, the body may exhibit a range of responses, including loss of nutrients and fluids, electrolyte imbalance, respiratory system failure, multi-organ and/or heart failure, and immune system suppression (Wang and Kimble, 2010).

Thermal injury releases large amounts of proinflammatory cytokines and chemical mediators, that include arachidonic acid, histamine, coagulation step products, and oxygen-free radicals. These burns induce an escalation in vascular permeability, which can result in hypovolemia and acute renal failure. Subsequently, wound infection and bacterial translocation from the gastrointestinal tract can further contribute to the development of sepsis. As a result, multiple organ failures and death occur (Church et al., 2006). Many physiological features of the burn environment are susceptible to infection and resistant to conventional antibiotic treatment. In burns, proteolysis and lipolysis are upregulated. An evident increase in matrix metalloproteinases (accompanied by a decline

in inhibitors) provokes protein degradation, which facilitates the entry of microbes into the tissue (Church et al., 2006).

Microbial species that colonize burns have a predictable time course. Gram-positive bacteria that can even survive thermal shock, such as *Staphylococci* that is found deep in the sweat glands and hair follicles, intensively colonize the wound surface within the first 2 days. After around 5-7 days, burns are colonized by the host's naturally found in upper respiratory and gastrointestinal flora or other microbes found in the hospital. Yeasts and fungi are the final colonizers (Church et al., 2006). Table 2.2 shows pathogens responsible of burn infections and their drug-resistance formation (Dai et al., 2010). Due to the susceptibility of the burn wound to bacterial infections, topical antimicrobial agents have been used to prevent and treat burn wound infections. The necessity of developing these agents came from the increasing multidrug resistance of the bacteria. Table 2.3 is a summary of topical antimicrobial agents that are used for burn wounds to prevent bacterial infection (Dai et al., 2010).

Table 2.2. Pathogens responsible for burn infections (Dai et al., 2010)

Group	Species	Drug Resistance
Gram-positive bacteria	*S. aureus*	-
	MRSA	By definition
	Coagulase-negative Staphylococci	MRSA increasing
	Enterococcus species	-
	Vancomycin-resistant Enterococci	By definition
Gram-negative bacteria	*P. aeruginosa*	High innate resistance
	E. coli	ESBL increasing
	Klebsiella pneumoniae	ESBL increasing
	Serratia marcescens	Increasing
	Enterobacter species	ESBL increasing
	Proteus species	ESBL increasing
	Acinetobacter species	Very common
	Bacteroides species	Uncommon
Viruses	*Herpes simplex virus*	-
	Cytomegalovirus	-
	Varicella-zoster virus	-
Fungi	*Cytomegalovirus*	-
	Varicella-zoster virus	-
	Fusarium species	Common in agriculture
	Alternaria species	Common in agriculture
	Rhizopus species	Azole resistance
	Mucor species	Azole resistance

Table 2.3. Antimicrobial agents used in burn wounds (Dai et al., 2010)

Agent Class	Specific Agent	Application
Skin substitutes	Duoderm	Clinical 2nd degree burns
	Trans-Cyte	Clinical 2nd degree burns
	Omniderm	Clinical 2nd degree burns
	Suprathel	Clinical 2nd degree burns
	Epigard	Clinical 2nd degree burns
	SYSpur-derm	Clinical 2nd degree burns
	Biobrane	Clinical 2nd degree burns
	Xenoderm	Clinical 2nd degree burns
Topical antibiotics	Mafenide acetate	Clinical 2nd/3rd degree burns
	Bacitracin	Clinical 2nd/3rd degree burns
	Mupirocin	Clinical 2nd/3rd degree burns
	Neosporin	Clinical 2nd/3rd degree burns
	Polymyxin B	Clinical 2nd/3rd degree burns
	Nitrofurazone	Clinical 2nd/3rd degree burns
	Nystatin	Clinical 2nd/3rd degree burns, fungal infections
Silver	Silver nitrate	Clinical 2nd/3rd degree burns
	Silver sulfadiazine	Clinical 2nd/3rd degree burns
	Silver foams	Clinical 2nd/3rd degree burns
	Flammacerium	Clinical 2nd/3rd degree burns
	Acticoat 7	Clinical 2nd/3rd degree burns
	Aquacel-Ag	Clinical 2nd/3rd degree burns
	Silvercel	Clinical 2nd/3rd degree burns
	Silver amniotic membrane	Clinical 2nd/3rd degree burns
Iodine	Povidone-iodine	Clinical 2nd/3rd degree burns
	Cadexomer iodine	Clinical chronic wounds
	Lipooal iodine, Repithel	Clinical 2nd degree burns
	Iocide	Oral infections

Table 2.3. Antimicrobial agents used in burn wounds (Dai et al., 2010) (continued)

Photodynamic therapy	TBO	Mouse wound infections
	PEI-ce6	Mouse burn infections (A. baumannii)
	XF73	In vitro, ex vivo skin infection
	BB6	In vitro, mouse wound infection
	Sylsens B	Mouse burn infection S. aureus
	DP/hemin	Guinea pig burn infections S. aureus
	Cat PC	In vitro, veterinary infections
	EtNBSe	In vitro
Chitosan	Hyrogel	Clinical 2nd degree burns
	Film	2nd degree burns in rabbits
	Bandage	Mouse burn infections
AMPs	Defensins	In vitro
	Demegel	Pseudomonas infected rat burns
	Histone H1.2	Pseudomonas infected rat burns
	Cecropin B	Pseudomonas infected mouse wounds
	rBPI	Clinical 2nd degree burns
	Ceragenins	In vitro
Miscellaneous	Chlorohexidine (LM Miller)	Infected rat burns, clinical trial
	Superoxidized water	In vitro
	BCTP nanoemulsion	In vitro
	FPQC	Mice burns, Pseudomonas
	Acidified nitrite	In vitro
	Phage therapy	Mice burns, Pseudomonas
	p38MAPK inhibitor	Rat burns, Pseudomonas
	Probiotics, Lactobacillus	Clinical trial, 2nd, 3rd degree
	Honey	Clinical trial, 2nd degree
	Essential oils	In vitro
	MEBO	Clinical trial, 2nd degree
	Papaya	Clinical trial, 2nd, 3rd degree

2.5. Wound dressings

The importance of wound healing has been acknowledged since ancient times due to continuous wars and terrible living conditions. As the medical comprehension of wounds developed, so did the healing ways, and different types of passive wound dressings started to appear (Figure 2.7). Carl Reyher, a surgeon of the Russian military, brought up a debridement for cleansing the wound from foreign bodies. In World War II, many dangerous weapons and ammunition were used, which increased the need for surgical dressings that helped eliminate the infection. In 1955, a poly-HEMA based hydrogel was synthesized by professors Wichterle and Lim (1960). Although passive dressings are cheap and partially provide protection to the wound site, they can not systematically deliver drugs nor respond to the changes occurring during the healing process. Active dressings were developed to overcome this problem as they contain functional materials such as antimicrobials to prevent infection (Van Hoorick et al., 2003; George et al., 2006; Simões et al., 2018).

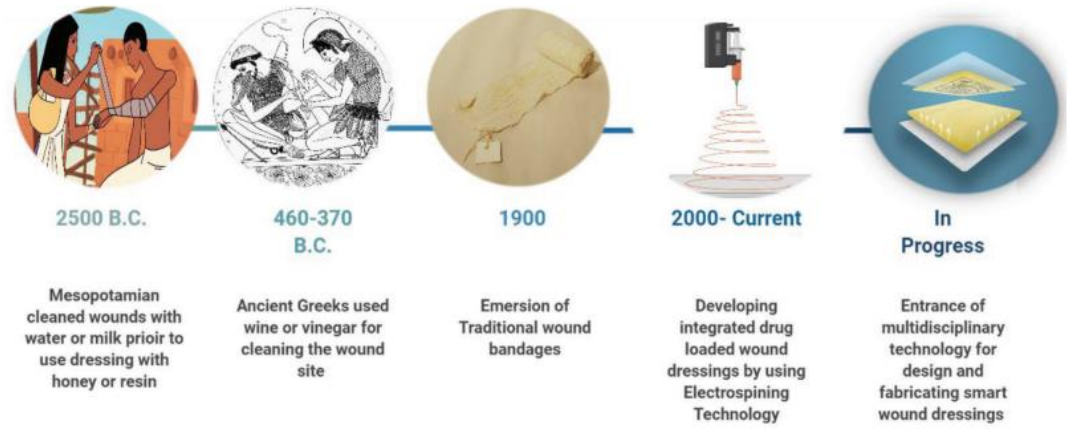

Figure 2.7. Timeline of wound dressings development over the years **(**Farahani and Shafiee, 2021)

Wound dressings are prepared in different physical forms (sponges, membranes, films, hydrocolloids or hydrogels) to allow the coverage of wounds, and each form has its distinct properties. Choosing the proper wound dressing is very important to accelerate the process of wound-healing and to prevent any further damage in the dressing-changing process (Hayes and Su, 2011). The main functions of wound dressings are accelerating

the wound healing process and protecting it from any external damaging factors such as microorganisms (Simões et al., 2018; Wang et al., 2018). In addition to the protection function, wound dressings provide a moist environment and absorb the exudates and this aids wound healing, especially in burn wounds (Jones et al., 2006; Queen et al., 2004). The wound dressing can transmit gas by allowing oxygen to enter, aiding the wound healing stages. Another essential function of wound dressings is that they can stop bleeding and provide support for the skin. Nevertheless, an ideal wound dressing should have the characteristics described in Figure 2.8 (Domb and Khan, 2014; Kokabi et al., 2007).

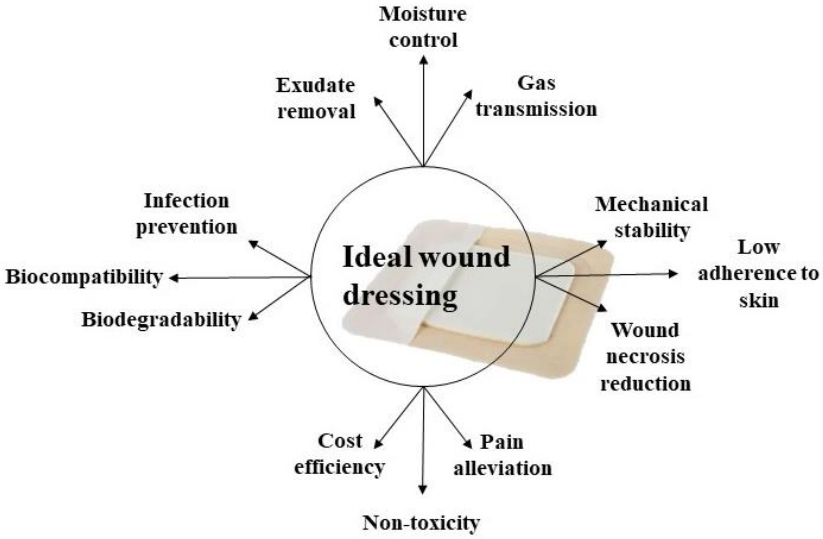

Figure 2.8. The features of ideal wound dressings

Wounds dressings can be classified into four types depending on their affinity to the wound: smart, passive, interactive, and advanced dressings (Figure 2.9). These kinds of dressings can be synthesized from synthetic and natural polymers. Passive dressings consist of a fiber network that allows gas exchange due to their porous structure, thus providing a suitable environment and protection to facilitate wound healing. Interactive dressings consist of a synthetic polymer and a biological agent to give an antibacterial characteristic to the dressing. Although it promotes wound healing and controls bacterial growth, its usage is limited due to impurities and immunogenic reactions. Liu et al. (2010) performed a study on a polylactide-polyglycolide

(PLGA)/collagen nanofiber that showed a remarkable resemblance to human fibroblasts, which eventually helped the wound healing hemostasis step. Drug-loaded nanofibers are an excellent example of advanced dressings as they can stop bacterial infection due to their ability to be loaded with a drug. The drug release profile depends on the type of polymer that the matrix is synthesized of, crosslinking, swelling capacity, and the drug itself. Soltanova et al. (2016) developed a coaxial polycaprolactone (PCL) based nanofiber loaded with ampicillin as an antibiotic. The coaxial nanofiber had a more controlled drug release rate (7% in 4 h) followed zero-order kinetics compared to blend nanofiber (85% in 4 h). Smart dressings are unique for different types of sensors that help surveil the wound while healing and other various functions. Pakolpakçıl et al. (2020) developed a SA/PVA-based nanofiber matrix and incorporated it with anthocyanins extracted from natural sources. The halochromic nanofibrous matrix exhibited detectable colors at pHs of 4.0–6.0 and 8.0–10.0, which align with the pH changes in the wound healing stages in a short response time.

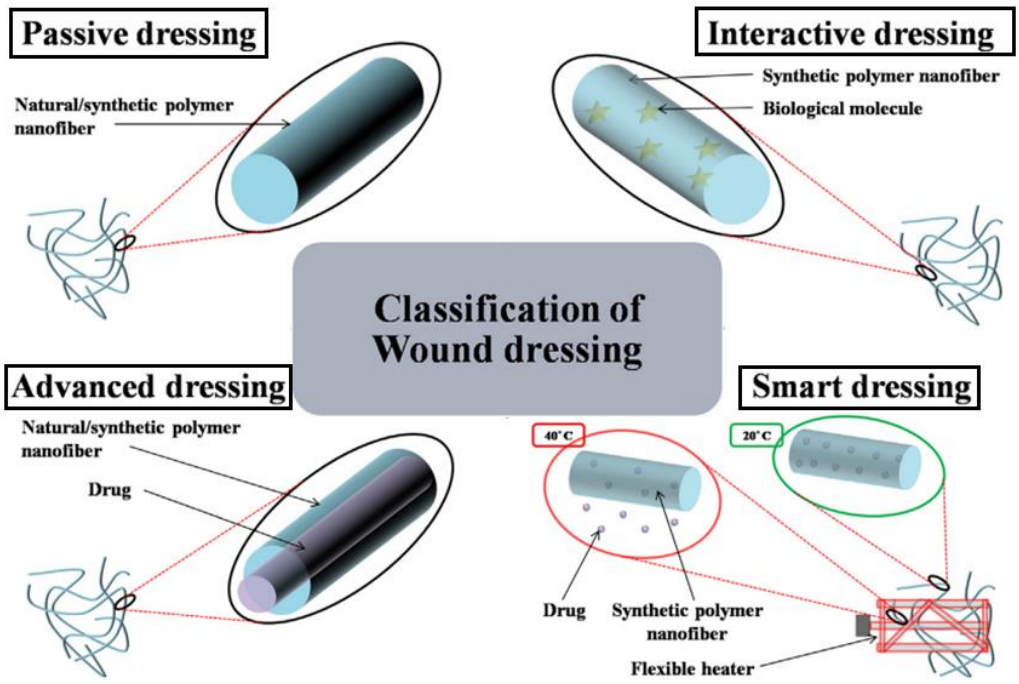

Figure 2.9. Classification of wound dressings (Ambekar and Kandasubramanian, 2019)

2.5.1. Antibacterial agents used in wound dressings

Antibiotics in wound dressings

Antibiotics can prevent bacterial infection in different ways; by inhibiting the cell wall synthesis of a bacteria cell, obstructing its metabolic pathway, intervening in protein synthesis, and inhibiting nucleic acid synthesis. Aminoglycosides, glycopeptides, beta-lactams, sulphonamides, quinolones, and tetracyclines are antibiotics known to be used in wound dressings (Table 2.4) (Simões et al., 2018). Tandi et al. (2015) developed PVA/cellulose-based hydrogels by freeze-thawing method and incorporated one with ciprofloxacin and the other with Tridax procumbens plant extract. Hydrogels loaded with both drugs showed almost similar swelling ability and antibacterial effect. In a study by Chhibber et al. (2020), chitosan-based hydrogels containing moxifloxacin were developed to treat *S. aureus* infected burn wounds. The novel hydrogel had Boswellia gum and ethylenediaminetetraacetic acid (EDTA) and the drug. Drug release studies showed that a burst drug release was exhibited in the first 60 minutes, then increased linearly to 360 minutes. Both conventional and novel hydrogels were effective in eliminating *MRSA* four hours post-infection treatment. The drug's minimum inhibitory concentration (MIC) and minimum bactericidal concentration (MBC) were determined for *S. aureus* and were found to be 0.06 μg/ml and 78.13 μg/ml respectively.

Table 2.4. Antibiotic incorporated wound dressings (Simões et al., 2018)

	Antibiotic	**Wound dressing**	**Materials**	**Tested bacteria**
Beta-lactams	Ceftadizime	Electrospun membrane	SF/G	*P. aeruginosa*
		Film	Collagen/CMGG/EDA	*S. aureus* *P. aeruginosa*
	Ampicillin	Electrospun membrane	PCL	*S. aureus* *K.pneumoniae*
		Hydrogel	PVA/SA	*E. coli*
	Cefazolin	Electrospun membrane	G	*S. aureus*
Tetracyclines	Doxycycline	Film	Collagen/DHBA/GMs	*P. aeruginosa*
	Tetracycline hydrochloride	Membrane	BC	*E. coli* *S. aureus*
		Hydrogel	OAlg/CMCS/GMs	*B. subtilis* *E. coli* *S. aureus*

Table 2.4. Antibiotic incorporated wound dressings (Simões et al., 2018) (continued)

Aminoglycosides	Streptomycin	Electrospun membrane	PU/CA/ZN	*E. coli* *S. aureus* *S. typhimurium* *V. vulnificus* *B. subtilis*
		Hydrogel	PVA/Cellulose	*S. aureus* *E. coli*
	Gentamicin	Electrospun membrane	CS	*P. aeruginosa* *S. aureus* *E. coli*
	Neomycin	Electrospun membrane	PSSA-MA/PVA	*S. aureus* *E. coli*
	Ciprofloxacin	Electrospun membrane	PVP; PU/Dextran	*E. coli* *B. subtilis* *S. aureus* *S. typhimurium* *V. vulnificus*
	Levofloxacin	Sponge	CS/PHEA	*MSSA* *MRSA* *P. aeruginosa*
	Norfloxacin	Film	CS	*S. aureus* *B. cereus* *E. coli* *K. pneumoniae*
	Moxifloxacin	Electrospun membrane	PVA/SA	*P. aeruginosa* *S. aureus*
Sulphonamides	Sulfadiazine	Film	BC/SA; CS/CHI	*E. coli* *S. aureus*
		Sponge	CS	*E. coli* *S. aureus* *B. subtilis*
		Electrospun membrane	PCL/PVA	*S. aureus*
	Sulfanilamide	Fiber	SA	*E. coli* *S. aureus*
Glycopeptides	Vancomycin	Hydrogel	SF/GMs	*E. coli* *S. aureus*
		Film	SA/HNTs/Gelatin	*E. coli* *S. aureus* *S. epidermidis* *S. aureus* *S. haemolyticus* *S. pneumoniae* *S. pyogenes*

Nanoparticles as antimicrobial agents in wound dressings

Nanoparticles are preferred over classical antibiotics because of their broad-spectrum activity against bacterial cells, and lots of side effects of conventional drugs can be avoided using them (Salouti and Ahangari, 2014; Yang et al., 2017). Their main disadvantage is that they can be dangerous to humans because they can easily penetrate many biological barriers and disrupt healthy human cells (Bahadar et al., 2016; Sanyicens and Marco, 2008). Khampieng et al. (2014) prepared γ-irradiation cross-linked PVP hydrogel and incorporated it with SNPs to create an antibacterial wound dressing. The 5 mM SNP-incorporated PVP hydrogel intercepted bacterial infection and boosted wound healing. Silver nanocomposite SA/PVA hydrogels were synthesized by acrylamide (AAm) monomer graft polymerization onto SA and PVA by Ghasemzadeh and Ghanaat (2014). Ammonium persulfate (APS) was used as an initiator, and finally, the hydrogel was cross-linked with N,N-methylenebisacrylamide (MBA). Swelling tests showed that the swelling ratio of the hydrogels could be affected by many factors; APS concentration, monomer weight ratio, drying time and temperature, reaction temperature, and SA/PVA weight ratio. As the alginate content increased, the hydrogels' water uptake capacity also increased due to the hydroxyl and carboxyl groups found in alginate. SEM imaging showed that the hydrogel's porosity increased distinctly with increasing SA content. From the antibacterial activity tests, nanocomposite hydrogels exhibited an inhibitory effect against gram-negative *E. coli* and gram-positive *S. aureus* cultures. MIC for *E.coli* was 31.25 μg ml^{-1} and MBC was 125 μg ml^{-1}, while for *S. aureus*, they were 250 μg ml^{-1} and 1000 μg ml^{-1}, respectively. Table 2.5 shows other examples of nanoparticle incorporated wound dressings (Simões et al., 2018).

Table 2.5. Nanoparticle incorporated wound dressings (Simões et al., 2018)

Type of nanoparticles	Wound dressing	Materials	Tested bacteria
Iron oxide	Electrospun membrane	CS/Gelatin	*E. coli* *S. aureus*
Titanium dioxide (TiO_2)	Composite	CS/human ECM sheet; CS/PVP	*E. coli* *S. aureus* *B. subtilis*
	Electrospun membrane	PVA/Plur/ PEI	*P. aeruginosa* *E. coli* *S. aureus* *S. typhi*
Zinc oxide (ZnO)	Hydrogel	CS; SA/gum Acacia	*E. coli* *S. aureus* *B. cereus*
	Composite	BC	*E. coli* *S. aureus* *P. aeruginosa* *C. freundii*
	Hydrogel	Alginate	*E. coli* *S. aureus* *MRSA*
Silver (Ag)	Sponge	CS/HA SF/ CMCS	*K. pneumoniae* *MRSA* *E. coli* *S. aureus* *P. aeruginosa*
	Hydrogel	AMPS; PVP	*S. aureus* *P. aeruginosa* *S. epidermidis* *MRSA* *E. coli* *A. iwoffii* *B. cereus* *S. pyogenes*

Natural product in wounds dressing

Many natural products that show an antibacterial effect have been used in wound dressings. The products are natural polymers like CS and its derivatives, essential oils, or even honey (Essa and Sukumar, 2012; Saleem et al., 2010). Saberian et al. (2021) have prepared and characterized SA/CS hydrogels combined with honey (H) and aloe vera

(Alv). Antibacterial studies showed that all hydrogels had an inhibitory effect against *S. aureus* as a gram-positive bacteria and *P. aeruginosa* as a gram-negative bacteria. Alg-CS-Alv-H hydrogel exhibited the best inhibitory impact for *S. aureus* (inhibitory zone =23 mm) and *P. aeruginosa* (14 mm). In contrast, the basic hydrogel of Alg-CS showed the lowest inhibitory effect for both bacterium types. Table 2.6 shows some wound dressings incorporated with natural products exhibiting antibacterial effects.

Table 2.6. Wound dressings incorporated with natural antibacterial agents (Simões et al., 2018)

Natural products	***Wound dressing***	***Materials***	***Tested bacteria***
Henna (Lawsonia inermis)	Electrospun membrane	CS/PEO;gelatin/oxidized Starch	*E. coli* *S. aureus*
St John's-wort EO (Hypericum perforatum)	Film	CS	*E. coli* *S. aureus*
	Electrospun membrane	PCL	*E. coli* *S. aureus*
Curcumin	Composite	PVA	*E. coli* *S. aureus* *B. subtilis* *P. vulgaris* *E. faecalis* *S. epidermidis* *K. pneumoniae* *E. aerogenes* *P. mendocina*
	Electrospun membrane	CA/PVP	*S. aureus*
Aloe vera	Electrospun membrane	PLGA	*S. epidermidis* *S. aureus*
Thymol	Electrospun membrane	PCL/PLA	*E. coli* *S. aureus*

2.6. Antimicrobial peptides

AMPs are a type of small peptides that are found in different organisms, starting from prokaryotes to humans. The importance of AMPs can be attributed to their role in the immune system (Diamond et al., 2009; Huan et al., 2020). AMPs have an inhibitory effect against bacteria, viruses, fungi, and parasites. In addition, AMPs can facilitate wound healing by encouraging cell migration and angiogenesis (Hashemi et al., 2018; Huan et al., 2020). AMPs' structure consists of a polar, cationic and hydrophobic parts (Hartman

et al., 2010). The mechanism of action of AMPs is based on the initial, selective electrostatic interaction between its positively charged groups and the negative groups of the target membrane.

On the other hand, the hydrophobic part of the AMPs can not get into the membrane, and when found in an adequate concentration, AMPs cause a disturbance in the membrane, which ends in the death of the target cell (Ding et al., 2002). Rezaei et al. (2020) incorporated an AMP, piscidin-1 in different concentrations into a thermo-responsive CS hydrogel as a wound dressing. The swelling test showed that the water uptake increased sharply in the first 4 h and reached a swelling equilibrium after 10 h. Drug release studies showed that the hydrogels exhibited a burst release of more than 40% of the AMP on the first day, which carried on for 7 days. Disk diffusion assay showed that the hydrogels containing 4, 8, and 16 μg ml^{-1} AMP exhibited an inhibitory effect against common strain bacteria. Resistant *A. baumannii* was only inhibited by 16 μg ml^{-1} AMP containing hydrogel.

AMPs can be classified based on activity, source, aminoacid-rich species and structural characteristics into four main groups (Figure 2.10) (Huan et al., 2020).

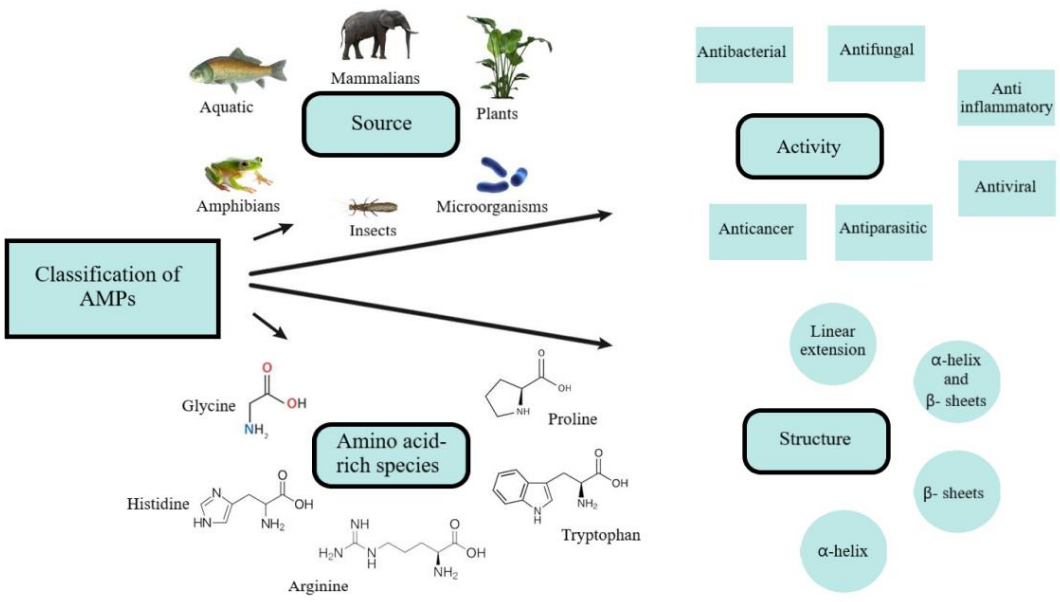

Figure 2.10. Classification of AMPs

2.7. Ceragenins

Unfortunately, even with the tremendous antimicrobial inhibitory effects of AMPs and their wound-healing characteristics, there are limiting factors that discourage their clinical applications. Some of these factors include their large-scale production and high expenses, vulnerability against bacterial proteases, problems in folding during the production of large AMPs, and decreased activity while immobilizing (Bahar and Ren., 2013).

Ceragenins are non-peptide mimics of AMPs that are synthesized from cholic acid which is a bile acid (Epand et al., 2008). Ceragenins were first discovered by Li and Savage (2009) and patented as a new antimicrobial agent for treating infections. Due to being non-peptide-based, ceragenins are not hydrolyzed like AMPs by ubiquitous proteases. Ceragenins are prepared and purified relatively straightforwardly, stable under physiological conditions, and their antibiotic activities can be conserved even under long-term storage in solution (Hashemi et al., 2017; Isogai et al., 2009). Those characteristics make ceragenins unique and overtop AMPs. However, ceragenins have an amphiphilic structure similar to AMPs which makes them also exhibit a similar inhibitory activity against bacteria, lipid-enveloped viruses and fungi (Surel et al., 2014). In Figure 2.11, the structures of selced ceragenins were given.

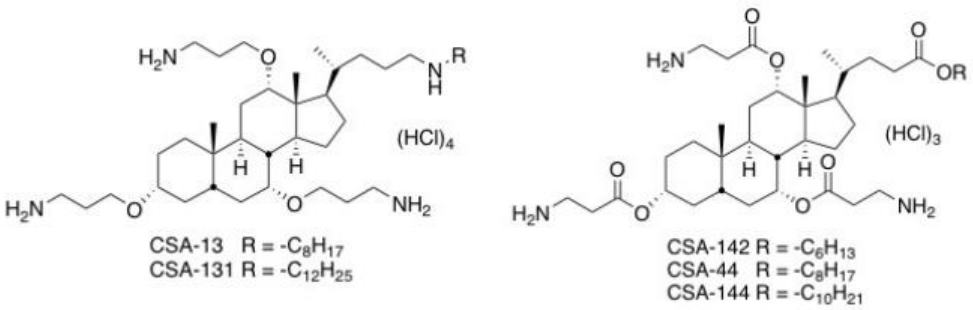

Figure 2.11. Structures of selected ceragenins (Hashemi et al., 2018)

The initial structure of ceragenins was based on the presumption of the ability to bind lipid A to polymyxin B (Ding et al., 2004). Lipid A, which is an amphipathic molecule, serves as the lipid core of lipopolysaccharides (Scott et al., 2017). Three primary amines

were bonded to cholic acid to mimic the arrangement of the primary amines in the polymyxin B molecule. The basic structure of ceragenins has exhibited inhibitory activity against *E. coli*. Later, it was concluded that adding lipophilic groups to the D ring of the cholic acid increased ceragenins activity against gram-negative bacteria and granted it a broad-spectrum antibacterial activity. This can be attributed to the ability of these lipophilic groups to cause a disturbance in the bacterial outer membrane and eventually pass it to the cytoplasmic membrane (Schmidt et al., 2001).

Furthermore, other methods were used to synthesize ceragenins in which the ether bonds binding amines to the cholic acid were replaced with amide and ester groups. Most resulting compounds exhibited less antibacterial activity than ceragenins with ether bonds. Nevertheless, in ester-based compounds, ester groups were immediately hydrolzed in water (Savage, 2001; Savage, 2002; Taotafa et al., 2000).

2.7.1. Mechanism of action of ceragenins

Like AMPs, ceragenins selectively interact with microbial membranes by ion pairing between positively charged ceragenins and negatively charged bacterial cell membranes. Also, ceragenins segregate bacterial endotoxins, which construct the membranes of gram-negative and gram-positive bacteria (Bucki et al., 2005; Bucki et al., 2007; Wimley, 2010).

The association between ceragenin and the outer membrane is inadequate for cell death. It also needs access to the cytoplasmic membrane. This can be achieved through the lipid chain of ceragenins, consisting of at least 24 carbons. The interaction of ceragenins with the cytoplasmic membrane causes the membrane to weaken, depolarize and eventually cause cell death (Ding et al., 2004; Kichler et al., 2005; Pogoda et al., 2014). The mechanism of action of ceragenins on viruses and fungi is not understood; however, some fungal and viral cells treated with ceragenins showed changes in cell shapes or lipid envelopes.

Antimicrobial activities of ceragenins have been studied on a wide range of drug-resistant gram-positive and gram-negative bacteria. Results showed that ceragenins exhibited a broad range of activity on both types of bacteria. As a result of these studies, it was

concluded that ceragenins could be used for medical applications with the growth of antibiotic-resistant bacteria (Schmidt et al., 2001; Wnorowska et al., 2015). Some tested ceragenins showed antibacterial activity when compared with the antimicrobial peptide cathelicidin LL-37. Table 2.7 shows MIC [MBC] μg ml^{-1} of LL-37 and ceragenins against tested strains associated with some oral infections (Leszczyńska et al., 2013)

Table 2.7. Antibacterial activity of ceragenins against tested strains associated with oral infections compared to LL-37 (Leszczyńska et al., 2013)

Strains	**MIC [MBC] μg ml^{-1}**			
	LL-37	**CSA-13**	**CSA-90**	**CSA-92**
***Staphylococcus aureus* ATCC 29213**	14 [28]	0.7 [1.4]	0.7 [2.8]	0.75 [0.75]
***Streptococcus salivarius* ATCC 13419**	14 [28]	0.7 [1.4]	0.7 [1.4]	1.5 [3.0]
***Streptococcus sanguinis* ATCC 10556**	14 [28]	0.7 [0.7]	1.6 [1.4]	1.5 [3.0]
***Streptococcus mutants* ATCC 35668**	28 [28]	0.7 [1.4]	0.7 [1.4]	0.75 [1.5]
***Enterococcus faecalis* ATCC 29212**	14 [56]	2.8 [2.8]	1.4 [2.8]	8.0 [3.0]
***Moraxella catarrhalis* ATCC 23246**	28 [28]	1.4 [1.4]	0.7 [1.4]	0.35 [1.5]
***Peptostreptococcus Anaerobius* ATCC 27337**	224 [224]	5.6 [5.6]	22.4 [22.4]	5.8 [11.7]
***Lactobacillus casei* ATCC 393**	224 [224]	22.4 [44.8]	44.8 [44.8]	46.8 [46.8]
***Fusobacterium nucleatum* ATCC 25586**	224 [224]	11.2 [22.4]	11.2 [11.2]	11.7 [23.4]

Due to the drug-resistant fungal pathogens, the antifungal activity of ceragenins was also studied. Since AMPs exhibit antifungal activity, some ceragenins were tested compared to LL-37 and other antifungal drugs against fungal strains (Durnaś et al., 2016; Zhang et al., 2018). Table 2.8 shows MIC [minimum fungicidal concentration (MFC)] μg ml^{-1} of

ten clinical isolates of *C. auris* to chosen ceragenins and three major types of antifungal agents (Hashemi et al., 2018).

Table 2.8. Ceragenins antifungal activity against *C. auris* compared to antifungal agents (Hashemi et al., 2018)

Strains	MIC [MFC] µg mL^{-1}						
	CSA 44	**CSA 131**	**CSA 142**	**CSA 144**	**Caspofungin**	**Amphotericin**	**Fluconazole**
***C. auris* CDC381**	0.5 [2.0]	0.5 [8.0]	4.0 [32]	0.5 [2.0]	2.0 [64]	1.0 [48]	16 [>100]
***C. auris* CDC382**	0.5 [4.0]	0.5 [8.0]	4.0 [24]	1.0 [8.0]	nm	nm	nm
***C. auris* CDC 383**	0.5 [8.0]	1.0 [10]	2.0 [64]	1.0 [8]	32 [64]	1.0 [32]	64 [>100]
***C. auris* CDC384**	0.5 [4.0]	0.5 [4.0]	4.0 [24]	1.0 [8.0]	nm	nm	nm
***C. auris* CDC385**	0.5 [16]	0.5 [4.0]	8.0 [32]	1.0 [8.0]	nm	nm	nm
***C. auris* CDC386**	0.5 [8.0]	1.0 [8.0]	4.0 [32]	0.5 [8]	2.0 [64]	2.0 [48]	64 [>100]
***C. auris* CDC387**	0.5 [8.0]	0.5 [8.0]	4.0 [32]	0.5 [8]	nm	nm	nm
***C. auris* CDC388**	1.0 [8.0]	0.5 [4.0]	4.0 [24]	2.0 [8.0]	nm	nm	nm
***C. auris* CDC389**	0.5 [8.0]	0.5 [8.0]	4.0 [24]	1.0 [8.0]	nm	nm	nm
***C. auris* CDC390**	0.5 [8.0]	0.5 [4.0]	4.0 [16]	1.0 [8.0]	2.0 [100]	4.0 [64]	64 [8.0]
***C.albicans* ATCC 90028**	0.5 [8.0]	0.5 [4.0]	2.0 [8.0]	2.0 [8.0]	2.0 [32]	2.0 [100]	24 [>100]
nm : not measured							

These days most infections that include chronic wounds and cystic fibrosis pneumonia, are thought to be caused by biofilms. Biofilms are groups of cells that form a cluster through a protective extracellular polymeric membrane (Davey and O'toole, 2000). The relatively small size of ceragenins enables them to pass through the extracellular membrane of biofilms (Hashemi et al., 2017). Ceragenins, like AMPs, can also kill bacterial and fungal cells despite their rapid growth, dividing, or being still (Olekson et al., 2017).

CSA-13 was studied against the vaccina virus. It exhibited strong antiviral activity by happened through aiming the viral envelope. A topical application of CSA-13 showed a serious decrease in viral replication in epidermis of the infected mice (Howell et al., 2009).

Ceragenins also have anti-parasite activity. The mechanism of action of AMPs has been ascribed to direct contact with cell membranes. Some tested ceragenins (CSA-13, CSA-44, CSA-131, CSA-138) showed great activity against *T. vaginalis* and metronidazole-susceptible and resistant strains. However, CSA-13 has exhibited the highest activity (Polat et al., 2016).

2.7.2. Medical applications of ceragenins

Contact lenses

Contact lenses are surfaces that are susceptible to pathogens and infections. To eliminate the bacterial infection, AMPs were incorporated into them. Although this method was successful at reducing bacterial colonization, it is hard to be applied due to the high price of AMPs and their low thermal stability (Szczotka-Flynn et al., 2010). On the other hand, ceragenins also defend against pathogens that can invade lenses while being cheaper. Ceragenins have no chromophore groups and are soluble in the polymers that lenses are made of, which are advantageous characteristics in producing contact lenses. Gu et al. (2013) developed hydrogel lenses from lotrafilcon B silicone-acrylate prepolymers by photosensitizing and irradiating under UV light for 1 min. CSA-138 was chosen to be incorporated into the lens solution after a few other experiences with CSA-120. These ceragenins inhibited bacterial infection for 15 days with *P.aeruginosa* and 30 days with *S.*

aureus. Drug delivery studies of CSA-138 elution showed that concentrations of the ceragenins were never higher than 5 μg/ml in 24 hours. After 4 days of elution, concentrations decreased to <0.5 μg/ml, maintaining antibacterial activity.

Implanted medical device coatings

Infections after implants are common. To eliminate these infections, those implants need a coating that releases a drug for a relatively long period. However, conventional antibiotics added to the coatings can not protect the implants due to the formation of biofilms. From here, ceragenins became necessary as they exhibit antibiofilm and antibacterial activity without being affected by proteases (Hashemi et al., 2.18). Williams et al. (2013) were the first to develop a CSA-13-incorporated polydimethylsiloxane (PDMS) coating for a fracture fixation plate. Their study showed that CSA-13 had no specific effect on PDMS physical properties. SEM imaging showed that CSA-13 has evenly dispersed within the coating. Within 30 days, CSA-13 continued being released from the coating, which protected the implant from forming biofilm and infections for over 12 weeks. CSA-13 incorporated coating exhibited thermal stability, bone healing effect, and no cytotoxicity. Another medical device that is susceptible to microbial invasion is endotracheal tubes. Hashemi et al. (2017) developed a polyurethane (PU)-based hydrogel coating and incorporated it with 10% CSA-131. The endotracheal tube coated with CSA-131 incorporated PU was tested against *MRSA*, *P. aeruginosa*, *K. pneumoniae*, *C. albican*, and *C. auris*. There was no trace of pathogens within 16 days, and no biofilm was formed within 4 days.

Bone fractures

Since AMPs exhibit bone healing activity, this ability was also tested for CSA. Schindeler et al. (2015) studied the effect of CSA on osteoblast differentiation and mineralization and its bacterial inhibitory effect in a rat open fracture. CSA-90 showed the most suitable activity. When CSA-90 was used synergistically with bone morphogenic protein-2, the infection was eliminated, and the bone healing process was slightly impacted. On the other hand, the open fracture left without CSA-90 observed a decline in health due to infections usually caused by pathogens like *S. aureus*.

Imaging infections

As ceragenins have exhibited an affinity towards bacterial membranes, several studies were conducted to label them with imaging agents to image bacterial infections. Hoppens et al. (2014) developed iron incorporated silver shell nanoparticle that is functionalized with a monolayer of CSA-124 (DANs). MRI imaging shows that DANs can successfully adhere to and contrast *S. aureus* in vitro. DANs inhibited *S. aureus* at 12 mg/l and *E. coli* at 24 mg/l, five times more effective than just silver. DANs can be further used to diagnose and treat deep tissue infections, as concluded from these results.

Gastrointestinal diseases

The role of ceragenins in gastrointestinal diseases was mainly studied on *H. pylori* which affect the world's half-adult population, and *C. difficile*. In a study by Leszczynska et al. (2009), CSA-13 bactericidal effect against *H. pylori* was compared to LL-37 and WLBU2 peptides. The results showed that CSA-13 needs fewer concentrations to inhibit bacterial activity after the same incubation time. However, *H. pylori* showed a slight resistance to ceragenins due to cholesterol in the bacterial membrane. In another study performed by Wang et al. (2018), the effect of CSA-13 on the infection caused by *C. difficile* was investigated in a mouse model. Subcutaneous and oral administration of CSA-13 showed an inhibitory effect on *C. difficile* as its concentration decreased in mouse fecal samples. However, the disadvantage of using CSA-13 in this application was the increase of *Peptostreptococcaceae* bacteria which can be linked to the CSA-13 mechanism on *C. difficile* that alters the intestinal microbiota.

2.8. Hydrogels as wound dressings

Recent advances in wound dressings include synthesizing a non-invasive wound dressing with the ability of a controlled release that promotes wound tissue regeneration with less scar formation and the least possible pain (Andreu et al., 2015). One of the best wound healing techniques to achieve the goals above is moist healing, suggested by George Winter (Winter, 1995). Dressing types used these days are films, hydrocolloids, foams, and hydrogels. Table 2.9 summarizes the advantages and disadvantages of those four forms of wound dressings with some of their available commercial forms. Hydrogels were the best choice compared to the mentioned forms of wound dressings due to their ideal wound-dressing properties. However, hydrogels are mechanically unstable in a swollen state (Kamoun et al., 2017).

Hydrogels have a high water absorption ratio depending on the cross-linking affinity of the functional groups found in the three-dimensional polymeric matrix, such as amide, amino, carboxyl, and hydroxyl groups (Miguel et al., 2014). Their high water content, biocompatibility, easy removal, and mimicking characteristics of the living tissues make them perfect candidates for an ideal wound dressing (Gupta et al., 2019).

Hydrogels play a significant role in wound healing by creating a moist environment that facilitates healing and provides a soothing effect. In addition, hydrogels are easily removed due to their limited adhesion, making them less painful and traumatic for patients. Hydrogels can also be enhanced by incorporating a drug or an active biomolecule, as they can release those two in a controlled manner (Gupta et al., 2019). Due to all these properties, hydrogels are used globally in various types of wounds.

Table 2.9. Summary of four types of wound dressings (Kamoun et al., 2017).

Type of dressing	Characteristics	Cautions	Proprietary products
Film dressings	•Polyurethane films with an adhesive to hold the dressing •Create moist healing environment • Elastic, durable and conformable •Waterproof and transparent •Semi-permeable to water vapour and gases •Impermeable to bacteria •Impervious to liquids such as wound fluid •No secondary dressing required	•Being non-absorbent, limited use for highly exuding wounds •Being adhesive, newly formed epithelium could be disrupted during removal •Frequently develop leakage channels	Opsite® Films (Smith & Nephew) Tegaderm™ (3M™, UK Plc.) Mepitel®Film (Mölnlycke Health Care Limited)
Hydrocolloid dressings	• Moist wound dressing • Capable of absorbing wound exudate • Usually made of polyurethane film with an adhesive mass • Adhesive mass is often composed of gelatin, pectin and sodium carboxymethyl cellulose (CMC) which swells on absorbing exudate • Impermeable to water and gases	• Not indicated for infected or heavy exudating wounds • Being opaque difficult to follow the healing process without prior removal • May produce a distinct odour at wound site	DuoDERM® (ConvaTec Inc.) 3M™ Tegaderm™ hydrocolloid dressing (3M™, UK Plc.) Replicare ® (Smith and Nephew)

Table 2.9. Summary of four types of wound dressings (Kamoun et al., 2017) (continued)

Foam dressings	•Bilaminate (or trilaminate) moist wound dressing with varying thickness • Excellent absorption capacity • Can expand and conform to wound shape • Easy to remove • Can be loaded with antimicrobials and other active agents	•Not suitable for low exudating wounds • Frequent change may be required for heavy exudating wounds • May cause maceration on saturation with exudate	Mepilex® and Mepilex Ag® (Molnlycke Health Care) Allevyn (Smith and Nephew) Aquacel® (ConvaTec Inc.) Cutimed® Siltec B (BSN medical Inc.) Biatain® Silicone Ag (Coloplast Ltd.)
Hydrogel dressings	•Insoluble aqueous gels as moist wound dressing • Moisture retention and donation properties • Usually non-adhesive so easy to remove • Can be loaded with antimicrobials and several active wound healing agents • Can be smart and stimuli responsive • Can be injected • Can be cross-linked in situ	• Some hydrogels are mechanically weak in swollen state, but mechanical properties can be enhanced by copolymerisation with appropriate polymer(s). • May cause maceration after accumulation of exudate • May require secondary dressing	Purilon® Gel (Coloplast Ltd) Derma-Gel (Medline Ind. Inc.) Intrasite® Gel (smith & Nephew)

Burn wounds damage the skin's protective function, making it susceptible to many infections and complications. As a result, a primary treatment for the burn wound is needed, especially for patients incompatible with skin grafting. As hydrogels have various wound healing properties, such as providing moisture through swelling, being non-adherent, and mimicking the natural ECM of the skin, they are considered to be the most suitable dressings for burn wounds (Dhaliwal and Lopez, 2018; Stoica et al., 2020). Figure 2.12 explains the uses of hydrogels in burn wound care (Madaghiele et al., 2014).

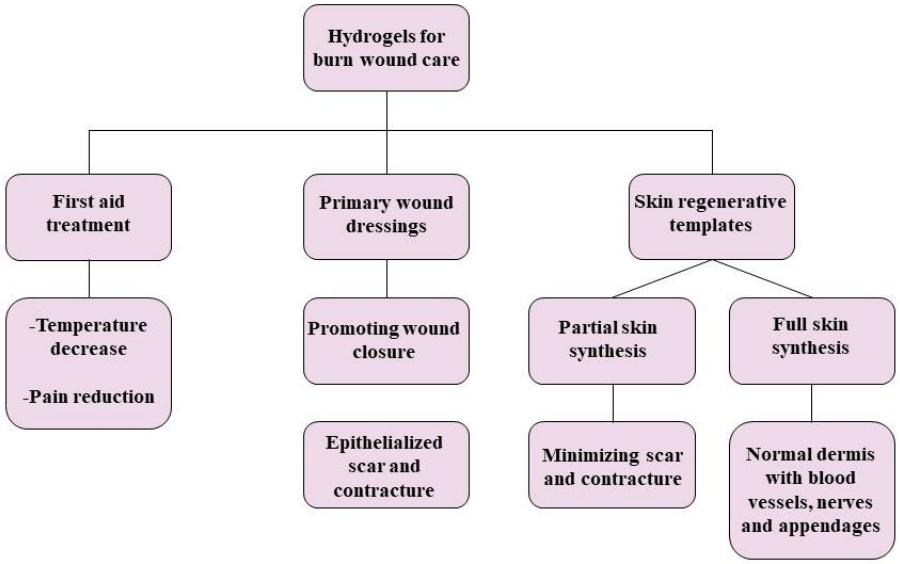

Figure 2.12. Hydrogels in burn wound care

Nevertheless, most hydrogels can not terminate pathogens threatening wound healing. Due to this, hydrogels loaded with different types of antimicrobial agents are being developed to enhance the efficiency of the wound-healing process (Kaur et al., 2019; Francesko et al., 2018). Table 2.10 summarizes some examples in the literature of hydrogel dressings used for partial and full-thickness burns (Madaghiele et al., 2014).

Table 2.10. Examples of hydrogel dressings that are used for partial and full thickness burns (Madaghiele et al., 2014).

Burn Depth	Hydrogel precursor(s)	Additional component(s)
Partial-thickness	AMPS/PEGDA	—
	AMPS	Silver nanoparticles
	Chitin	ZnO nanoparticles
	Chitosan	—
	Keratin	—
	Laponite®/alginate	Mafenide
	PVA/chitosan	Silver sulfadiazine
	PVA	Silver nanoparticles
	PVA/lysine/vanillin	—
	PVP/PEG	Honey
	PVP/PEG	Sea cucumber
	Self-assembling peptides	—
Full-thickness	Chitosan	—
	Chitosan/collagen	Lysostaphin
	Collagen/PEG/fibrin	—
	Dextran/PEGDA	—
	Dextran	Chitosan microparticles with EGF and VEGF
	Hyaluronan	—

Some polymers have been frequently used in synthesizing hydrogels due to their unique characteristics, such as their biocompatibility, porosity, and biodegradability. PVA, SA, and G usage in hydrogel synthesis have increased as single-component or mixed components hydrogels.

PVA is a linear synthetic polymer prepared by hydroxylation of polyvinyl acetate. Hydroxylation can be complete or partial, and its amount regulates the yielding PVA's physical, chemical, and mechanical properties (Tubbs, 1966). For example, the higher the

degree of hydroxylation of PVA, the less soluble it becomes in water and the more challenging to crystallize (Jones, 1973). The structure of PVA can be seen in Figure 2.13.

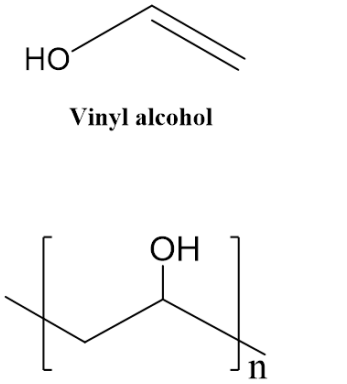

Figure 2.13. Polyvinyl alcohol

PVA has unique characteristics that make it preferable for medical uses. While PVA is very soluble in water, it is insoluble in most organic solvents. It has low protein adsorption, high biocompatibility, and good chemical resistance (Baker et al., 2012). Due to its properties, PVA has been used in many medical applications, such as eye drops, contact lenses, tissue adhesion barriers, embolization particles, and nerve cuffs.

As a hydrogel, PVA has been used in injectable implants, artificial organs, drug delivery systems, aesthetic surgeries, and wound dressings (Hassan and Peppas, 2000). In hydrogels, PVA is preferred to be blended with other polymers due to its relative stiffness and insufficient water uptake (Kamoun et al., 2015).

In a study by Oliveira et al. (2015), a propolis-loaded PVA hydrogel was synthesized by the freeze-thawing method for burn wound healing applications. All the hydrogels containing different concentrations of propolis exhibited a maximum swelling degree near 400% in 4 days in both PBS and aqueous solution at pH 4.0. Based on the drug release studies, high propolis release in the initial hours was observed, and the cumulative release reached constant values up to 1 day of immersion. PVA–propolis gels with concentrations of 15% propolis or more had an inhibitory effect against *S.*

aureus. Varguez-Catzim et al. (2021) developed a bilayer hydrogel membrane from PVA and poly (2-acryloamido-2- methyl-1-propanesulfonic acid) (PAMPS) and cross-linked it with succinic acid for wound dressing applications. Cell cytotoxicity studies showed that all membranes did not exhibit any cytotoxic effect. The antimicrobial activity test showed that PVA/PAMPS membranes exhibited an inhibitory effect against *E. coli* and *S. aureus*, which increased by increasing PAMPS ratio in the blend. Tamahkar et al. (2020) developed a multilayer hydrogel of four layers for wound dressing applications. The layers comprised of carboxylated polyvinyl alcohol, gelatin, hyaluronic acid (HA), and gelatin. The HA layer was loaded with an ampicillin antibiotic. The degradation test showed that the hydrogel exhibited a degradation with good stability that lasted for 15 days. The results of the drug release study showed that the hydrogel had a burst release of 34.5% within 6 h. Within seven days, the hydrogel has exhibited a release of almost 65% of the total ampicillin, which marks the ability of these hydrogels to achieve a long-term drug release profile.

G is a heterogeneous mixture of multi-stranded or single polypeptides derived from hydrolyzed collagen protein with thermal, acid, or alkaline treatment. It contains between 300-4000 amino acids (Figure 2.14) (Liu et al., 2015; Harrington and Von Hippel, 1962).

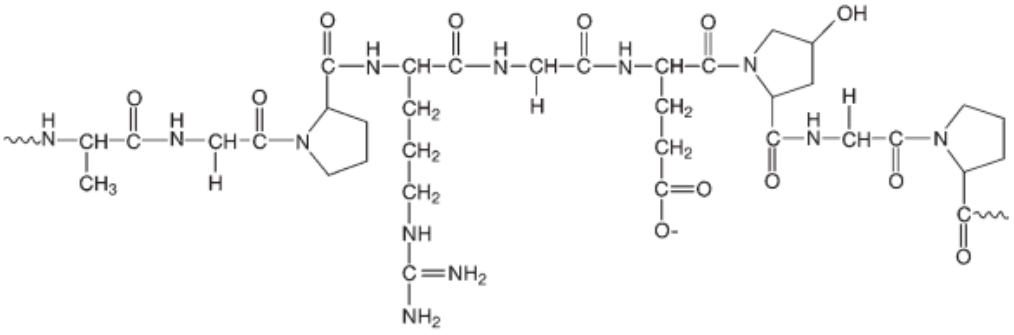

Figure 2.14. General structure of gelatin

Due to the biocompatibility, low cytotoxicity, biodegradability, low antigenicity, and the ability to facilitate cellular growth and attachment, G has been used for several applications such as drug and gene delivery, tissue engineering, wound healing, food industry, and cosmetic industries (Suarato et al., 2018).

In wound dressing, G has been widely used due to its previously mentioned properties. In addition, it can absorb 5-10 times the water of its weight, which enables it to absorb wound fluids and debris. Its resemblance to the extracellular matrix has made gelatin an excellent candidate for wound dressing (Ye et al., 2019). However, G has some limitations as it has low flexibility and water solubility. These limitations can be resolved by cross-linking and/or mixing it with another polymer (Inal and Mülazımoğlu., 2019). For instance, a work performed by Stubbe et al. (2019) where G and SA polymers were modified by photo cross-linkable functional group methacrylamide (MAA) and combined them to develop hydrogel films (G-MAA/SA-MAA) for burn wound treatment. The G-SA films showed increased swelling compared to the G hydrogel due to the extreme swelling potential of alginate. Imtiaz et al. (2019) prepared Nigella sativa seeds encapsulated PVA/G hydrogel by esterification followed by solvent casting. PVA and G were cross-linked in the presence of hydrochloric acid (HCl). Further, the loaded hydrogel was found to have the same swelling ability as the control hydrogel. Loaded hydrogel exhibited an inhibitory effect against the gram-negative *P. aeruginosa* and the gram-positive *S. aureus*.

Alginate is an anionic polymer usually derived from brown seaweed processed with alkali solutions, generally with sodium hydroxide (NaOH). The extract was added with calcium chloride ($CaCl_2$) or ether sodium (Smidsrød and Skja, 1990). Alginate consists of linear copolymers containing blocks of α-L-guluronate and (1,4)-linked β-D-mannuronate residues. The blocks are arranged in a certain way, either consecutive or alternating. Alginates usually differ in these arrangements based on the source they were extracted from (Figure 2.15) (Lee and Mooney, 2012).

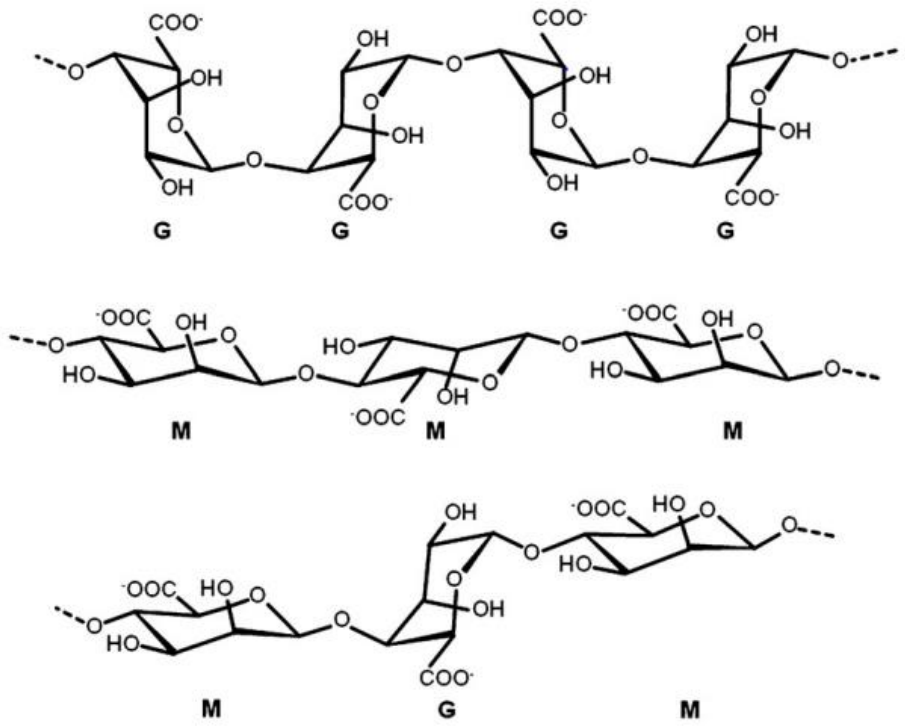

Figure 2.15. Alginate structure

In hydrogel preparation, it is believed that only the α-L-guluronate blocks of alginate participate in intermolecular cross-linking with divalent cations (e.g., Ca^{2+}) (George and Abraham, 2006).

Alginates have been used in various biomedical applications owing to their biocompatibility, gelation ability, low toxicity, swelling capacity, and resemblance to the extracellular matrices. Alginates are widely used in wound healing, delivery of drugs and proteins, in addition to cell transplantation. Alginates are used in wound dressing applications because they preserve a moist environment, inhibit bacterial infections to some extent, and accelerate the wound healing process. The release of drugs and proteins in a controlled way can be achieved via the cross-linking (Lee and Mooney, 2012).

Sodium ampicillin incorporated PVA/ SA hydrogel membranes were developed by Kamoun et al. (2015) for wound dressing application. Hydrogels were prepared by the freeze-thawing method after mixing different ratios of PVA and SA solutions. Burst release of ampicillin was observed from drug release studies as it reached 38–45% in the first 15 min. This was ascribed to ampicillin dispersal, which was close to the hydrogels'

surface. The drug release behavior did not significantly increase after 6 h. It was found that the addition of SA decreased the percentage of the released drug. From the swelling test, it was found that the hydrogels which had no SA, presented lower water uptake of 1500%. After increasing SA content to 75%, it increased to 4200%.

In a study by Nuutila (2020), an antibiotic containing alginate hydrogel was prepared by lyophilization to be used cooperatively with a platform wound device (PWD). The added antibiotics were gentamicin, minocycline, and vancomycin, each into a different hydrogel. Porcine studies showed that using alginate hydrogels containing a high concentration of antibiotics with PWD decreased the number of bacteria and depth of the burn compared to the control. Results also showed no toxicity or adverse effects exhibited in any animals during or after treatment. From the drug release studies, all hydrogels exhibited burst release kinetics as most of the drugs were released into the supernatant within the first few hours.

3. MATERIALS and METHODS

3.1. Materials (Chemicals)

Table 3.1. Chemicals used in this study.

Chemical	Brand	Code
Polyvinyl alcohol	Aldrich	363081
Sodium alginate	Sigma	A2033
Gelatin	Sigma	G2500
Gluteraldehyde	Merck	S5223003
Acetone	Merck	I462812
Hydrochloric acid	Merck	K47224017
Chloroform	Merck	K48774144
Benzoic anhydride	Aldrich	385980
Triethylamine	Merck	S4940052
Methanol	Merck	K27693618
Sodium chloride	Merck	K37352804
Potassium chloride	Merck	K47220436
Disodium hydrogen phosphate (Na_2HPO_4)	Sigma-Aldrich	04272
Potassium dihydrogen phosphate (KH_2PO_4)	Ph.Eur.	26922.295
Phosphorus pentoxide	Riedel-de Haen	04113

3.2. Methods

3.2.1. Preparation of PAG hydrogel

Firstly, the composition of PVA/SA/G hydrogel was investigated. For this purpose, PAG hydrogels were prepared by solvent-casting method using different polymer ratios. A solution of 10% PVA (w/v) was prepared by dissolving PVA in deionized water using a water bath at 90 ^oC. In the same way, solutions of 2% SA (w/v) and 5% G (w/v) were prepared and dissolved in a water bath at 40 ^oC. PVA, SA, and G ratios used to prepare hydrogels are given in Table 3.2. After the preparation, 18 ml of each PAG mixture was poured into petri dishes of 9 cm in diameter. The hydrogels were dried at 37 ^oC for a night.

Table 3.2. The PVA, SA and G ratios used for hydrogel preparation

Hydrogel/Polymer	PVA	SA	G
PAG1	1	1	1
PAG2	1.5	0.5	1
PAG3	0.5	1.5	1
PAG4	0.5	1	1.5
PAG5	1.5	1	0.5
PAG6	1	0.5	1.5
PAG7	1	1.5	0.5

The prepared hydrogels, PAG1, PAG2, PAG3, PAG4, PAG5, PAG6, and PAG7 were cross-linked with glutaraldehyde solutions (v/v) prepared at different concentrations (0.5%, 0.375%, 0.1875%, 0.125%) for 5 minutes and tested for swelling and hydrolytic degradation. PAG1, PAG4, and PAG6 hydrogels were cross-linked with 0.375% GA solution to investigate the cross-linking time for 10 min, 20 min, and 30 min.

3.2.2. Swelling and hydrolytic degradation tests

The swelling test was performed at room temperature in distilled water. For this purpose, the dry weight of the hydrogels was determined, then the hydrogels were soaked in 30 ml of distilled water. The wet hydrogels were weighed after the excess water was carefully removed. By weighing the wet samples at certain time intervals, the time of the swelling equilibrium was determined. Swelling (%) was calculated using Equation 3.1.

$$Swelling\ \% = \frac{W_s - W_i}{W_i} \times 100 \qquad (3.1)$$

where W_i is the dry weight (g) and W_s is the wet weight (g).

The hydrolytic degradation test was performed at room temperature in distilled water. Hydrogels' initial weights were taken, and then the degradation rate was determined at different intervals by drying the soaked hydrogels' pieces and weighing them. The degradation test was carried out for one month. Degradation (%) was calculated using Equation 3.2.

$$Degradation\% = \frac{W_i - W_d}{W_i} \times 100 \qquad (3.2)$$

where W_i is initial dry weight (g), W_d is the dry weight after being soaked in the water.

3.2.3. Preparation of PAG-CSA hydrogel

Considering the results of optimization studies, PAG6 hydrogel formulation was selected to prepare PAG-CSA hydrogel. The hydrogel mixture PAG was prepared by mixing PVA, SA, and G in the ratio of 2:1:3, respectively. PVA and SA were mixed for 2 h, then G was added and left to mix all overnight. The next day, CSA-44 was added with a ratio of 1.77% (w/w) and left to mix in the hydrogel solution for half an hour until it totally dissolved. The solution was divided into 6-well plates (d=3.5 cm each well), which were previously coated with glycerol, by pouring 2 ml of the mixture into each well. The final CSA-44 incorporated hydrogel PAG-CSA was left in the deep freezer section of the lyophilizer overnight (Figure 3.1). The next day, 6-well plates containing PAG-CSA hydrogel mixtures were lyophilized for 24 hours using MCGS lyophilizer in Bursa Uludağ University, Chemistry Department, Biochemistry Research Laboratory.

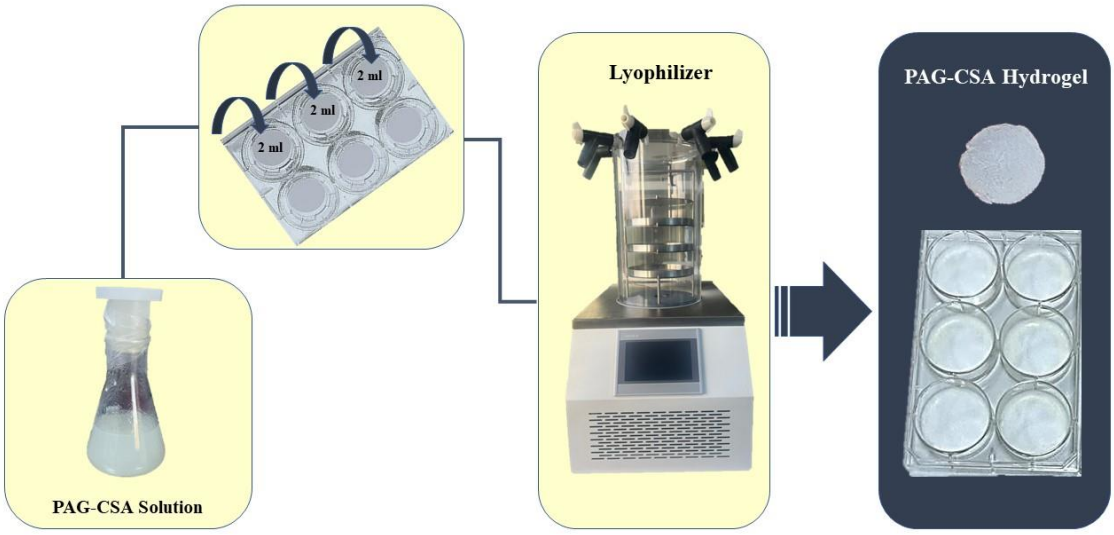

Figure 3.1. PAG-CSA hydrogel lyophilization process

PAG and PAG-CSA hydrogels were cross-linked in 0.125% (v/v) GA solution for 20 min. The solution was prepared by mixing GA and HCl in acetone as a solute. PAG and PAG-CSA hydrogels were washed in acetone and dried in a refrigerator (4 ^{o}C). After that, the lyophilized hydrogels were stored in a desiccator containing phosphorus pentoxide in the fridge for further usage.

3.2.4. Characterization og PAG-CSA hydrogel

The characterization studies for lyophilized PAG and PAG-CSA (cross-linked and non-cross-linked) were conducted by Fourier Transform infrared spectroscopy (FTIR), scanning electron microscopy (SEM), and mercury porosimetry, Swelling (%), hydrolytic and enzymatic degradation (%), dehydration, water vapor transmission rate (WVTR), air permeability, tensile strength, water contact angle (WCA) and thickness of the lyophilized hydrogels were also determined.

Fourier transform infrared spectroscopy (FTIR) analysis

FTIR analysis of PAG and PAG-CSA (cross-linked and non-cross-linked) was conducted in a frequency range of 400-4000 cm^{-1}. The analysis was performed by FTIR spectrophotometer with ATR apparatus (Perkin Elmer Spectrum 100 Waltham, MA, USA).

Scanning electron microscopy (SEM) analysis

The morphological features of the prepared PAG and PAGS-CSA hydrogels were determined by SEM analysis. The SEM images of cross-linked PAG and non-cross-linked and cross-linked PAG-CSA were taken by SEM at different magnifications. In addition, the cross-section of the cross-linked PAG-CSA structure was visualized by SEM. CSA-44 integration was demonstrated by analyzing the cross-linked PVA/SA/G lyophilized hydrogel with and without CSA-44 by SEM-EDX. SEM analyses were carried out at Bursa Technical University using GeminiSEM 300.

WCA measurement

The WCAs of PAG and PAG-CSA cross-linked hydrogels (1×1 cm) were measured using a contact angle instrument (KSV attention Tetha, Hamburg, Germany) in Bursa Uludağ University, Chemistry Department, Biochemistry Research Laboratory. The sessile drop method was used to measure the contact angle. The contact angle was determined by taking 40 separate photos of the water drop from different parts of the hydrogels' surfaces utilizing the instrument's software.

Mercury porosimetry analysis

The cross-linked PAG-CSA hydrogel's porosity and pore size distribution was determined through mercury porosimetry analysis using Quantachrome Corporation, Poremaster 60. The applied pressure was 25000 psi.

Thickness measurement

The thickness of the PAG and PAG-CSA, both cross-linked and non-cross-linked hydrogels, was determined using an Insize brand digital micrometer. The thickness was measured from 15 different points of the hydrogel, and the average was calculated with the standard deviation value. The thickness measurement was performed in Bursa Uludağ University Textile Engineering Department Research Laboratory.

Tensile test

To prepare PAG and PAG-CSA hydrogels for analysis, 12 ml of PAG and PAG-CSA hydrogel solutions were separately poured into plastic petri dishes (d = 9 cm) and lyophilized as previously described. The hydrogels were cross-linked by 0.125% GA solution for 20 min and left to dry in the lyophilizer. Samples were sprayed with distilled water prior to analysis. The tensile strength test was performed using a Shimadzu AG Xplus brand mechanical strength test device in Bursa Uludağ University, Textile Engineering Department Laboratory. Samples with dimensions of 20 mm X 25 mm were placed between the test device's grips and pulled until they broke using a 50 N load cell at a jaw speed of 15 mm/min with a distance of 25 mm between the grips. This test was based on the ASTMD 3822 standard. The test was repeated three times, then the mean and standard deviations were calculated. The elongation and stress values at the maximum

point were determined, and the tensile stress (TS) at the maximum point was calculated using Equation 3.3.

$$TS = \frac{F}{A_R} \qquad (3.3)$$

where F (N) is the break force of the film and A_R (m^2) is the cross-sectional area.

Air permeability test

To determine the air permeability of cross-linked PAG and PAG-CSA hydrogels, SDL ATLAS M021A Air Permeability Tester located in Bursa Uludağ University, Textile Engineering Laboratory was used. The test area was 5 cm^2, and the pressure applied was 98 Pa, based on the BS 5636 standard. Measurements were repeated three times, and the mean and standard deviation were calculated.

WVTR test

The water vapor transmission test was applied using the E96-00 standard method at 37 ^oC and 85% relative humidity (ASTM E 96-95, Annual Book of ASTM,1995). The cross-linked PAG-CSA was cut into a circle (d=1.35 cm), placed on the mouth of a 1.35 cm diameter glass bottle containing 10 ml of pure water, and weighed all together. Then, the bottle was kept in a desiccator containing saturated ammonium sulfate solution at 37 ^oC for 24 hours. The bottle was weighed again after 24 h, and the WVTR ($g/m^2/day$) was calculated using Equation 3.4. The experiment was repeated three times.

$$WVTR = \frac{W_o - W_f}{10^6} \qquad (3.4)$$

Where W_o is the weight of the bottle with hydrogel before keeping it for 24 h and W_f is their weight after 24 h.

Dehydration test

The dehydration test was conducted by soaking cross-linked PAG and PAG-CSA hydrogels in pH 7.4 PBS solution until they had reached the swelling equilibrium time. Then wet hydrogels were incubated at 37 ^oC. After that, the weight of the hydrogels was

measured during definite time intervals until it completely dried out. The test was repeated three times. Dehydration% was calculated using Equation 3.5.

$$Dehydration\ \% = \frac{M_i - M_{DEH}}{M} \times 100 \qquad (3.5)$$

where M_i is the initial weight of the wet hydrogel, M_t is the weight of the wet hydrogel at time *t*, and *M* is the water content of the hydrogel.

Swelling test

The swelling test for the cross-linked PAG and PAG-CSA hydrogels was performed in PBS solution of pH 7.4 at 37 °C. For this purpose, first, the dry weight of the hydrogels was determined, then the hydrogels were soaked in a 30 ml pH 7.4 PBS buffer. The wet weight of the hydrogels was determined after the excess buffer solution was carefully removed. By weighing the wet samples at certain time intervals, the time of the swelling equilibrium was determined. Experiments were repeated three times. Swelling (%) was calculated using Equation 3.1.

Hydrolytic and enzymatic degradation tests

The hydrolytic degradation test of cross-linked PAG and PAG-CSA was performed by soaking the hydrogels in 50 ml PBS solution of pH 7.4. 1% lysozyme enzyme solution (50 ml PBS at pH 7.4) was used for enzymatic degradation. Hydrogels' initial weights were taken, and then the degradation rate was determined at different intervals by drying the soaked hydrogel pieces and weighing them. The degradation test was carried out for one month. This test was repeated three times. Degredation (%) was calculated using Equation 3.2.

3.2.5. Drug release studies

In order to plot a calibration graph for CSA-44, solutions of 5, 10, 20, 50, and 100 mg/l of CSA-44 were prepared. Since the CSA-44 molecule does not contain chromophore groups, solutions were derivatized for High Performance Liquid Chromotography (HPLC)-UV detection. For this purpose, benzoic anhydride (BA) was used. 1 ml of each CSA-44 solution was firstly mixed with BA at a ratio of 10:0.25 (Solution: BA) (v/v) and then triethylamine (TEA) at a ratio of 10:1 (Solution: TEA) (v/v) and incubated for 1 h at

37 °C at a stirring rate of 100 rpm. Then, 1 ml of chloroform equal to the sample volume was added, mixed, and the resulting mixture was centrifuged at 5000 rpm. Later, 800 µl of chloroform phase was separated and dried with N_2 gas. The samples were reconstituted in 800 µl methanol prior to analysis using HPLC. In HPLC analysis (C3 column), the mobile phase was acetonitrile/water, and the flow rate was 0.5 ml/min. A calibration graph was plotted using the resulted values of the averages of 2 sets of solutions.

For drug release studies 0.02 g CSA-44 was added to 18 ml of PAG solution (1.77% (w/w) CSA-44). The solution was then divided into well plates 2 ml each and lyophilized. The hydrogel which was used for drug release studies weighed 0.1464 g and contained 2.69 mg CSA-44. The release studies from the PAG-CSA hydrogel were conducted using 5 ml of PBS buffer (pH 7.4) as a release medium. All samples were incubated at 37 ^{o}C at a stirring rate of 90 rpm, and the release medium was replaced with fresh PBS (5 ml) at each analysis time at certain time intervals. The amount of CSA-44 in the release medium was determined by HPLC after each sample was derivatized. The derivatization technique was the same that was used in the calibration graph preparation as 1 ml of the release medium was taken at specific time interval then dervatized and analyzed using HPLC. The HPLC analysis was conducted at SEM Research and Development Laboratories using Agilent HPLC 1290 Infinity.

The cumulative release (%) vs. time plots of the CSA-44 release were prepared using the obtained release data. Cumulative release (%) values were calculated using Equation 3.6.

$$Cumulative\ release\% = \frac{W_t}{W_c} \times 100 \qquad (3.6)$$

where W_t is the total CSA-44 amount released into the release medium at time t (g), and W_c is the total amount of incorporated CSA-44.

CSA-44 release kinetics was investigated using zero order, first order, Higuchi, and Korsmeyer-Peppas kinetic models.

4. RESULTS and DESCUSSION

4.1. Optimization of the PAG hydrogel composition

The hydrogels prepared at seven different compositions exhibited high swelling and degradation ratios maintaining a fair mechanical stability when 0.375% (v/v) GA solution was used for cross-linking (Table 4.1). PAG3 and PAG7 hydrogels prepared with 0.375% (v/v) GA solution have high swelling ratios, but they were mechanically highly unstable. This can be attributed to the high SA content of these hydrogels. PAG2 and PAG5 had the lowest swelling ratios. PAG1, PAG4 and PAG6 hydrogels crosslinked with 0.375% GA solution were mechanically stable. The hydrolytic degradation ratios of PAG1, PAG4 and PAG6 hydrogels ranged between 67 % and 84 % for 1 month.

Table 4.1. Swelling (%) and hydrolytic degradation (%) of the crosslinked PAG hydrogels (crosslinking time: 5 min)

	Degradation (%)				**Swelling (%)**			
Hydrogels	**0.5%**	**0.375%**	**0.187%**	**0.125%**	**0.5%**	**0.375%**	**0.187%**	**0.125%**
PAG1	67	67	78	81	350	424	349	312
PAG2	64	79	72	81	249	208	228	2.6
PAG3	92	93	92	96	186	554	1096	967
PAG4	79	84	92	79	2608	1181	2373	1053
PAG5	92	85	94	95	428	338	401	367
PAG6	90	83	86	96	504	439	338	537
PAG7	94	86	95	95	185	414	297	342

To study the effect of crosslinking time on swelling and degradation profiles of the hydrogels, PAG1, PAG4, and PAG6 hydrogels crosslinked with 0.375% GA solution were selected because they had suitable swelling and degradation ratios, and they were relatively mechanically stable. The crosslinking time intervals were set as 10 min, 20 min, and 30 min. The obtained results are given in Table 4.2. As it can be clearly seen that cross-linking time did not significantly affect the swelling behavior, but it caused an increase in the degradation time for PAG1, PAG4, and PAG6. Additionally, PAG4 exhibited poor mechanical stability despite the high swelling ratio. Therefore, the cross-linking time was determined as 20 min to use a lower amount of GA.

Table 4.2. Swelling (%) and hydrolytic degradation (%) of PAG1, PAG4 and PAG6 hydrogels with different cross-linking time at 0.375% GA

Parameters	**Hydrogel**	**Crosslinking time**		
		10 min	**20 min**	**30 min**
Swelling (%)	***PAG1***	398	338	247
	PAG4	734	1116	1070
	PAG6	265	246	277
Hydrolytic degradation (%)	***PAG1***	69	67	67
	PAG4	55	64	72
	PAG6	56	60	55

PAG1, PAG4, and PAG6 were also lyophilized at -75 ^{o}C for 24 h to improve both the swelling properties and mechanical stabilities. The swelling ratios of PAG1 and PAG6 significantly increased after lyophilization because lyophilization enable to preparation of hydrogels with more prominent pores. However, no significant difference was observed for the swelling ratio of PAG4. Although lyophilized PAG4 had the highest swelling ratio, it had poor mechanical stability even after lyophilization. As a result, the lyophilized PAG6 hydrogel was the most mechanically stable, and its swelling ratio improved enough (722%) after lyophilization, maintaining an excellent porous structure (Figure 4.1). Thus, PAG6 formulation, including PVA, SA, and G in the ratio of 2:1:3, was determined as the optimal hydrogel composition and used to prepare ceragenins (CSA-44) loaded lyophilized hydrogel. The final cross-linking ratio with GA was determined to be 0.125% for 20 minutes.

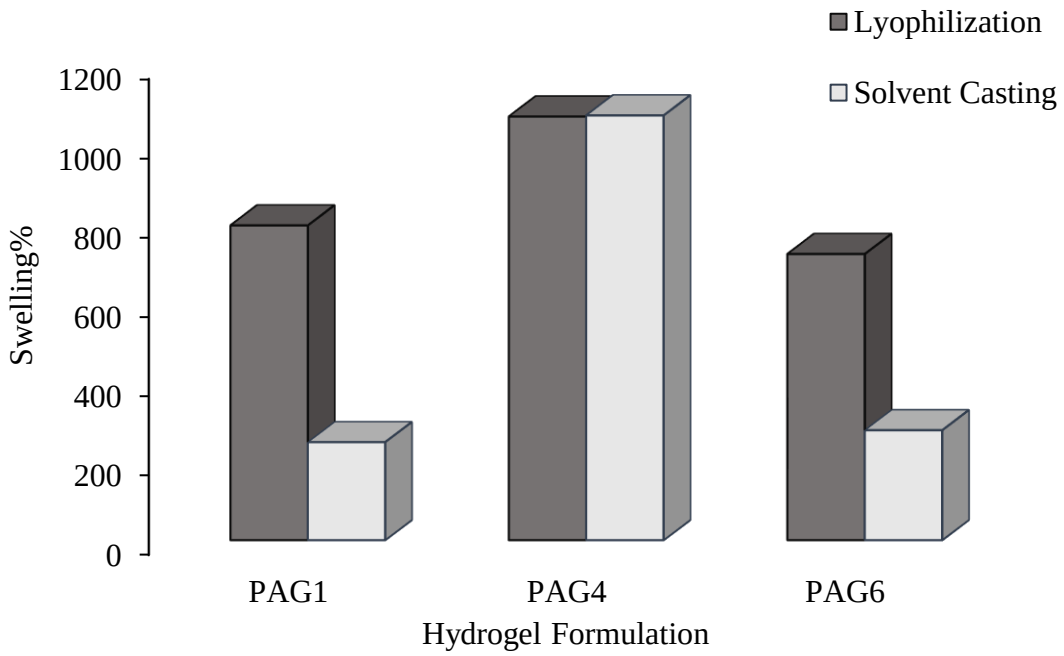

Figure 4.1. The swelling ratios of PAG hydrogels prepared via solvent casting and lyophilization methods (cross-linking time: 30 min)

4.2. Properties of PAG-CSA hydrogel

4.2.1. Chemical properties

The FTIR spectra of PAG and PAG-CSA hydrogel were taken for chemical characterization before and after crosslinking with GA. The polymeric components of the hydrogel were also investigated by FTIR analysis to ensure that all the polymers entered the structure of the hydrogel. The FTIR spectrum of PVA is given in Figure 4.2. At around 3303 cm^{-1}, the hydroxyl group stretching can be seen. The absorption band at 2937 cm^{-1} is referred to as the asymmetric stretching of the C-H alkyl group, while 2910 cm^{-1} is related to the symmetric stretching of C-H. The bands seen at 1714 and 1731 cm^{-1} refer to the stretching of C=O and C-O bonds of the ester carbonyl group. It can be concluded from the C=O and C-O bands that polyvinyl acetate wasn't fully hydrolyzed to form PVA.

The FTIR spectrum of SA (Figure 4.3) shows a vibrational band at 3242 cm^{-1}, attributed to hydroxyl group stretching. The band at 2923 cm^{-1} is related to the stretching of the CH_2. Asymmetric and symmetric stretching bonds of carboxylic salt ions can be seen at 1594 and 1406 cm^{-1}, respectively. The N-H stretching band was observed at 3278 cm^{-1}

in the FTIR spectrum of G (Figure 4.4). The band at 2937 cm^{-1} is related to the asymmetric stretching of CH_2, whereas the band around 2850 cm^{-1} represents the symmetric stretching of CH_2. The band at 1629 cm^{-1} is associated with C-O stretching of amide I. The N-H bond bending of amide II is observed at 1523 cm^{-1}. While the bond at 1238 cm^{-1} is related to the C-H stretching of amide III.

FTIR spectrum of the CSA-44 is given in Figure 4.5. The N-H stretching was observed as a weak band at 3412 cm^{-1}. The absorption band at 2924 cm^{-1} is related to the asymmetric stretching of CH_2, while the band around 2850 cm^{-1} represents the symmetric stretching of CH_2. C=O stretching of the ester group was seen as a strong band at 1728 cm^{-1}. The C-O stretching was observed at 1208 cm^{-1}. At 1099 cm^{-1}, the C-N stretching of the amines appeared as a weak band.

All hydrogels' functional groups of the hydrogel's polymers can be observed in the FTIR spectrum. However, CSA characteristic bands in PAG-CSA, whether cross-linked or not, are not apparent due to its small quantity compared to other components of the hydrogel (Figure 4.6).

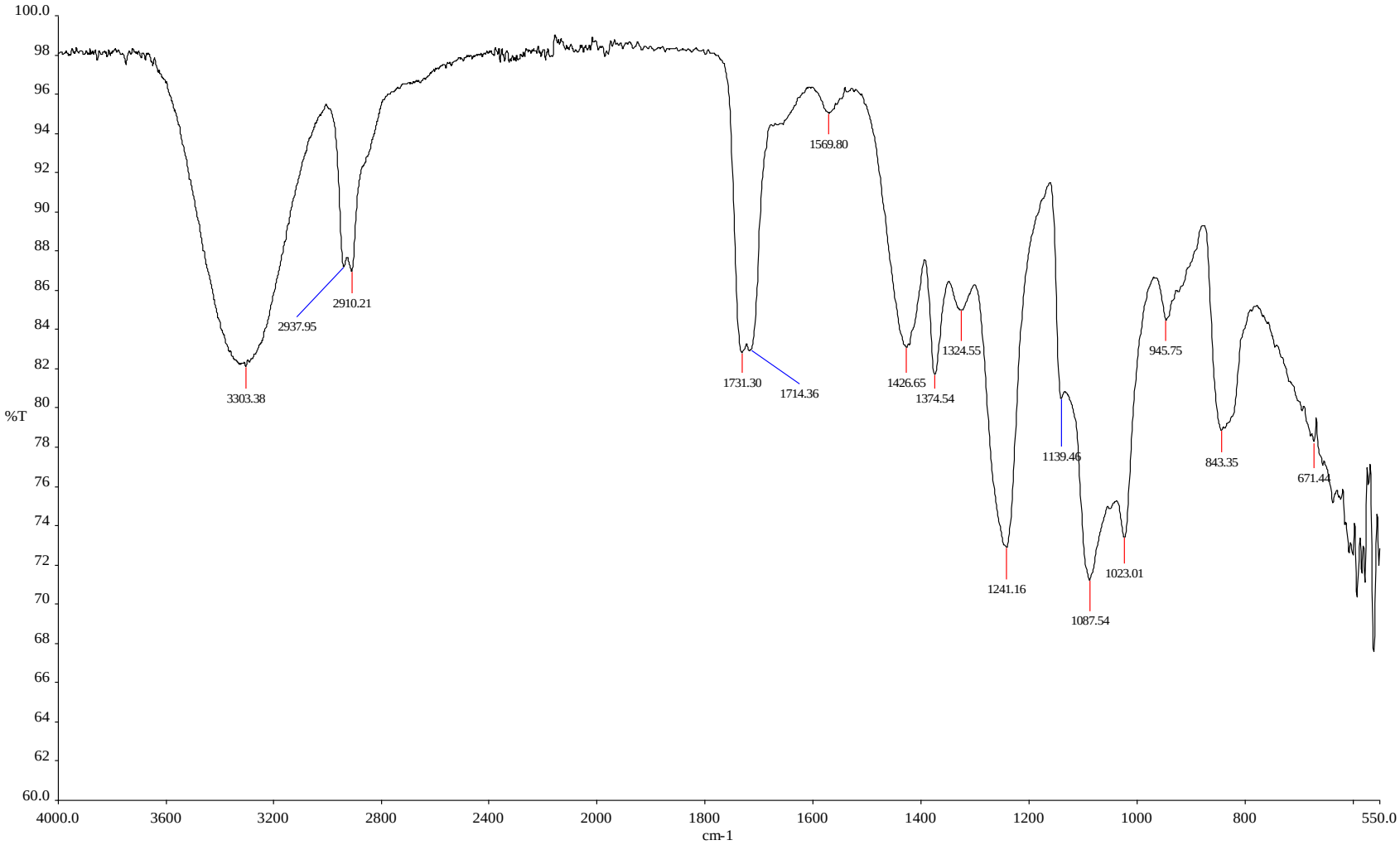

Figure 4.2. FTIR spectrum of PVA

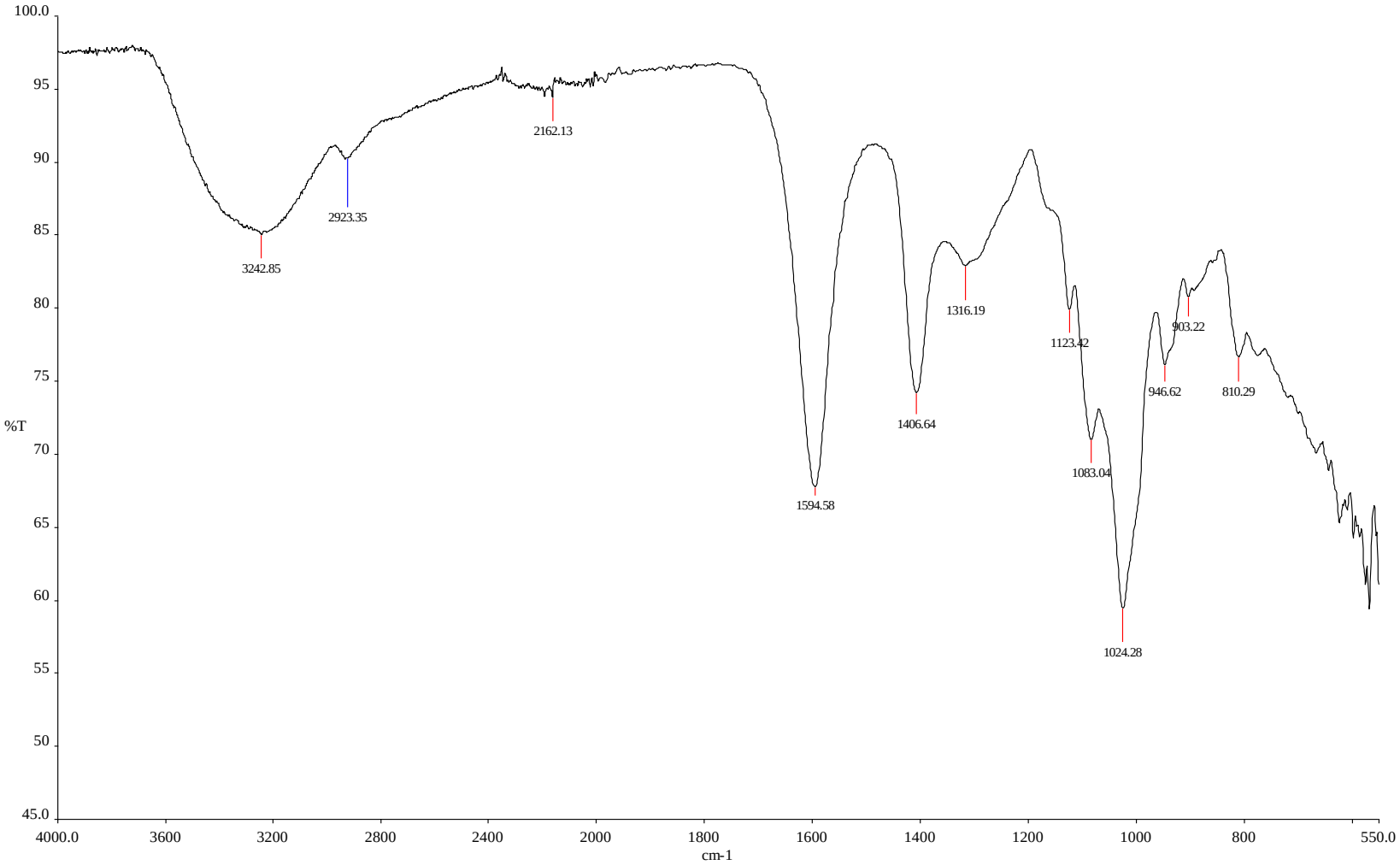

Figure 4.3. FTIR spectrum of SA

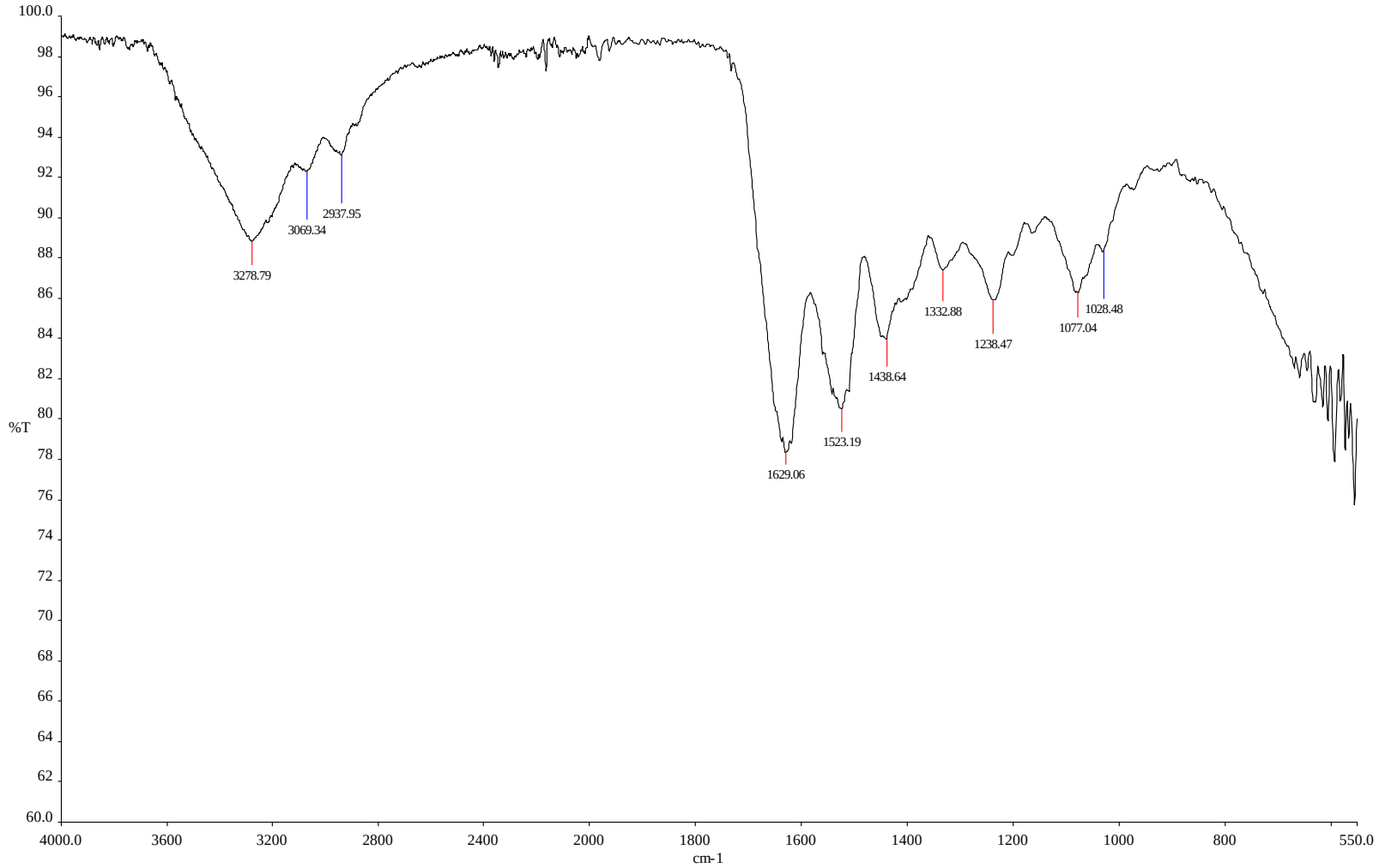

Figure 4.4. FTIR spectrum of gelatin

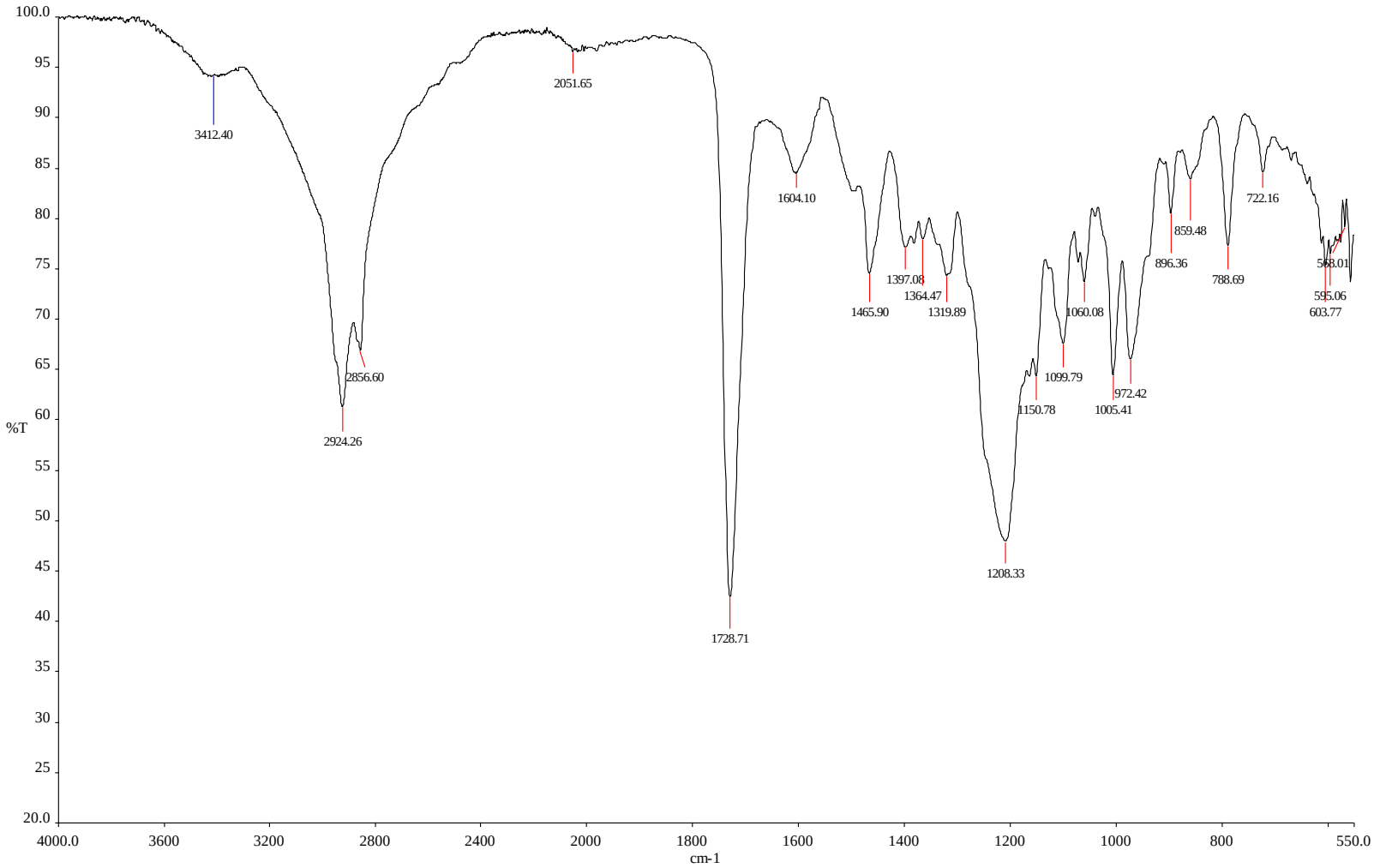

Figure 4.5. FTIR spectrum of CSA-44

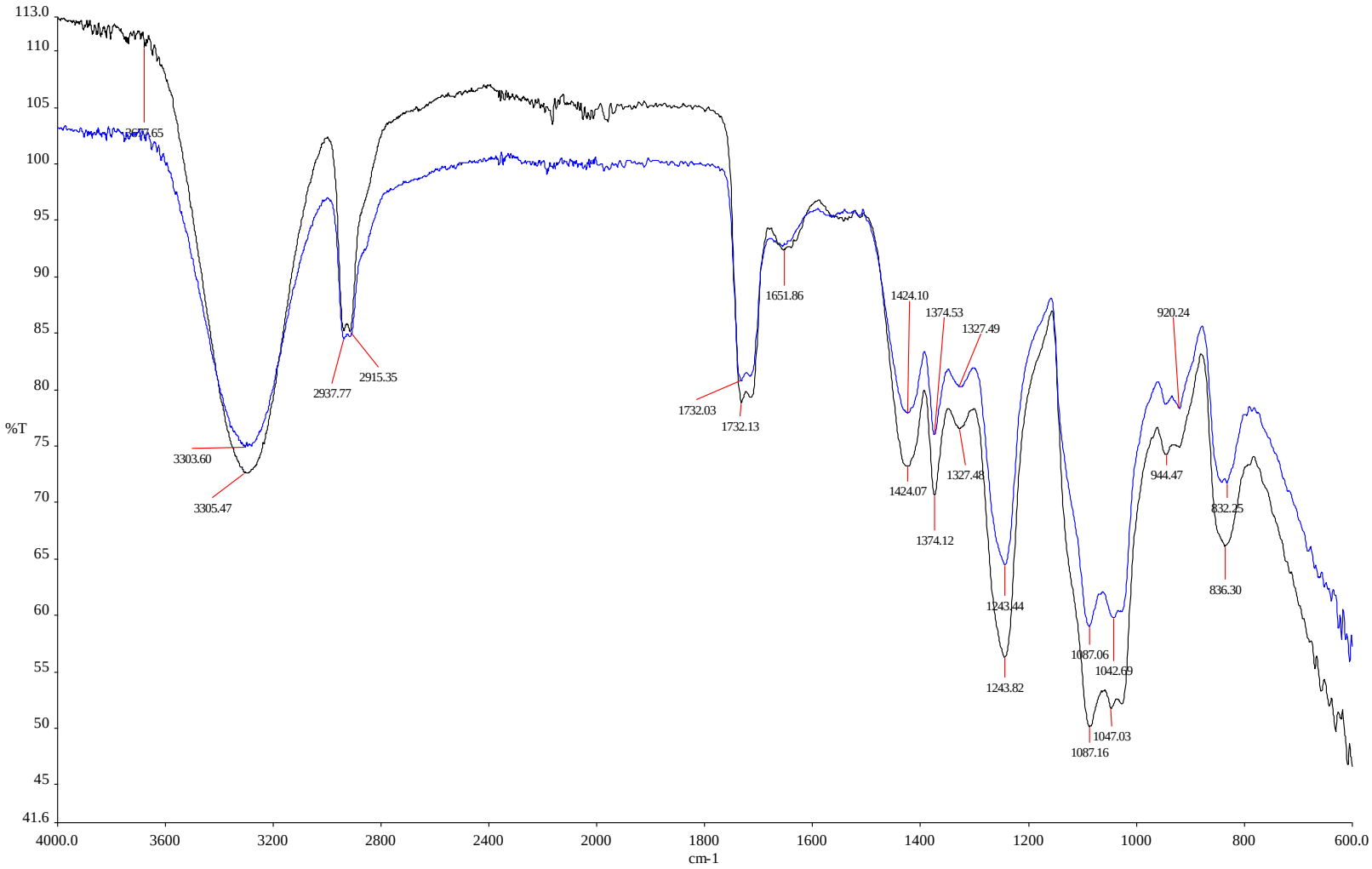

Figure 4.6. FTIR spectra of Noncross-linked PAG hydrogel (black) and noncross-linked PAG-CSA (blue) hydrogels.

In both cross-linked PAG and PAG-CSA (Figure 4.8) hydrogels, a band can be observed at 2867 cm^{-1} of C-H stretching is related to aldehydes from the unreacted GA, a duplet absorption band is attributed to the alkyl chain (symmetric and asymmetric), and by cross-linking PVA with GA, the O-H stretching vibration peak at around 3300 cm^{-1} decreased compared to the non-cross-linked hydrogel. This result suggests that the free hydroxyl groups decreased by forming an acetal group during cross-linking. In addition, the C-O stretching at approximately 1087 cm^{-1} in the non-cross-linked hydrogel is replaced by a broader absorption band at 1095 cm^{-1}, which can be attributed to C-O and the acetal bonds (C-O-C) formed by the cross-linking reaction of PVA with GA (Figure 4.7). Therefore, it can be assumed that PVA was successfully cross-linked with GA (Sapalidis, 2020).

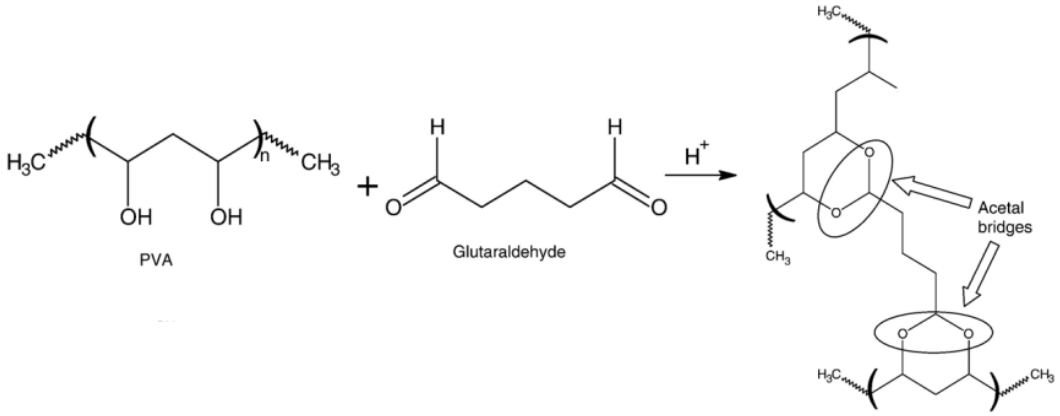

Figure 4.7. The crosslinking of PVA with GA (Sapalidis, 2020)

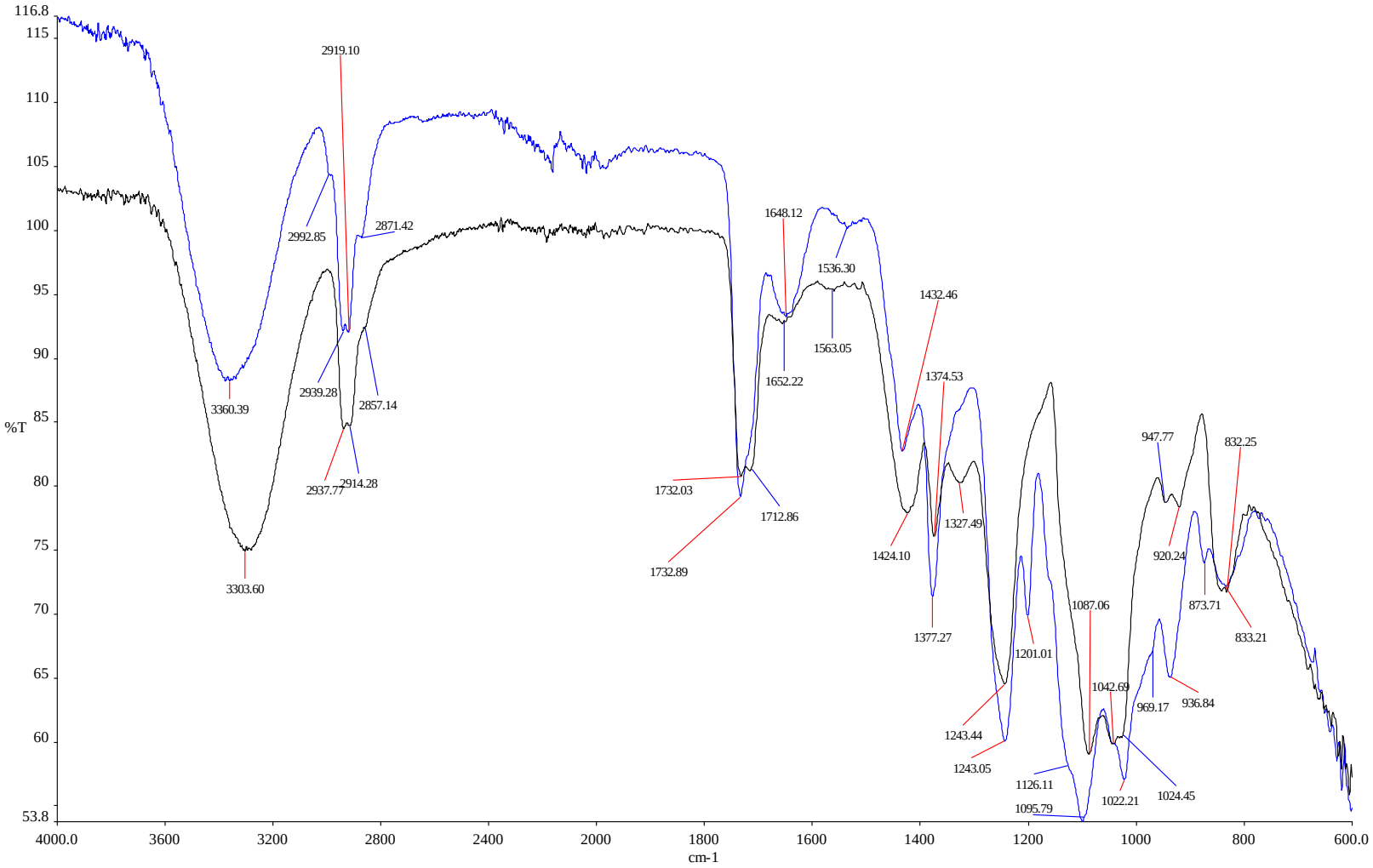

Figure 4.8. FTIR spectra of noncross-linked PAG-CSAhydrogel (black) and cross-linked PAG-CSA (blue) hydrogels

4.2.2. Morphological properties

The SEM photos of the cross-linked PAG, non-crosslinked PAG-CSA and the cross-linked PAG-CSA hydrogels were given in Figure 4.9 and Figure 4.10, respectively. The SEM images clearly showed that all hydrogels (cross-linked PAG and cross-linked and non-cross-linked PAG-CSA) have heterogeneously distributed pores of different sizes. In Figure 4.10 (a-d), the SEM photos of the cross-linked PAG and the non-cross-linked PAG-CSA hydrogel at different magnifications are shown, demonstrating no significant difference between the morphology of the cross-linked PAG and the non-cross-linked PAG-CSA hydrogel. However, the GA cross-linking enormously affected the morphology of PAG-CSA hydrogel, supporting the success of the applied cross-linking procedure (Figure 4.11 a,b). The cross-linked PAG-CSA hydrogel is more porous than the cross-linked PAG hydrogel. The morphological change may be attributed to CSA-44 interacting with the polymer chains of the PAG hydrogel through non-covalent interactions.

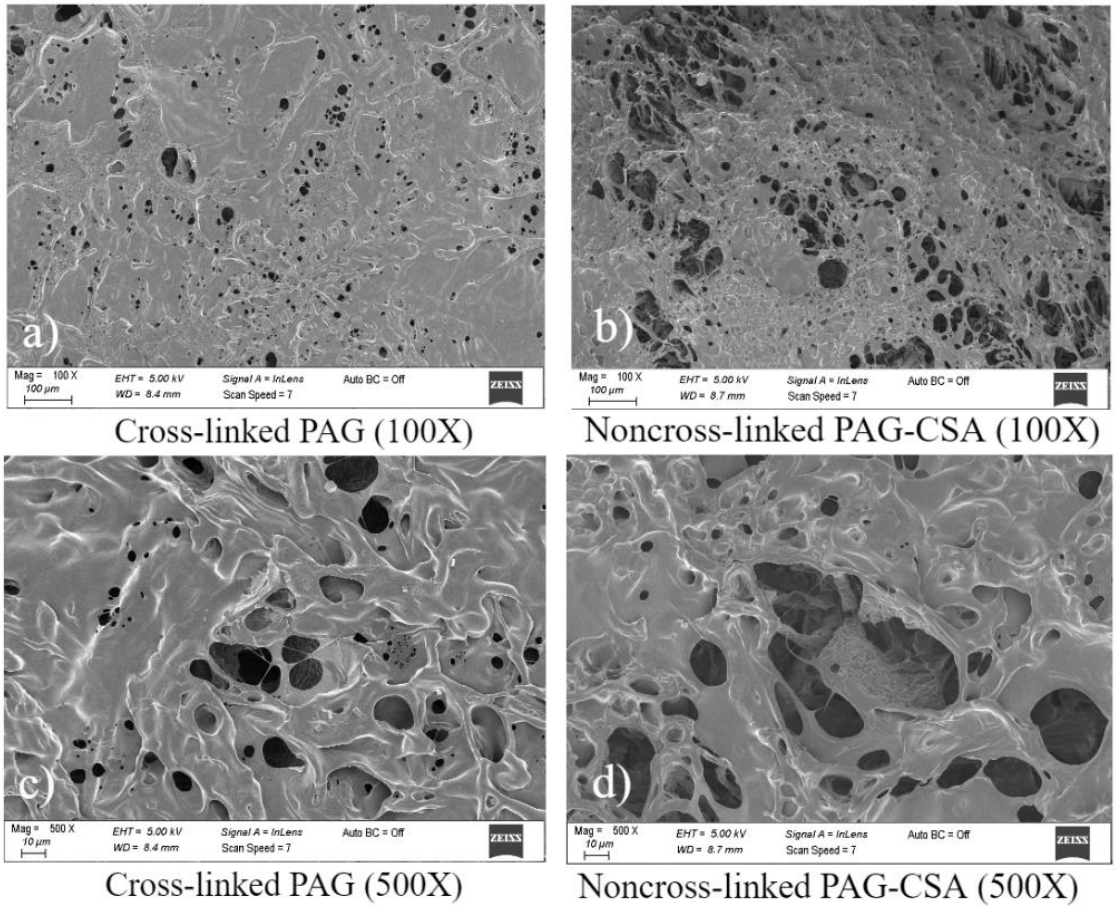

Figure 4.9. SEM images of cross-linked PAG (100X (a) & 500X (c)) and noncross-linked PAG-CSA (100X (b) & 500X (d)) hydrogels

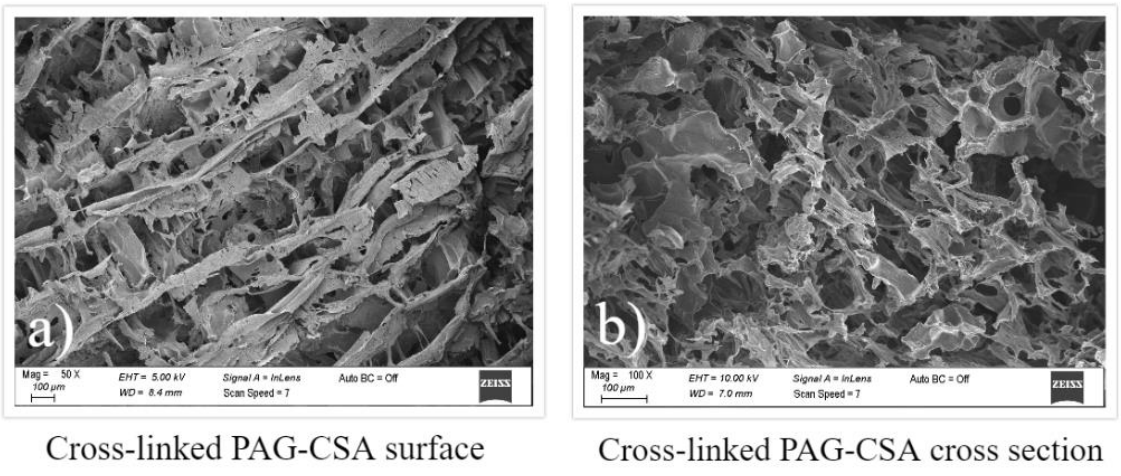

Figure 4.10. SEM images of cross-linked PAG-CSA hydrogel surface (a) and cross-linked PAG-CSA hydrogel cross section (b)

4.2.3. Hyrophilicity of the hydrogel

WCA measurement is used to determine the hydrophilicity of the materials. A WCA higher than 90^o indicates that the material's surface is hydrophobic; thus, the water droplet does not spread on the material's surface. The surface is hydrophilic if the WCA is lower than 90^o (Kim et al., 2009). The WCAs of the cross-linked PAG and PAG-CSA hydrogels were measured. For cross-linked PAG, the WCA was 76.8^o at the first second, and then, it decreased to 31.8^o after eight seconds. The graph representing the changes in the WCAs over time is given in Figure 4.11.

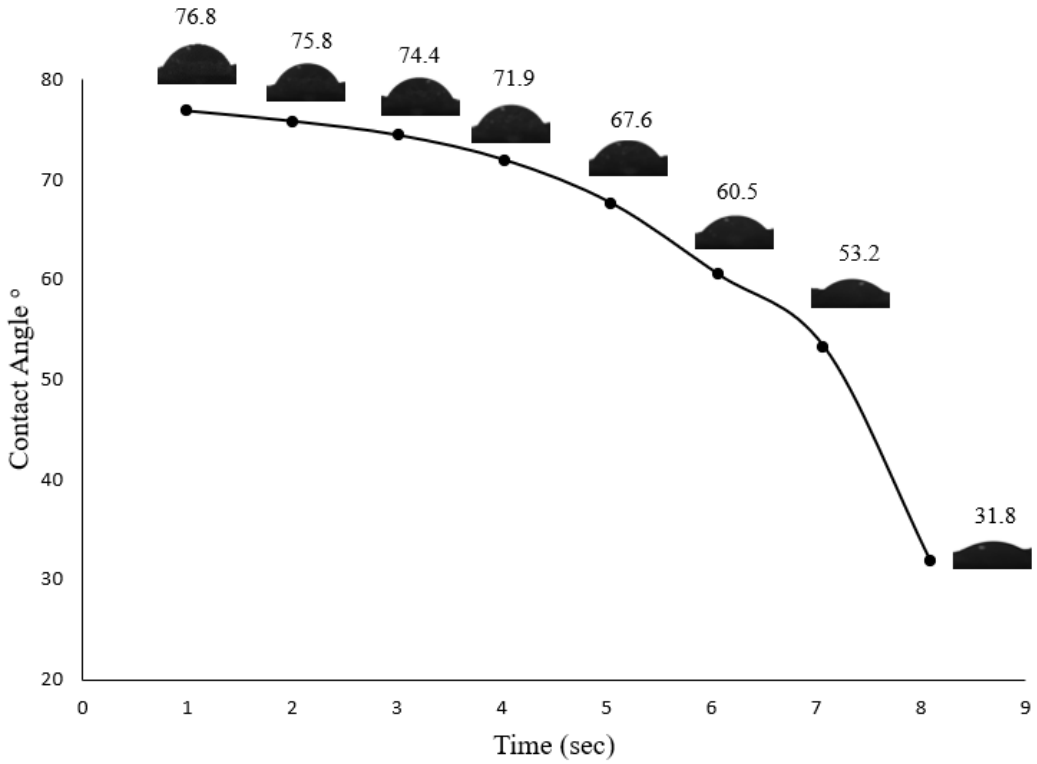

Figure 4.11. PAG-CSA the decrease of contact angle value within 8 seconds

The cross-linked PAG-CSA hydrogel, on the other hand, presented great hydrophilicity. The WCA can not be measured due to the super hydrophobicity of the cross-linked PAG-CSA hydrogel. The water droplet spread over the surface in the first second, probably because of the presence of CSA-44, a hygroscopic compound, and the high porosity of the cross-linked PAG-CSA hydrogel (Figure 4.12).

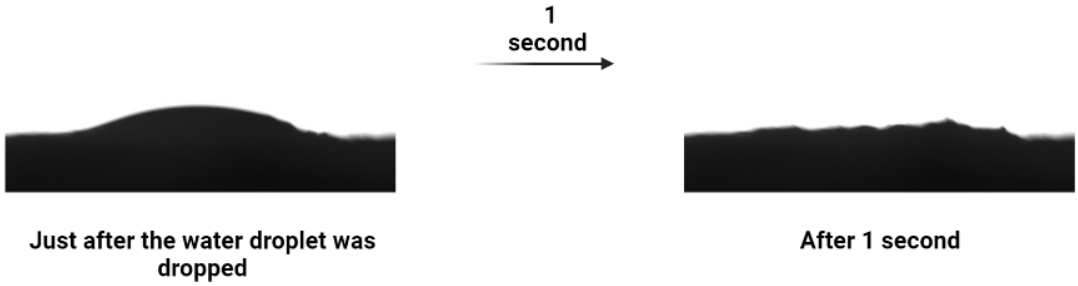

Figure 4.12. PAG-CSA contact angle measurement

Jiang et al. (2019) developed hydrogels composed of different PVA, SA, and Hyaluronic acid (HA) ratios. The hydrogel was prepared by freeze-thawing method and cross-linked using $CaCl_2$. They determined that increasing the PVA amount resulted in a high WCA, while increasing alginate decreased the WCA, which was attributed to the high hydrophilicity of SA. The value of the contact angle ranged from 20o to 50o. It was concluded that adjusting the ratio of PVA and SA can alter the hydrophilicity of the hydrogel to serve the application it is needed for. Kadri et al. (2016) prepared alginate/methacrylated gelatin (GMA) hybrid hydrogels and incorporated them with curcumin-encapsulated nanoliposomes. The WCAs of alginate, G, and their mixture with or without liposomes ranged between 8.7o and 33.4o. Alginate hydrogel had lower WCA (10^o) than GMA (33.4o) due to the hydrogen bonds between the free carboxylic groups and water molecules.

4.2.4. Dehydration and swelling properties of the hydrogels

Rapid dehydration is undesired in wound dressings. Wounds that result in high exudate need wound dressings with a high swelling capacity and quick dehydration rate to avoid maceration (Broussard and Powers, 2013). There was no significant difference between the cross-linked PAG hydrogel and the cross-linked PAG-CSA hydrogel dehydration rates as they completely dried out after around 3 hours (Figure 4.13).

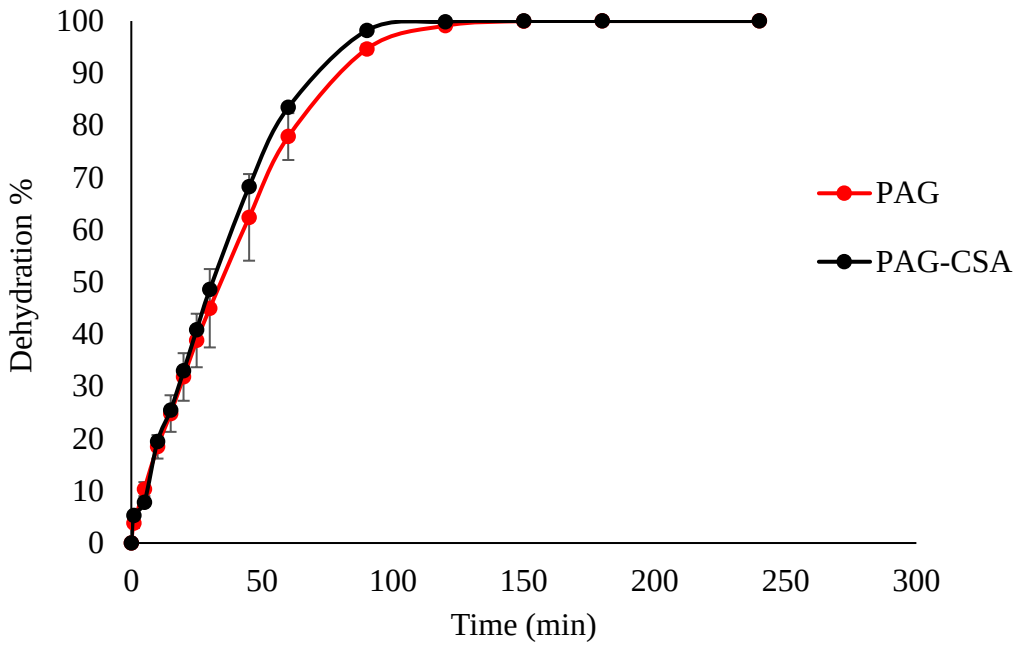

Figure 4.13. Dehydration (%) of PAG and PAG-CSA hydrogels

Tamahkâr (2021) prepared a BC/PVA hydrogel by freeze-thawing method for wound dressing application. A dehydration test was performed, and the results showed that the hydrogel dried after 2 hours. Increasing the number of freezing cycles and PVA ratio has enhanced the water loss of the hydrogel due to the formation of smaller pores. Luo et al. (2016) developed a transparent doxorubicin-loaded nanodiamonds/cellulose nanocomposite membranes by the tape casting method as a wound dressing material. All membranes have reached dehydration equilibrium after 6 hours. Dehydration properties were improved via the incorporation of carboxylated nanodiamonds.

Swelling is one of the most critical parameters in hydrogel production as it helps to keep a moist wound environment which is essential, especially for burn wounds. A moist wound environment provides a better wound healing quality. It reduces pain and scarring, facilitates wound healing by activating collagen synthesis, promotes keratinocyte migration over the wound surface, and supports the presence of nutrients, growth factors, and other healing mediators. Hydrogels can swell up to 10 times their weight. Despite the cross-linking of PAG and PAG-CSA hydrogels, they managed to keep a high swelling ratios, which is a tremendous advantage for wound healing.

The maximum swelling ratio for cross-linked PAG hydrogel was 973.22% ± 18.42 (almost 10 times its weight), which was achieved after 15 minutes of soaking in PBS pH 7.4. For the PAG-CSA, it was found to be 780.48 ± 14.80 after 15 minutes of soaking in PBS pH 7.4 (Figure 4.14). The slight difference can be attributed to the physical cross-link effect of CSA-44.

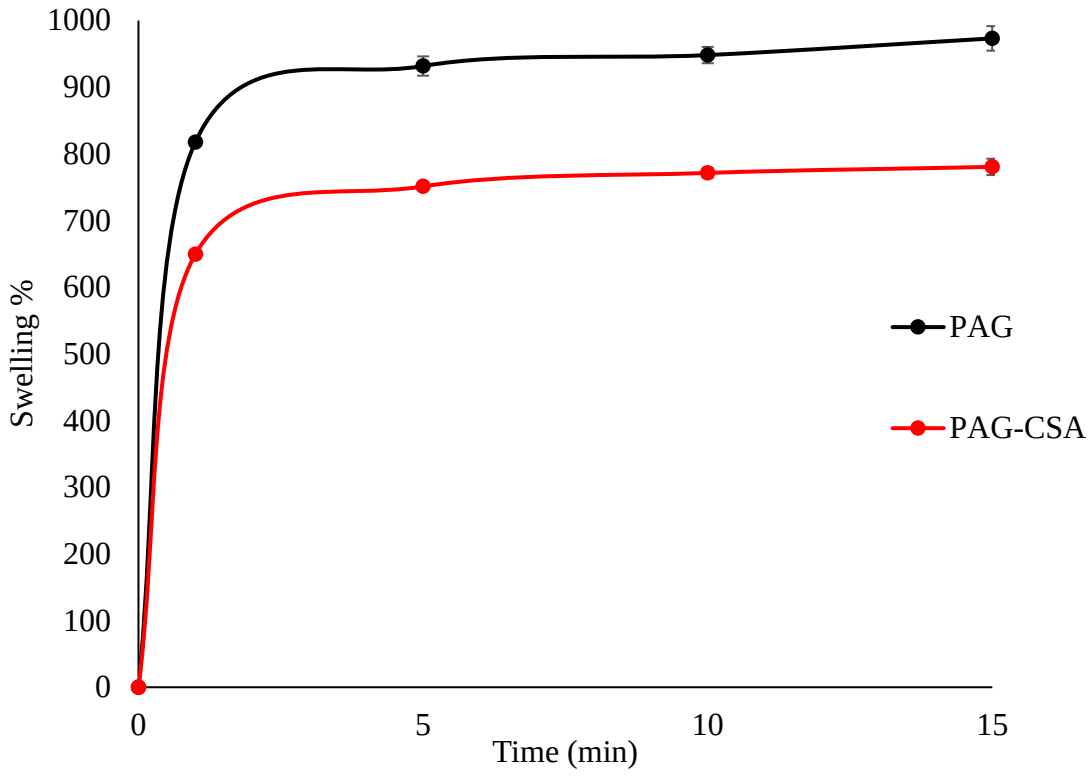

Figure 4.14. Swelling rates of PAG and PAG-CSA

In a study performed for pancreatic differentiation of iPS cells by Kuo et al. (2019), PVA, SA, and G were conjugated with MA and then were photo-cross-linked to prepare PVAMA-SAMA-GMA hydrogels using a water-in-oil self-assembly method. The swelling studies showed that hydrogels containing higher SAMA had higher swelling ratios due to the hydrophilicity of SA polymer. The highest swelling ratio was 500% only due to the compact structure of hydrogel caused by cross-linking.

Satish et al. (2018) designed an SA/G/PVA hydrogel by lyophilization. Triiodothyronine was integrated into the hydrogel to help regenerate the wound's tissue. The hydrogel was cross-linked with 2% $CaCl_2$ solution for 15 h. The swelling test in PBS showed that the

hydrogel incorporated with triiodothyronine had a swelling rate of 750% in 48 h before the degradation started.

4.2.5. Hydrolytic and enzymatic degradation properties

Both hydrogels have shown hydrolytic and enzymatic degradation resistance at the given cross-linking ratio (0.125% GA). After 31 days, the hydrolytic degradation ratios for PAG and PAG-CSA hydrogels were 71.17% ± 0.08 and 61.17% ± 9.31, respectively. In comparison, the enzymatic degradation ratios for PAG and PAG-CSA hydrogels were 72.21 ± 1.22 and 48.16% ± 4.29, respectively. There was a difference between PAG and PAG-CSA hydrogels in both cases, which can be ascribed to the fact that CSA-44 can provide an extra cross-linking for PAG hydrogel (Figure 4.15 and Figure 4.16).

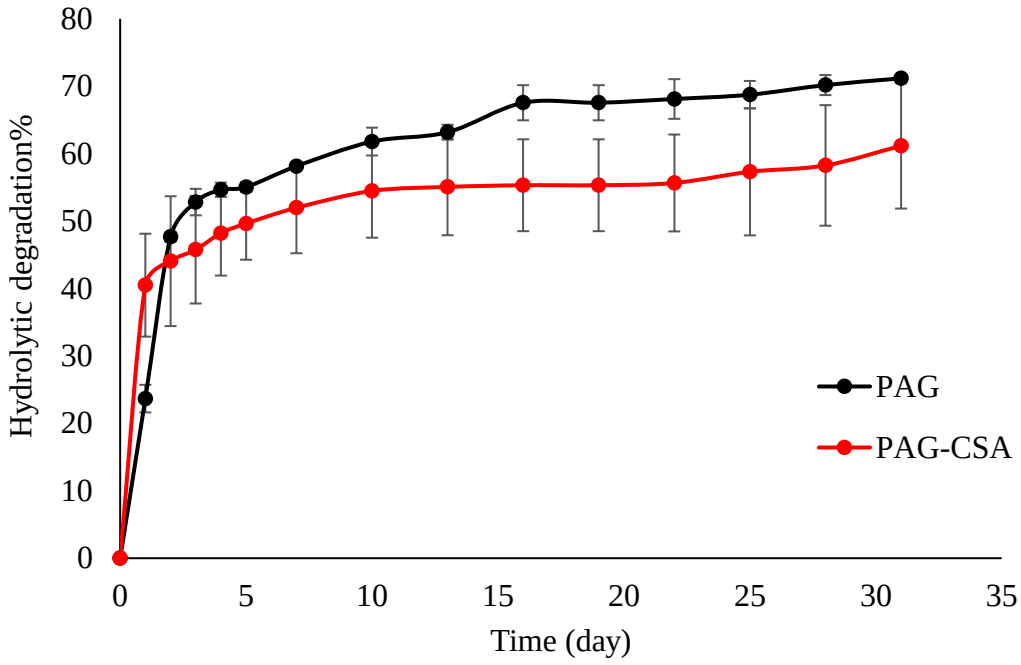

Figure 4.15. Hydrolytic degradation (%) of PAG and PAG-CSA hydrogels

Bahadoran et al. (2020) have developed hydrogels of PVA/SA in different ratios by freeze-thawing method and incorporated it with basic fibroblast growth factor (bFGF)-encapsulated PCL microspheres. Swelling and hydrolytic degradation studies showed that by increasing alginate content the swelling and degradation rate have increased. The hydrogel that had the highest SA ratio had the highest degradation rate of around 50% after 30 days.

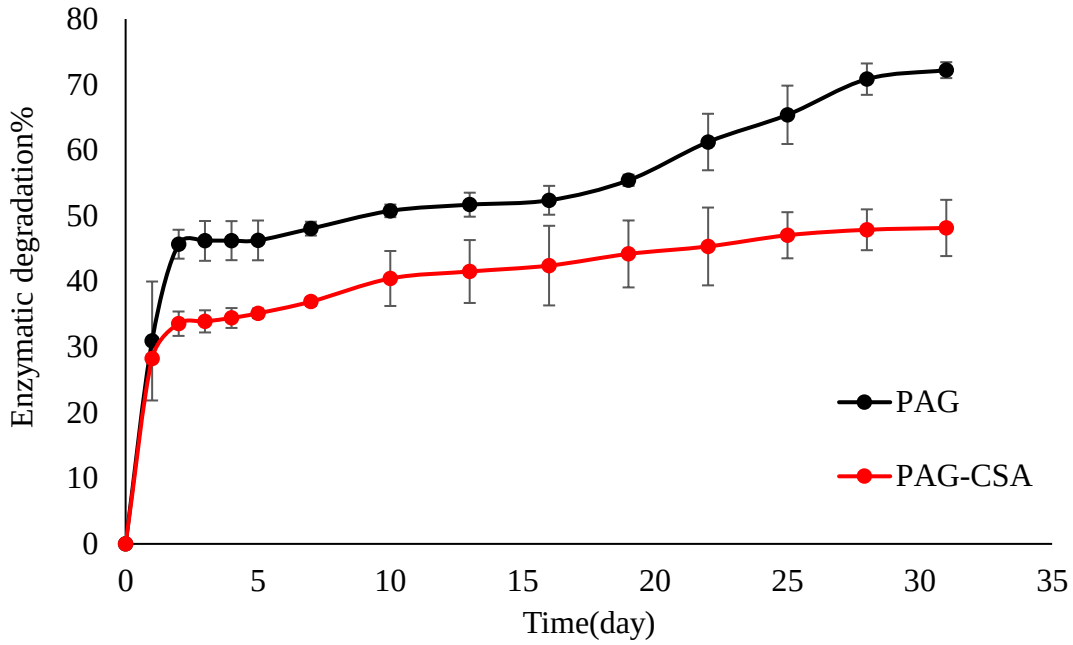

Figure 4.16. Enzymatic degradation (%) of PAG and PAG-CSA hydrogels

CS/ PVA/G freezing-thawed hydrogels incorporated with different concentrations of honey were developed by Shamloo et al. (2020) for wound healing applications. It was concluded from the enzymatic degradation studies in lysozyme solution that the higher the honey concentration was the quicker the degradation of the hydrogel happened. After 7 weeks of time the hydrogel containing no honey has reached a degradation of 40% while the hydrogel that contained the highest honey concentration has reached 50%.

4.2.6. Thickness measurement

The thickness of the wound dressing plays a significant role in defining its air permeability and WVTR. Increasing the thickness of the wound dressing causes a decrease in both WVTR and air permeability. A high value of WVTR could be a reason for wound dehydration and scar formation (Maver et al., 2015; Morgado et al., 2014). Good air permeability can help prevent infections (Li et al., 2019). The thicknesses of cross-linked PAG-CSA and non-cross-linked PAG-CSA hydrogels were 1.664 ± 0.18 mm and 1.559 ± 0.17 mm, respectively. The thickness of the cross-linked PAG-CSA hydrogel provided good WVTR and air permeability results, demonstrating that PAG-CSA can be used as a wound dressing.

4.2.7 Tensile strength

A good indicator of the strength and elasticity of a wound dressing is the tensile strength test, which can be measured by load and elongation at break. A suitable wound dressing material should be stable and flexible. The elastic and flexible dressing can control external stress on the skin (Pandima Devi et al., 2012). The tensile strengths of cross-linked PAG-CSA and PAG hydrogels at maximum elongation were 9.14 ± 2.39 kPa and 9.63± 1.74 kPa, respectively, which can be considered low. It can be concluded that the cross-linked PAG hydrogel elongated for a longer time than the cross-linked PAG-CSA hydrogel before it was broken (Figure 4.17). This result indicates that CSA-44 presence increases the physical fragileness of the hydrogel due to the possible physical cross-linking effect it creates between the hydrogel's polymer chains.

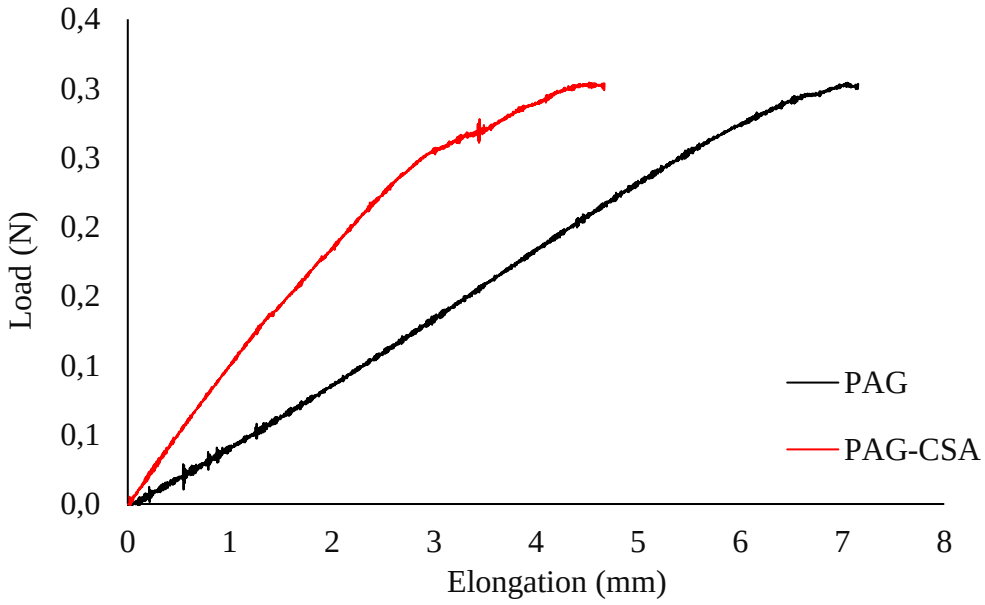

Figure 4.17. Elongation curve of PAG and PAG-CSA

Satish et al. (2018) have developed an SA/G/PVA hydrogel by lyophilization and incorporated it with triiodothyronine for exudate-intensive wound therapy. The tensile strength of the hydrogel was found to be 3 ± 0.2 MPa. Shamloo et al. (2021) developed a CS, PVA, and G (2:1:1) hydrogel containing different concentrations of honey. It was physically cross-linked by freeze-thawing. The ultimate tensile strength of the hydrogel decreased by increasing honey concentration. The hydrogel incorporated with the highest concentration of honey reached a tensile strength of 0.54 ± 0.08 kPa and had the lowest

elastic modulus of 1.3 ± 0.36 kPa. However, the same hydrogel had one of the highest elongations at the breakpoint (46.8 ± 6.2 (%)). It was concluded from these results that the ultimate strain and flexibility of hydrogels were improved by increasing H concentration. Franco et al. (2011) Prepared a bilayered scaffold consisting of an upper layer of electrospun PCL and poly (lacto-co-glycolic acid) and a sublayer of a CS\G lyophilized hydrogel which was cross-linked using (3.5% v/v) GA. The tensile strength of both layers was quite similar as they ranged between 216.7 ± 21.1 and 225.7 ± 33.5 kPa in the dry state while it reduced 9 times after immersing the scaffolds in PBS. Nevertheless, the electrospun nanofiber still had higher tensile strength than lyophilized CS\G hydrogel alone.

4.2.8 Porosity and pore size distribution of the PAG-CSA hydrogel

The porosity of the hydrogel is an essential characteristic as it affects the swelling ability, dehydration, water-vapor and air permeability, cell adhesion, and drug release rate. The pore size is related to the cell type, nevertheless it should be larger than the size of the cell (i.e.,10 µm). However, pore sizes of a few hundred micrometers are also important for excellent cell migration (Pu et al., 2015). The desired porosity value for a wound dressing is (60-90%) (Morgado et al., 2015). Still a porosity of 90% or higher is generally desired to maintain a good cell infiltration. The cross-linked PAG-CSA hydrogel exhibited an 89.55%. The pore size ranged between 20 and 200 µm (Figure 4.18).

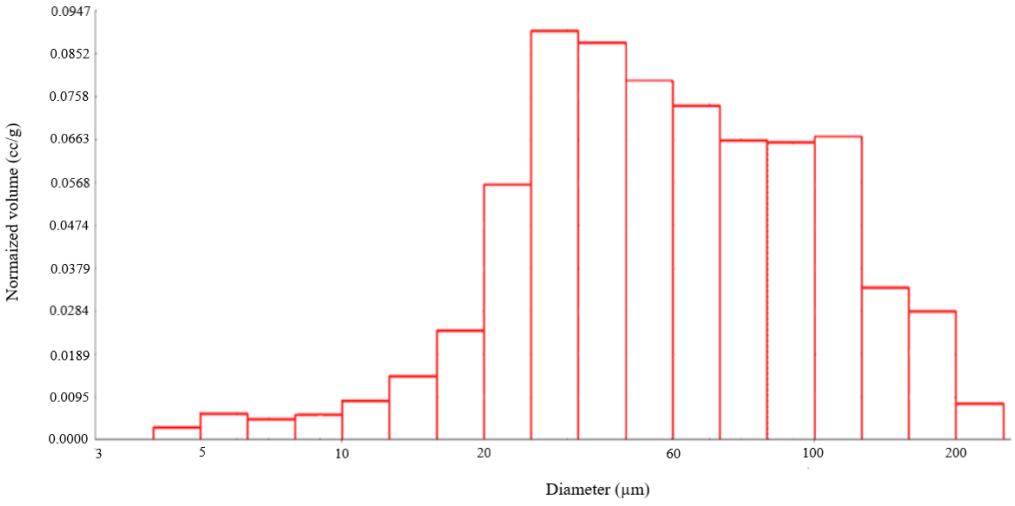

Figure 4.18. Pore size distribution of the PAG-CSA hydrogel

Franco et al. (2011) prepared a bilayer scaffold consisting of an upper layer of electrospun PCL and poly(lacto-co-glycolic acid) and a sublayer of a CS\G lyophilized hydrogel which was cross-linked using (3.5% v/v) GA. The porosity of each material was determined with a mercury porositymeter. The porosity of the lyophilized hydrogel was found to be 97.49% with an average pore diameter of 290 ± 109 micrometer which is considered to be highly porous.

4.2.9 Air permeability and WVTR

An air-permeable wound dressing facilitates oxygen access into the wound site, reducing the wound's susceptibility to infection. The porosity of the plays a significant role in determining the air permeability of wound dressings (Yang and Hu, 2017). Air permeability values of the cross-linked PAG-CSA and cross-linked PAG were 88.24 ± 10.75 $l/m^2/s$ and 50.7 ± 1.69 $l/m^2/s$, respectively. As seen, PAG-CSA had a higher value of air permeability which can be attributed to the presence of CSA-44, which causes a total alteration in the morphology of the hydrogel.

Anjum et al. (2016) developed a wound dressing by coating a piece of cotton fabric with a CS/poly(ethylene glycol) (PEG)/PVP blend. Air permeability tests showed that the cotton fabric alone had an air permeability value of 200 $l/m^2/s$, while after coating it with CS, it significantly decreased to 40.1 $l/m^2/s$. The addition of PEG increased the air permeability to 80.6 $l/m^2/s$, but when a further increase of PEG amount (%50), the air permeability decreased again to 50 $l/m^2/s$. Liu et al. (2012) prepared cellulose acetate (CA)/polyester urethane nanofibrous membranes as wound dressings. Polyhexamethylene biguanide was incorporated into the nanofibers. Increasing the CA ratio in the nanofiber improved the membrane's air permeability because it provided the structure with more pores. The permeability of the electrospun mats was between 5 and 40 $l/m^2/s$. Uppal et al. (2011) prepared electrospun HA and tested its air permeability. They compared the HA nanofiber with gauze with vaseline and found that the HA nanofiber had an air permeability value of 504.7 $l/m^2/s$ which was way higher than the vaseline gauze was 89 $l/m^2/s$.

As mentioned previously, a high value of WVTR could be a reason for wound dehydration and scar production, while a low WVTR value may not provide enough moisture for wound healing. The WVTR value of PAG-CSA hydrogel was 905.41 ± 35.38 g/m^2/d, a good value compared to some commercial wound dressings (Table 4.3). Consequently, it can be said that the WVTR value of PAG-CSA hydrogel is enough to retain a moisture environment for the wound to heal (Gharibi et al., 2018).

Table 4.3. Some commercial wound dressings and their WVTR values (Gharibi et al., 2018)

Wound dressing	**WVTR (g/m^2/d)**
Op Site (Smith & Nephew)	792 ± 32
Metoderm (ConvaTec Ltd)	823 ± 45
Duoderm (ConvaTec Ltd)	886 ± 60
Biobrain®	1565 ± 51

4.3 CSA-44 release from the cross-linked PAG-CSA hydrogel

Conventional drugs used to be pills or capsules that released the drug instantly when it interacted with water. It wasn't possible to control this instant release of the drug until 1952 when Smith Klein Beecham came up with the first controlled drug release system, Spansule technology, which lasted for 12 h (Lee and li, 2010). Over the years, new and various controlled drug delivery systems were developed and given different names, with slight distinctions from each other. Between the 1950 and 1980s, the basics of drug release mechanisms were understood. Back then, drug release mechanisms used were dissolution and controlled diffusion, which were the most famous, in addition to osmosis-based and ion-exchange-based systems. The techniques used at that time were more focused on oral and transdermal delivery. From 1980 to 2010, the developed drug delivery systems were less successful based on clinical products produced due to their incapability to overcome biological barriers. The studies in this period focused more on targeted delivery, and more complicated and smart delivery systems were used (nanoparticles, smart polymers, and hydrogels). The current approach aims to produce strategies to overcome physicochemical and biological barriers. All recent studies aim to create

delivery systems that deliver poorly water-soluble drugs, peptides, proteins, and nucleic acids to specific targets without toxic effects (Yun et al., 2015).

The primary purpose of developing drug delivery systems is to release the drug sufficiently at an appointed time to a specific target site. Drug delivery systems are needed because many drugs have poor solubility in physiological fluids and can't get through bio-barriers (Vijaya Shanti and Mrudula, 2011). Conventional methods, such as capsules or pills, often have negative impacts due to their random distribution and uncontrolled drug release (Liu et al., 2016). Drug release systems aim to increase drug solubility and patient compliance and decrease the side effects and toxicity of the drug. Nowadays, many drug delivery systems have been developed and used to deliver existing drugs to a specified target instead of developing new drugs. (Laffleur and Keckeis, 2020).

One of the novel drug delivery systems is hydrogels. The uniqueness of hydrogels is attributed to their similitude to the living tissue and their ability to swell. Hydrogels can also respond to different stimuli by a change in volume or by incorporating specific detectors (Lee et al., 2013; Vashist et al., 2014). The high porosity of hydrogels that could be easily controlled by a cross-linking method facilitated the incorporation of drugs. Hydrogels are good candidates for obtaining a sustained drug release due to these properties. Drugs incorporated into hydrogels are released in different mechanisms: diffusion-controlled, swelling-controlled, chemically controlled, and environmentally responsive release (Hoare and Kohane, 2008).

Diffusion-controlled drug delivery systems grant the drug to be released through the hydrogel's matrix and can be explained in reservoir or matrix models (Figure 4.19). The reservoir delivery system consists of a drug incorporated into a core-shell surrounded by a hydrogel membrane layer. Due to the high drug concentration in the core, a sustained drug release is obtained. In a matrix system, the drug is homogeneously distributed throughout the hydrogel matrix. The drug is released via the macropores of the hydrogel (Caló and Khutoryanskiy, 2015).

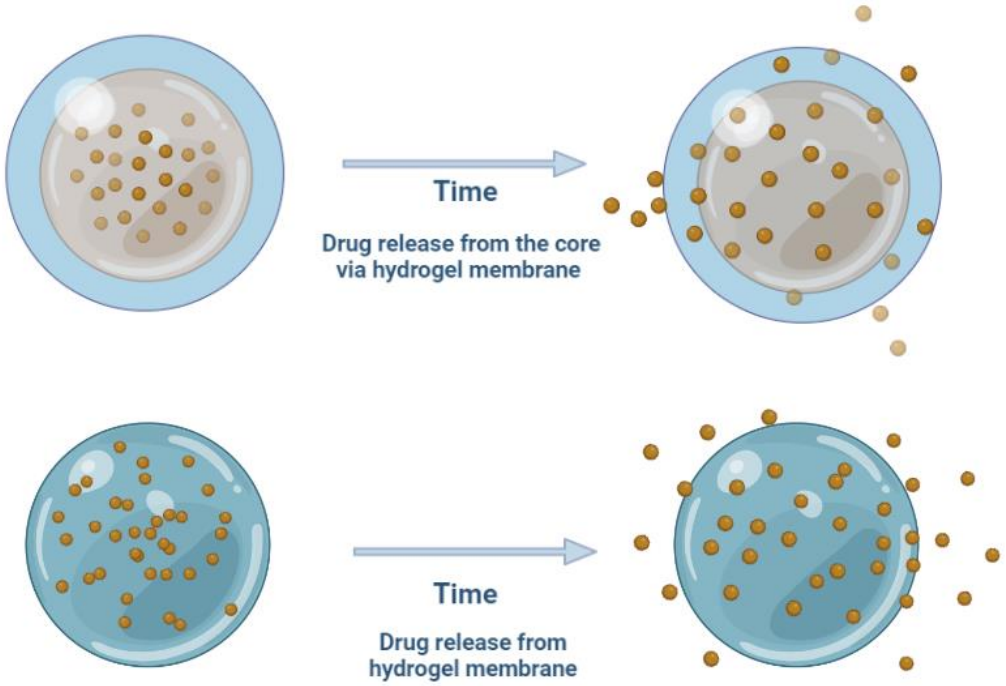

Figure 4.19. Diffusion controlled drug delivery systems

In swelling-controlled systems, the drug distributed within the hydrogel matrix gets released when the hydrogel meets physiological fluids and swells. Due to swelling, the polymer chains loosen, and the hydrogel expands, allowing the drug diffusion of the hydrogel matrix. The drug release is constant and time-independent in these systems (Caló and Khutoryanskiy, 2015).

Mathematical models were developed to understand drug release processes thoroughly. This understanding is vital in developing and enhancing the design of drug release systems. When novel model approaches were compared, it was found that the most used ones were drug-release fitting models. From those models, the most used equations appear to be: zero-order, first-order Higuchi's, Peppas', Hixon-Crowell's, and other equations (Figure 4.20) (Caccavo, 2019).

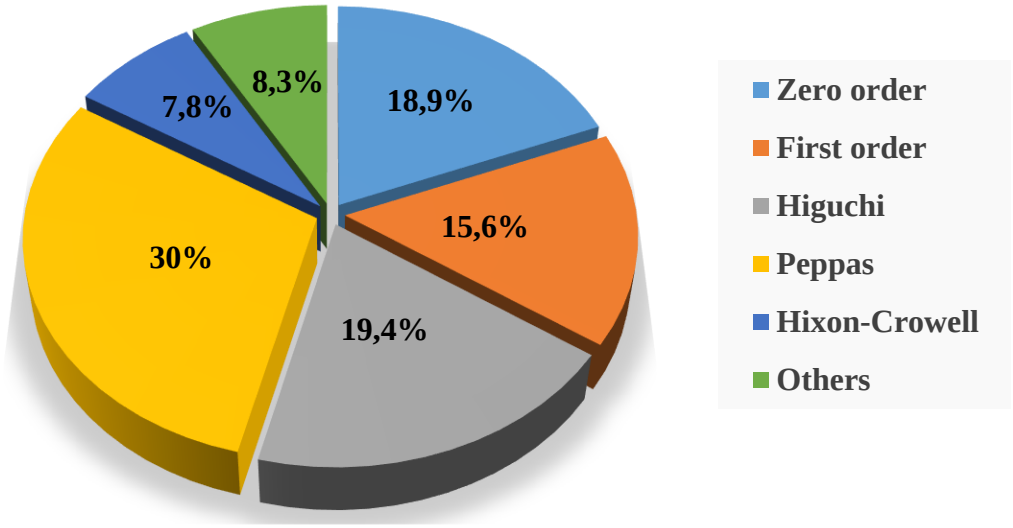

Figure 4.20. Most used mathematical models for drug release systems

Zero order model model describes some drug release systems that aim for a specific target and time course, like coated low-soluble drugs and osmotic systems. This model can be represented by Equation 4.1

$$Q_t = Q_0 + K_0 t \qquad (4.1)$$

Q_t is the amount of drug dissolved in a specific time t, Q_0 is the initial amount of drug in the solution, and K_0 is the zero-order release constant expressed in units of concentration/time (Dash et al., 2010).

First order model explains the drug release systems impacted by the drug concentration. This model can be described by Equation 4.2.

$$\log Q_t = \log Q_0 + \frac{k_1 t}{2.303} \qquad (4.2)$$

Where Q_0 is the initial concentration of the drug and Q_t is the concentration of the drug in solution at time t (Bruschi, 2015).

Higuchi mathematical model was introduced in 1963 to describe drug release from a matrix system. This model aims to study drug release for drugs soluble in water or low solubility from the solid or semisolid matrix. This model can be represented by Equation 4.3.

$$Q = K_H t^{1/2} \qquad (4.3)$$

The slope of the plot of the cumulative drug release rate (Q) versus the square root of time represents the Higuchi dissolution constant (K_H). The main advantages of using this equation are that it eases the drug-loaded system's optimization and helps recognize the drug release mechanism (Higuchi, 1963).

Korsmeyer - Peppas model is the most used. This equation has described the drug release mechanism from polymeric systems. Ritger and Peppas and Korsmeyer and Peppas developed an equation to investigate swelling and non-swelling polymeric systems by determining whether the system follows Fickian or Non-Fickian diffusion. This model can be represented by Equation 4.4.

$$\frac{M_t}{M_a} = K_{KP} t^n \qquad (4.4)$$

The model graph can be obtained by plotting the cumulative drug release rate log versus the time log. Where Mt/Mα is the fraction of drug released at time t, k is the rate constant including structural and geometric characteristics of the delivery system, and n is the release exponent indicative of the drug transport mechanism through the polymer. The n value is used to characterize different release mechanisms (Table 4.4) (Paarakh et al., 2018; Dash et al., 2010).

Table 4.4. Release mechanism based on n value (Paarakh et al., 2018; Dash et al., 2010)

Release exponent (n)	Drug transport mechanism	Rate as a function of time	Drug release mechanism
n < 0.5	Quasi-Fickian diffussion	t^{n}	Non swellable matrix-diffusion
0.5	Fickian diffusion	$t^{0.5}$	
0.5 < n < 1.0	Anomalous (Non - fickian transport)	t^{n-1}	For both diffusion and relaxation (erosion)
1.0	Case II transport	(Time-independent)	Zero order release
Higher than 1.0	Super case II transport	t^{n-1}	Relaxation/erosion

Fickian diffusional release (Case I) happens due to a potential chemical gradient (diffusion). In the Fickian system, the diffusion rate is higher than the polymer relaxation rate and depends on time. Non-Fickian mechanism (Case II) relates to the polymer chains' relaxation and their swelling in biological fluids (Ambekar and Kandasubramanian, 2019).

Hixson-Crowell model describes systems that do not undergo any geometrical change, but only the surface area of the particles or tablets change, and then dissolution occurs. This model is suitable only when the drug release occurs due to dissolution and not diffusion. When the fraction of the unreleased drug is plotted against time, a linear line should be formed if the drug release mechanism obeys the Hixson-Crowell model (Dash et al., 2010). This model can be represented by Equation 4.5.

$$Q_0^{1/3} - Q_t^{1/3} = K_{HC}\, t \qquad (4.5)$$

The cumulative realease graph was plotted using the slope equation in the calibration graph (Figure 4.21). From the cumulative release graph (Figure 4.22) we can see that a burst release of around 23% of CSA-44 was achieved within 480 minutes (8 hours). After

that the realease had gradually increased to reach a plateau after 7 days. The ratio of the drug release are shown in Table 4.4.

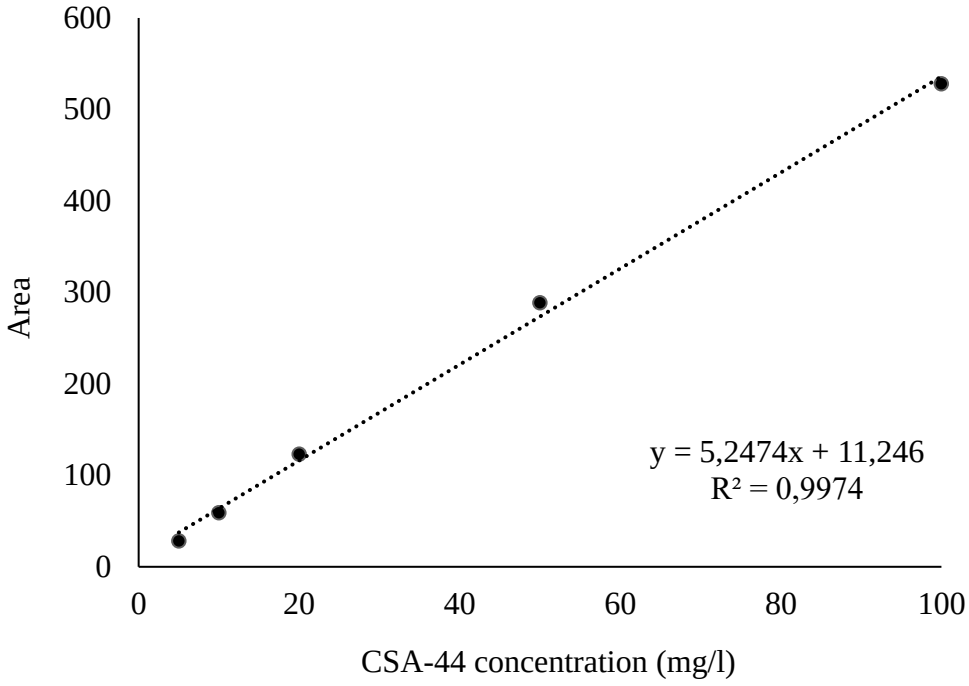

Figure 4.21. CSA-44 calibration graph

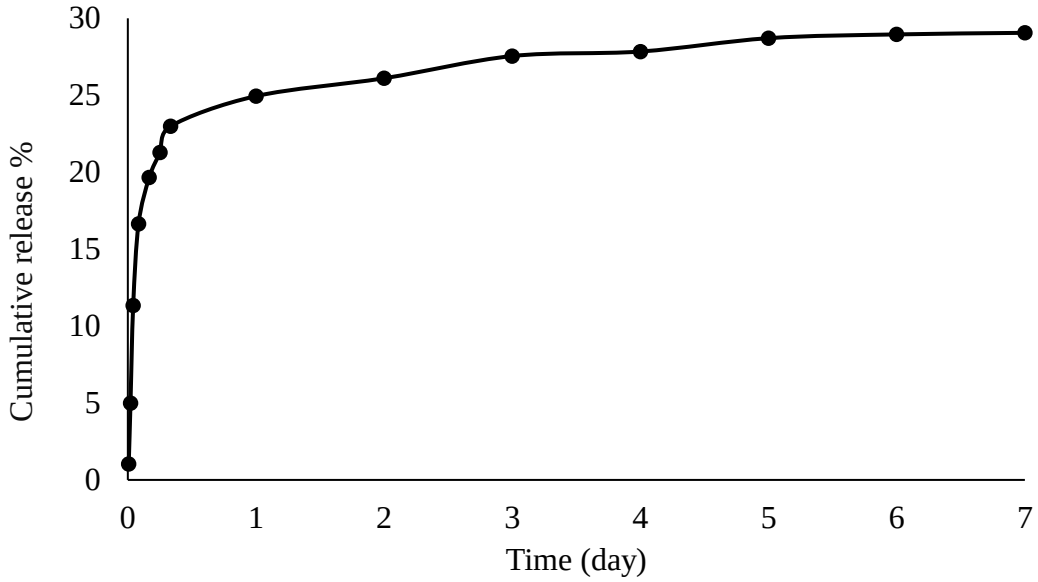

Figure 4.22. Cumulative release (%) of CSA-44 from cross-linked PAG-CSA hydrogel

Table 4.4. The cumulative release (%) of CSA-44

Time equivalent	Time (min)	Cumulative release (%)
	10	1.04
	30	4.98
1 h	60	11.34
2h	120	16.63
4h	240	19.65
6h	360	21.28
8h	480	22.98
1 day	1440	24.94
2 days	2880	26.10
3 days	4320	27.55
4 days	5760	27.84
5 days	7200	28.71
6 days	8640	28.95
7 days	10080	29.05

After applying these values on the drug release fitting models (Figure 4.23), CSA-44 release from PAG-CSA hydrogel has appeared to follow Korsmeyer-Peppas model. It was found to follow non-fickian distribution as 0.5 < n < 1 (n=0.61) which means that the drug release is swelling and degradation controlled (Table 4.5).

Table 4.5. CSA-44 release parameter from PAG-CSA hydrogel

Models		(%0,25 GA, 20 min)
Zero order $Q_t = Q_o + K_o$	**Equation**	y = 0.0018x + 15.429
	R^2	0.4976
	K_o (min^{-1})	0.0018
	Q_o (%)	15.429
	Qe	≈ 29
First order $logQ_t = logQ_o + \frac{K_1 t}{2{,}303}$	**Equation**	y = 0.000057x + 1.049256
	R^2	0.25300
	K_1(min^{-1})	0.00013
	Q_o (%)	11.201
	Qe	≈ 29
Higuchi $Q_t = K_H . t^{1/2}$	**Equation**	y = 0.2117x + 11.791
	R^2	0.67
	K_H(min$^{-1/2}$)	0.2117
Korsmeyer-Peppas $log\frac{Q_t}{Q_\infty} = logK_{KP} + nlogt$	**Denklem**	y = 0,2742x + 1,4873
	R^2	0.8117
	K_{KP}(min^{-1})	1.8159
	n	0.6103

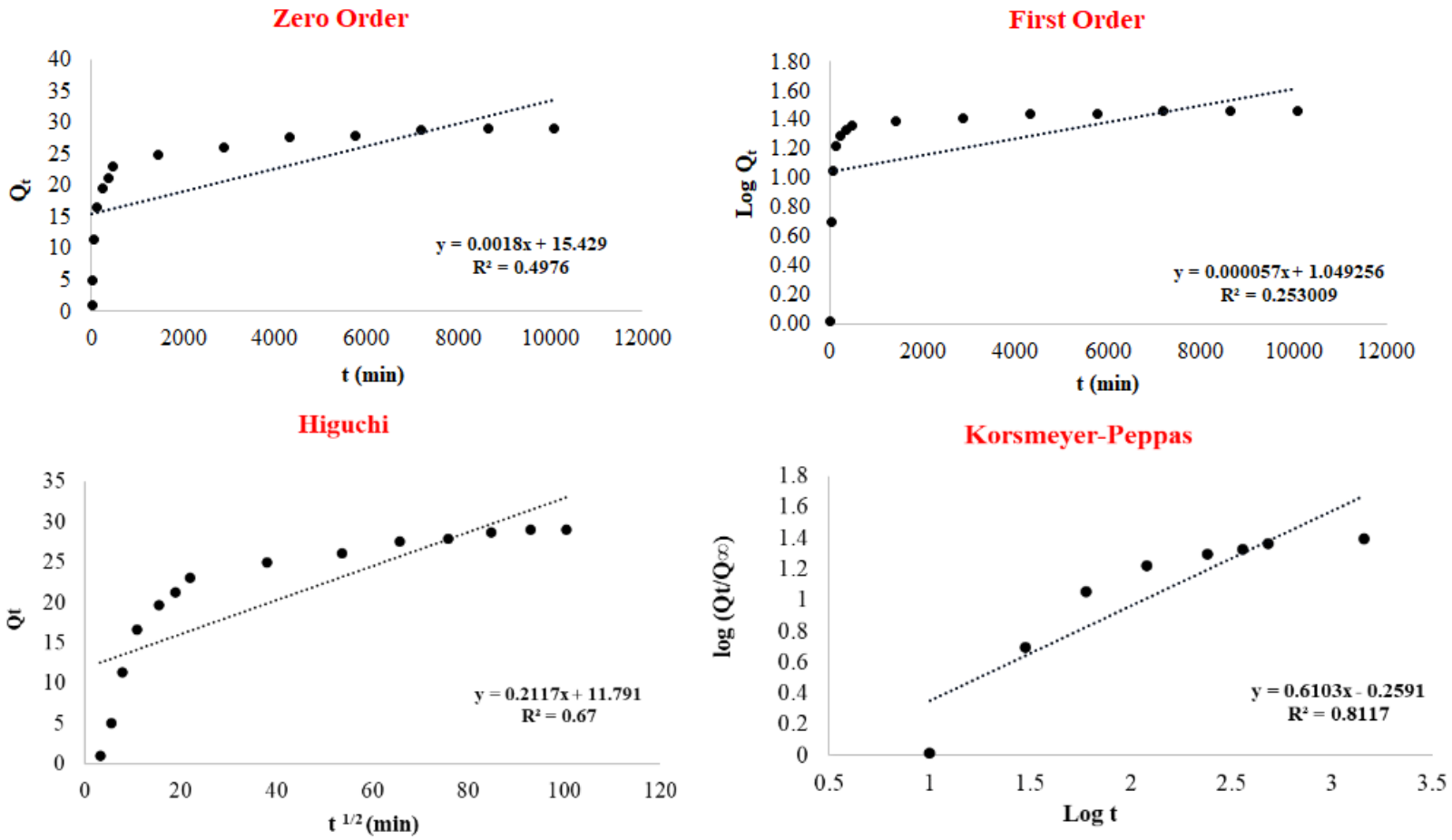

Figure 4.23. Graphs of release patterns of CSA-44 release from cross-linked PAG-CSA hydrogel

5. CONCLUSION

In this study, a PAG hydrogel was prepared in the ratio 2:1:3 (PVA:SA:G) respectively and was incorporated with %1.77 (w/w) CSA-44 to prepare lyophilized PAG-CSA hydrogel. The synthesized hydrogel mixture was poured into proper casts and lyophilized to reach the needed hydrogel structure with optimal characteristics. This study's final product was a hydrogel that can release CSA-44 which is a ceragenin. The hydrogel was further tested and characterized as follows:

- PVA:SA:G ratio for PAG-CSA hydrogel was determined as 2:1:3 and PAG and PAG-CSA hydrogels were prepared via lyophilization.
- Both the PAG and the PAG-CSA hydrogel were synthesized and characterized by the FTIR technique before and after cross-linking with 0.125% GA for 20 minutes.
- SEM images of the cross-linked PAG, non-crosslinked PAG-CSA, and cross-linked PAG-CSA hydrogels were used to characterize and show the structural differences between the hydrogels. SEM imaging confirmed the highly porous structure of the hydrogels and the contribution of both CSA-44 and cross-linking in altering the structure.
- The WCA was measured for both cross-linked PAG and PAG-CSA hydrogels. The WCA of PAG hydrogel dropped from 76.8 ^{o} to 31.8 ^{o} within 8 s, while PAG-CSA hydrogel absorbed the water droplet immediately after a second. These results indicated the high hydrophilicity of both PAG and PAG-CSA hydrogels and demonstrated the hygroscopic nature of CSA-44.
- The dehydration and swelling properties of the cross-linked PAG and PAG-CSA hydrogels were tested. Dehydration test results of the cross-linked PAG and PAG-CSA hydrogels showed insignificant difference caused by incorporation of CSA-44 into the hydrogel as they completely dried out within 3 h. However, swelling studies' results showed that the maximum swelling ratio of PAG hydrogel was 973.22% ± 18.42 while a percentage of 780.48% ± 14.80 was obtained for PAG-CSA hydrogel. This difference can be linked to the physical cross-link effect of CSA-44 that tightens the structure of the hydrogel, as was also observed in SEM

images. These results indicated that both PAG and PAG-CSA hydrogels can remarkably absorb wound exudates.

- The cross-linked PAG and PAG-CSA hydrogels were tested for hydrolytic and enzymatic degradation for a month. The hydrolytic degradation ratio for PAG hydrogel was 71.17% ± 0.08, while for PAG-CSA hydrogel, it was 61.17% ± 9.3. Enzymatic degradation ratios were 72.21 ± 1.22 and 48.16% ± 4.29 for PAG and PAG-CSA hydrogel, respectively. These results indicated that both hydrogels resist degradation at 0.125% GA cross-linking ratio and can be used for prolonged periods.
- The thickness of PAG-CSA hydrogel before and after cross-linking was determined as 1.664 ± 0.18 mm and 1.559 ± 0.17 mm, respectively. The thickness of PAG-CSA hydrogel is suitable for wound dressing purposes.
- A tensile test was performed for cross-linked PAG and PAG-CSA hydrogels. The tensile strengths of cross-linked PAG-CSA and PAG hydrogels at maximum elongation were 9.14 ± 2.39 kPa and 9.63± 1.74 kPa, respectively, indicating the fragile nature of the hydrogels. PAG hydrogel elongated for a bit longer than PAG-CSA hydrogel before it was broken. These results suggested that the incorporation of CSA-44 increased the fragileness of the hydrogel.
- Porosity and pore size distribution measurements were performed for the cross-linked PAG-CSA hydrogel. It exhibited a porosity of 89.55%, an excellent value for wound dressings, while the most abundant pore sizes ranged between 20 and 200 μm.
- Air permeability values for cross-linked PAG and PAG-CSA hydrogel were measured as 88.24 ± 10.75 $l/m^2/s$ and 50.7 ± 1.69 $l/m^2/s$, respectively. The difference between the values can be due to the structure alteration caused by the incorporation of CSA-44. WVTR test was performed for cross-linked PAG-CSA and exhibited a value of 905.41 ± 35.38 $g/m^2/d$, which was good enough compared to some commercial wound dressings. Air permeability and WVTR test values showed that the hydrogel could retain water without causing dehydration of the wound bed and could facilitate the gas exchange.
- CSA-44 release from PAG-CSA hydrogel was studied as the final step of this work. The results showed that a burst release of 23% of the CSA-44 was achieved

within the first 8 hours, which then increased gradually to reach a plateau after 7 days (29.05%). The release data fitted the Korsmeyer-Peppas model with a non-Fickian distribution (0.61). These results indicated that the swelling and degradation of PAG-CSA hydrogel mainly control CSA-44 release.

- The results obtained in this study showed that drug release can be controlled by altering cross-linking ratio and time, causing a change in the degradation rate and affect the swelling ability of PAG-CSA hydrogel.
- Finally, the prepared PAG-CSA hydrogel exhibited great potential to be used as a burn wound dressing. It has excellent water retention ability, good gas permeability, ideal porosity, and the ability to perform a controlled drug release. Further studies and characterizations will be performed on PAG-CSA hydrogel to determine its antibacterial effect, biocompatibility, and in vivo wound healing studies.

REFERENCES

A., Galiano, R. D., & Tomic-Canic, M. (2005). Molecular pathogenesis of chronic wounds: the role of β-catenin and c-myc in the inhibition of epithelialization and wound healing. The American journal of pathology, 167(1), 59-69. https://doi.org/10.1016/S0002-9440(10)62953-7

Ahmed, E. M. (2015). Hydrogel: Preparation, characterization, and applications: A review. Journal of advanced research, 6(2), 105-121. https://doi.org/10.1016/j.jare.2013.07.006

Alonso, J. E., Lee, J., Burgess, A. R., & Browner, B. D. (1996). The management of complex orthopedic injuries. Surgical Clinics of North America, 76(4), 879-903. https://doi.org/10.1016/S0039-6109(05)70486-2

Ambekar, R. S., & Kandasubramanian, B. (2019). Advancements in nanofibers for wound dressing: A review. European Polymer Journal, 117, 304-336. https://doi.org/10.1016/j.eurpolymj.2019.05.020

Andreu, V., Mendoza, G., Arruebo, M., & Irusta, S. (2015). Smart dressings based on nanostructured fibers containing natural origin antimicrobial, anti-inflammatory, and regenerative compounds. Materials, 8(8), 5154-5193. https://doi.org/10.3390/ma8085154

Anjum, Sadiya, Abha Arora, M. S. Alam, and Bhuvanesh Gupta. "Development of antimicrobial and scar preventive chitosan hydrogel wound dressings." *International journal of pharmaceutics* 508, no. 1-2 (2016): 92-101. https://doi.org/10.1016/j.ijpharm.2016.05.013

Atiyeh, B. S., Dibo, S. A., & Hayek, S. N. (2009). Wound cleansing, topical antiseptics and wound healing. International wound journal, 6(6), 420-430. https://doi.org/10.1111/j.1742-481X.2009.00639.x

Baek R. M., Heo C. Y., Choe J. & Lee, J. H. (2006). Wound healing effect of silk fibroin/alginate-blended sponge in full thickness skin defect of rat. Journal of Materials Science: Materials in Medicine, 17(6), 547-552. https://doi.org/10.1007/s10856-006-8938-y

Bahadar, H., Maqbool, F., Niaz, K., & Abdollahi, M. (2016). Toxicity of nanoparticles and an overview of current experimental models. Iranian biomedical journal, 20(1), 1. https://doi.org/10.7508%2Fibj.2016.01.001

Bahadoran, M., Shamloo, A., & Nokoorani, Y. D. (2020). Development of a polyvinyl alcohol/sodium alginate hydrogel-based scaffold incorporating bFGF-encapsulated microspheres for accelerated wound healing. *Scientific reports*, *10*(1), 1-18. https://doi.org/10.1038/s41598-020-64480-9

Bahar, A. A., & Ren, D. (2013). Antimicrobial peptides. Pharmaceuticals, 6(12), 1543-1575. https://doi.org/10.3390/ph6121543

Bai, J., Chen, C., Wang, J., Zhang, Y., Cox, H., Zhang, J., Guo, L., Huang, H., Wang, X., Liu, X., & Xu, H. (2016). Enzymatic regulation of self-assembling peptide A9K2 nanostructures and hydrogelation with highly selective antibacterial activities. In H. Cox & J. Zhang (Eds.), ACS Applied Materials & Interfaces, 8(24), 15093-15102. https://doi.org/10.1021/acsami.6b03770

Baker, M. I., Walsh, S. P., Schwartz, Z., & Boyan, B. D. (2012). A review of polyvinyl alcohol and its uses in cartilage and orthopedic applications. Journal of Biomedical Materials Research Part B: Applied Biomaterials, 100(5), 1451-1457. https://doi.org/10.1002/jbm.b.32694

Berk, W. A., Welch, R. D., & Bock, B. F. (1992). Controversial issues in clinical management of the simple wound. Annals of emergency medicine, 21(1), 72-78. https://doi.org/10.1016/S0196-0644(05)82245-0

Bielefeld, K. A., Amini-Nik, S., & Alman, B. A. (2013). Cutaneous wound healing: recruiting developmental pathways for regeneration. Cellular and Molecular Life Sciences, 70(12), 2059-2081. http://doi.org/10.1007/s00018-012-1152-9

Boateng, J. S., Matthews, K. H., Stevens, H. N., & Eccleston, G. M. (2008). Wound healing dressings and drug delivery systems: a review. Journal of pharmaceutical sciences, 97(8), 2892-2923. https://doi.org/10.1002/jps.21210

Boonkaew, B., Barber, P. M., Rengpipat, S., Supaphol, P., Kempf, M., He, J., Leekitcharoenphon, P., & Cuttle, L. (2014). Development and characterization of a novel, antimicrobial, sterile hydrogel dressing for burn wounds: single-step production with gamma irradiation creates silver nanoparticles and radical polymerization. Journal of Pharmaceutical Sciences, 103(10), 3244-3253. https://doi.org/10.1002/jps.24095

Broussard, K. C., & Powers, J. G. (2013). Wound dressings: selecting the most appropriate type. American journal of clinical dermatology, 14(6), 449-459. https://doi.org/10.1007/s40257-013-0046-4

Bruschi, M. L. (2015). Strategies to modify the drug release from pharmaceutical systems. Woodhead Publishing. http://dx.doi.org/10.1016/B978-0-08-100092-2.00005-9

Bucki, R., Georges, P. C., Espinassous, Q., Funaki, M., Pastore, J. J., Chaby, R., & Janmey, P. A. (2005). Inactivation of endotoxin by human plasma gelsolin. Biochemistry, 44(28), 9590-9597. https://doi.org/10.1021/bi0503504

Bucki, R., Sostarecz, A. G., Byfield, F. J., Savage, P. B., & Janmey, P. A. (2007). Resistance of the antibacterial agent ceragenin CSA-13 to inactivation by DNA or F-actin and its activity in cystic fibrosis sputum. Journal of antimicrobial chemotherapy, 60(3), 535-545. https://doi.org/10.1093/jac/dkm218

Caccavo, D. (2019). An overview on the mathematical modeling of hydrogels' behavior for drug delivery systems. International journal of pharmaceutics, 560, 175-190. https://doi.org/10.1016/j.ijpharm.2019.01.076

Caló, E., & Khutoryanskiy, V. V. (2015). Biomedical applications of hydrogels: A review of patents and commercial products. European polymer journal, 65, 252-267. https://doi.org/10.1016/j.eurpolymj.2014.11.024

Chhibber, T., Gondil, V. S., & Sinha, V. R. (2020). Development of chitosan-based hydrogel containing antibiofilm agents for the treatment of Staphylococcus aureus–infected burn wound in mice. AAPS PharmSciTech, 21(2), 1-12. https://doi.org/10.1208/s12249-019-1537-2

Cho, H., Jammalamadaka, U., & Tappa, K. (2018). Nanogels for pharmaceutical and biomedical applications and their fabrication using 3D printing technologies. Materials, 11(2), 302. https://doi.org/10.3390/ma11020302

Chong, E. J., Phan, T. T., Lim, I. J., Zhang, Y. Z., Bay, B. H., Ramakrishna, S., & Lim, C. T. (2007). Evaluation of electrospun PCL/gelatin nanofibrous scaffold for wound healing and layered dermal reconstitution. Acta biomaterialia, 3(3), 321-330. https://doi.org/10.1016/j.actbio.2007.01.002

Chua, A. W. C., Khoo, Y. C., Tan, B. K., Tan, K. C., Foo, C. L., & Chong, S. J. (2016). Skin tissue engineering advances in severe burns: review and therapeutic applications. Burns & trauma, 4. https://doi.org/10.1186/s41038-016-0027-y

Chung, H. J., & Park, T. G. (2009). Self-assembled and nanostructured hydrogels for drug delivery and tissue engineering. Nano Today, 4(5), 429-437. https://doi.org/10.1016/j.nantod.2009.08.008

Church, D., Elsayed, S., Reid, O., Winston, B., & Lindsay, R. (2006). Burn wound infections. Clinical microbiology reviews, 19(2), 403-434. https://doi.org/10.1128/CMR.19.2.403-434.2006

Dai, T., Huang, Y. Y., K Sharma, S., T Hashmi, J., B Kurup, D., & R Hamblin, M. (2010). Topical antimicrobials for burn wound infections. Recent patents on anti-infective drug discovery, 5(2), 124-151. https://doi.org/10.2174/157489110791233522

Dash, S., Murthy, P. N., Nath, L., & Chowdhury, P. (2010). Kinetic modeling on drug release from controlled drug delivery systems. Acta Pol Pharm, 67(3), 217-223.

Daunton, C., Kothari, S., Smith, L., & Steele, D. (2012). A history of materials and practices for wound management. *Wound Practice & Research: Journal of the Australian Wound Management Association*, *20*(4).

Davey, M. E., & O'toole, G. A. (2000). Microbial biofilms: from ecology to molecular genetics. Microbiology and molecular biology reviews, 64(4), 847-867. https://doi.org/10.1128/MMBR.64.4.847-867.2000

Debats, I. B. J. G., Wolfs, T. G. A. M., Gotoh, T., Cleutjens, J. P. M., Peutz-Kootstra, C. J., & Van der Hulst, R. R. W. J. (2009). Role of arginine in superficial wound healing in man. Nitric Oxide, 21(3-4), 175-183. https://doi.org/10.1016/j.niox.2009.07.006

Dhaliwal, K., & Lopez, N. (2018). Hydrogel dressings and their application in burn wound care. British journal of community nursing, 23(Sup9), S24-S27. https://doi.org/10.12968/bjcn.2018.23.Sup9.S24

Diamond, G., Beckloff, N., Weinberg, A., & Kisich, K. O. (2009). The roles of antimicrobial peptides in innate host defense. Current pharmaceutical design, 15(21), 2377-2392. https://doi.org/10.2174/138161209788682325

Ding, B., Guan, Q., Walsh, J. P., Boswell, J. S., Winter, T. W., Winter, E. S., Li, H., Li, X., Li, Y., Li, J., & Savage, P. B. (2002). Correlation of the antibacterial activities of cationic peptide antibiotics and cationic steroid antibiotics. Journal of Medicinal Chemistry, 45(3), 663-669. https://doi.org/10.1021/jm0105070

Ding, B., Taotofa, U., Orsak, T., Chadwell, M., & Savage, P. B. (2004). Synthesis and characterization of peptide−cationic steroid antibiotic conjugates. Organic letters, 6(20), 3433-3436. https://doi.org/10.1021/ol048845t

Ding, B., Yin, N., Liu, Y., Cardenas-Garcia, J., Evanson, R., Orsak, T., Li, J., Li, Y., & Savage, P. B. (2004). Origins of cell selectivity of cationic steroid antibiotics. Journal of the American Chemical Society, 126(42), 13642-13648. https://doi.org/10.1021/ja046909p

Domb, A. J., & Khan, W. (Eds.). (2014). Focal controlled drug delivery. Springer Science & Business Media. https://doi.org/10.1007/978-1-4614-9434-8

Dorsett-Martin, W. A. (2004). Rat models of skin wound healing: a review. Wound Repair and Regeneration, 12(6), 591-599. https://doi.org/10.1111/j.1067-1927.2004.12601.x

Dubay, D. A., & Franz, M. G. (2003). Acute wound healing: the biology of acute wound failure. Surgical Clinics, 83(3), 463-481. https://doi.org/10.1016/S0039-6109(02)00196-2

Durnaś, B., Wnorowska, U., Pogoda, K., Deptuła, P., Wątek, M., Piktel, E., Gliński, J., Kuć, J., & Bucki, R. (2016). Candidacidal activity of selected ceragenins and human cathelicidin LL-37 in experimental settings mimicking infection sites. PloS one, 11(6), e0157242. https://doi.org/10.1371/journal.pone.0157242

Epand, R. M., Epand, R. F., & Savage, P. B. (2008). Ceragenins (cationic steroid compounds), a novel class of antimicrobial agents. Drug news & perspectives, 21(6), 307-311. https://doi.org/10.1358/dnp.2008.21.6.1246829

Essa, M. M., Manickavasagan, A., & Sukumar, E. (2012). Natural products and their active compounds on disease prevention. Nova Science Publishers, Inc..

Evers, L. H., Bhavsar, D., & Mailänder, P. (2010). The biology of burn injury. Experimental dermatology, 19(9), 777-783. https://doi.org/10.1111/j.1600-0625.2010.01105.x

Farahani, M., & Shafiee, A. (2021). Wound healing: From passive to smart dressings. Advanced Healthcare Materials, 10(16), 2100477. https://doi.org/10.1002/adhm.202100477

Forbes, S., McBain, A. J., Felton-Smith, S., Jowitt, T. A., Birchenough, H. L., & Dobson, C. B. (2013). Comparative surface antimicrobial properties of synthetic biocides and novel human apolipoprotein E derived antimicrobial peptides. Biomaterials, 34(22), 5453-5464. https://doi.org/10.1016/j.biomaterials.2013.03.087

Francesko, A., Petkova, P., & Tzanov, T. (2018). Hydrogel dressings for advanced wound management. Current medicinal chemistry, 25(41), 5782-5797. https://doi.org/10.2174/0929867324666170920161246

Franco, R. A., Min, Y. K., Yang, H. M., & Lee, B. T. (2013). Fabrication and biocompatibility of novel bilayer scaffold for skin tissue engineering applications. *Journal of biomaterials applications*, *27*(5), 605-615. https://doi.org/10.1177/0885328211416527

George Broughton, I. I., Janis, J. E., & Attinger, C. E. (2006). A brief history of wound care. Plastic and reconstructive surgery, 117(7S), 6S-11S. https://doi.org/10.1097/01.prs.0000225429.76355.dd

George, M., & Abraham, T. E. (2006). Polyionic hydrocolloids for the intestinal delivery of protein drugs: alginate and chitosan—a review. Journal of controlled release, 114(1), 1-14. https://doi.org/10.1016/j.jconrel.2006.04.017

Gharibi, R., Yeganeh, H., & Abdali, Z. (2018). Preparation of antimicrobial wound dressings via thiol–ene photopolymerization reaction. Journal of Materials Science, 53(3), 1581-1595. https://doi.org/10.1007/s10853-017-1622-4

Ghasemzadeh, H., & Ghanaat, F. (2014). Antimicrobial alginate/PVA silver nanocomposite hydrogel, synthesis and characterization. *Journal of Polymer Research*, *21*(3), 1-14. https://doi.org/10.1007/s10965-014-0355-1

Gibas, I., & Janik, H. (2010). Synthetic polymer hydrogels for biomedical applications. Chem. Chem. Technol, 4(4), 297-298.

Gizaw, M., Thompson, J., Faglie, A., Lee, S. Y., Neuenschwander, P., & Chou, S. F. (2018). Electrospun fibers as a dressing material for drug and biological agent delivery in wound healing applications. Bioengineering, 5(1), 9. https://doi.org/10.3390/bioengineering5010009

Gu, X., Jennings, J. D., Snarr, J., Chaudhary, V., Pollard, J. E., & Savage, P. B. (2013). Optimization of ceragenins for prevention of bacterial colonization of hydrogel contact lenses. Investigative ophthalmology & visual science, 54(9), 6217-6223. https://doi.org/10.1167/iovs.13-12664

Gupta, A., Kowalczuk, M., Heaselgrave, W., Britland, S. T., Martin, C., & Radecka, I. (2019). The production and application of hydrogels for wound management: A review. European Polymer Journal, 111, 134-151. https://doi.org/10.1016/j.eurpolymj.2018.12.019

Harrington, W. F., & Von Hippel, P. H. (1962). The structure of collagen and gelatin. Advances in protein chemistry, 16, 1-138. https://doi.org/10.1016/S0065-3233(08)60028-5

Hartmann, M., Berditsch, M., Hawecker, J., Ardakani, M. F., Gerthsen, D., & Ulrich, A. S. (2010). Damage of the bacterial cell envelope by antimicrobial peptides gramicidin S and PGLa as revealed by transmission and scanning electron microscopy. Antimicrobial agents and chemotherapy, 54(8), 3132-3142. https://doi.org/10.1128/AAC.00124-10

Hashemi, M. M., Holden, B. S., & Savage, P. B. (2018). Ceragenins as non-peptide mimics of endogenous antimicrobial peptides. Fighting Antimicrobial Resist, 1, 139-169.

Hashemi, M. M., Holden, B. S., Durnas, B., Bucki, R., & Savage, P. B. (2017). Ceragenins as mimics of endogenous antimicrobial peptides. J. Antimicrob. Agents, 3(1000141), 2472-1212.

Hashemi, M. M., Rovig, J., Holden, B. S., Taylor, M. F., Weber, S., Wilson, J., Wozniak, D. J., Lebar, M. D., & Savage, P. B. (2018). Ceragenins are active against drug-resistant Candida auris clinical isolates in planktonic and biofilm forms. Journal of Antimicrobial Chemotherapy, 73(6), 1537-1545. https://doi.org/10.1093/jac/dky085.

Hayes, T. R., & Su, B. (2011). Wound dressings. In Electrospinning for Tissue Regeneration (pp. 317-339). Woodhead Publishing. https://doi.org/10.1016/B978-1-84569-741-9.50015-X

Henríquez, C. M., Sarabia-Vallejos, M. A., & Rodriguez-Hernandez, J. (2017). Advances in the fabrication of antimicrobial hydrogels for biomedical applications. Materials, 10(3), 232. https://doi.org/10.3390/ma10030232

Hermans, M. H. (2005). A general overview of burn care. International wound journal, 2(3), 206-220. https://doi.org/10.1111/j.1742-4801.2005.00129.x

Higuchi, T. (1963). Mechanism of sustained-action medication. Theoretical analysis of rate of release of solid drugs dispersed in solid matrices. Journal of pharmaceutical sciences, 52(12), 1145-1149. https://doi.org/10.1002/jps.2600521210

Hixson, A. W., & Crowell, J. H. (1931). Dependence of reaction velocity upon surface and agitation. Industrial & Engineering Chemistry, 23(8), 923-931. https://doi.org/10.1021/ie50260a018

Hoare, T. R., & Kohane, D. S. (2008). Hydrogels in drug delivery: Progress and challenges. polymer, 49(8), 1993-2007. https://doi.org/10.1016/j.polymer.2008.01.027

Hoppens, M. A., Wheeler, Z. E., Qureshi, A. T., Hogan, K., Wright, A., Stanley, G. G., Peterson, M. K., & Hayes, D. (2014). Maghemite, silver, ceragenin conjugate particles for selective binding and contrast of bacteria. Journal of Colloid and Interface Science, 413, 167-174. https://doi.org/10.1016/j.jcis.2013.09.016.

Howell, M. D., Streib, J. E., Kim, B. E., Lesley, L. J., Dunlap, A. P., Geng, D., Petryk, A., Belk, K. A., & Leung, D. Y. (2009). Ceragenins: a class of antiviral compounds to treat orthopox infections. Journal of Investigative Dermatology, 129(11), 2668-2675. https://doi.org/10.1038/jid.2009.120.

Hu, Y., Ren, G., Deng, L., Zhang, J., Liu, H., Mu, S., & Wu, T. (2016). Degradable UV-cross-linked hydrogel for the controlled release of triclosan with reduced cytotoxicity. Materials Science and Engineering: C, 67, 151-158. https://doi.org/10.1016/j.msec.2016.05.003

Huan, Y., Kong, Q., Mou, H., & Yi, H. (2020). Antimicrobial peptides: classification, design, application and research progress in multiple fields. Frontiers in microbiology, 2559. https://doi.org/10.3389/fmicb.2020.582779

Hudson, D. A., Knottenbelt, J. D., & Krige, J. E. (1992). Closed degloving injuries: results following conservative surgery. Plastic and reconstructive surgery, 89(5), 853-855. https://doi.org/10.1097/00006534-199205000-00013

Inal, M., & Mülazımoğlu, G. (2019). Production and characterization of bactericidal wound dressing material based on gelatin nanofiber. International journal of biological macromolecules, 137, 392-404. https://doi.org/10.1016/j.ijbiomac.2019.06.119

Isogai, E., Isogai, H., Takahashi, K., Okumura, K., & Savage, P. B. (2009). Ceragenin CSA-13 exhibits antimicrobial activity against cariogenic and periodontopathic bacteria. Oral microbiology and immunology, 24(2), 170-172. https://doi.org/10.1111/j.1399-302X.2008.00464.x

Jayaramudu, T., Raghavendra, G. M., Varaprasad, K., Sadiku, R., & Raju, K. M. (2013). Development of novel biodegradable Au nanocomposite hydrogels based on wheat: for

inactivation of bacteria. Carbohydrate polymers, 92(2), 2193-2200. https://doi.org/10.1016/j.carbpol.2012.12.006

Jiang, Y., Hou, Y., Fang, J., Liu, W., Zhao, Y., Huang, T., Zhang, Y., Zou, L., & Zhou, Z. (2019). Preparation and characterization of PVA/SA/HA composite hydrogels for wound dressing. International Journal of Polymer Analysis and Characterization, 24(2), 132-141. https://doi.org/10.1080/1023666X.2018.1558567

Jones, J. I. (1973). Polyvinyl alcohol. Properties and applications. Edited by CA Finch. John Wiley, Chichester. 1973. Pp. xviii+ 622. Price:£ 14.00. https://doi.org/10.1002/pi.4980050608

Jones, V., Grey, J. E., & Harding, K. G. (2006). Wound dressings. Bmj, 332(7544), 777-780. https://doi.org/10.1136/bmj.332.7544.777

Kadri, R., Messaoud, G. B., Tamayol, A., Aliakbarian, B., Zhang, H. Y., Hasan, M., Kaskous, N., Huang, X. Y., & Arab-Tehrany, E. (2016). Preparation and characterization of nanofunctionalized alginate/methacrylated gelatin hybrid hydrogels. RSC Advances, 6(33), 27879-27884. https://doi.org/10.1039/C6RA03699F

Kakkar, P., & Madhan, B. (2016). Fabrication of keratin-silica hydrogel for biomedical applications. Materials Science and Engineering: C, 66, 178-184. https://doi.org/10.1016/j.msec.2016.04.067

Kamoun, E. A., Kenawy, E. R. S., & Chen, X. (2017). A review on polymeric hydrogel membranes for wound dressing applications: PVA-based hydrogel dressings. Journal of advanced research, 8(3), 217-233. https://doi.org/10.1016/j.jare.2017.01.005

Kamoun, Elbadawy A., El-Refaie S. Kenawy, Tamer M. Tamer, Mahmoud A. El-Meligy, and Mohamed S. Mohy Eldin. "Poly (vinyl alcohol)-alginate physically cross-linked hydrogel membranes for wound dressing applications: characterization and bio-evaluation." *Arabian Journal of Chemistry* 8, no. 1 (2015): 38-47. https://doi.org/10.1016/j.arabjc.2013.12.003

Katz, M. H., Alvarez, A. F., Kirsner, R. S., Eaglstein, W. H., & Falanga, V. (1991). Human wound fluid from acute wounds stimulates fibroblast and endothelial cell growth. Journal of the American Academy of Dermatology, 25(6), 1054-1058. https://doi.org/10.1016/0190-9622(91)70306-M

Kaur, P., Gondil, V. S., & Chhibber, S. (2019). A novel wound dressing consisting of PVA-SA hybrid hydrogel membrane for topical delivery of bacteriophages and antibiotics. International Journal of Pharmaceutics, 572, 118779. https://doi.org/10.1016/j.ijpharm.2019.118779

Kendrick, J. H., Casali, R. E., Lang, N. P., & Read, R. C. (1982). The complicated septic abdominal wound. Archives of Surgery, 117(4), 464-468. http://.org/10.1001/archsurg.1982.01380280048010

Khampieng, T., Brikshavana, P., & Supaphol, P. (2014). Silver nanoparticle-embedded poly (vinyl pyrrolidone) hydrogel dressing: gamma-ray synthesis and biological evaluation. Journal of Biomaterials Science, Polymer Edition, 25(8), 826-842. https://doi.org/10.1080/09205063.2014.910154

Khan, M. N., & Naqvi, A. H. (2006). Antiseptics, iodine, povidone iodine and traumatic wound cleansing. Journal of tissue viability, 16(4), 6-10. https://doi.org/10.1016/S0965-206X(06)64002-3

Kichler, A., Leborgne, C., Savage, P. B., & Danos, O. (2005). Cationic steroid antibiotics demonstrate DNA delivery properties. Journal of controlled release, 107(1), 174-182. https://doi.org/10.1016/j.jconrel.2005.08.002

Kim, B. C., Kim, H. T., Park, S. H., Cha, J. S., Yufit, T., Kim, S. J., & Falanga, V. (2003). Fibroblasts from chronic wounds show altered TGF-β-signaling and decreased TGF-β Type II Receptor expression. Journal of cellular physiology, 195(3), 331-336. https://doi.org/10.1002/jcp.10301

Kim, S. E., Heo, D. N., Lee, J. B., Kim, J. R., Park, S. H., Jeon, S. H., & Kwon, I. K. (2009). Electrospun gelatin/polyurethane blended nanofibers for wound healing. Biomedical Materials, 4(4), 044106. http://dx.doi.org/10.1088/1748-6041/4/4/044106

Kokabi, M., Sirousazar, M., & Hassan, Z. M. (2007). PVA–clay nanocomposite hydrogels for wound dressing. European polymer journal, 43(3), 773-781. https://doi.org/10.1016/j.eurpolymj.2006.11.030

Kuo, Y. C., Lee, I. H., & Rajesh, R. (2019). Self-assembled ternary poly (vinyl alcohol)-alginate-gelatin hydrogel with controlled-release nanoparticles for pancreatic differentiation of iPS cells. Journal of the Taiwan Institute of Chemical Engineers, 104, 27-39. https://doi.org/10.1016/j.jtice.2019.09.010

Laffleur, F., & Keckeis, V. (2020). Advances in drug delivery systems: Work in progress still needed?. International journal of pharmaceutics, 590, 119912. https://doi.org/10.1016/j.ijpharm.2020.119912

Lazarus, G. S., Cooper, D. M., Knighton, D. R., Margolis, D. J., Percoraro, R. E., Rodeheaver, G., & Robson, M. C. (1994). Definitions and guidelines for assessment of wounds and evaluation of healing. Wound repair and regeneration, 2(3), 165-170. https://doi.org/10.1046/j.1524-475X.1994.20305.

Lee, K. Y., & Mooney, D. J. (2012). Alginate: properties and biomedical applications. Progress in polymer science, 37(1), 106-126. https://doi.org/10.1016/j.progpolymsci.2011.06.003

Lee, P. I., & Li, J. X. (2010). Evolution of oral controlled release dosage forms. Oral controlled release formulation design and drug delivery. John Wiley & Sons, Inc, 21-31. https://doi.org/10.1002/9780470640487.ch2

Lee, S. C., Kwon, I. K., & Park, K. (2013). Hydrogels for delivery of bioactive agents: A historical perspective. Advanced drug delivery reviews, 65(1), 17-20. https://doi.org/10.1016/j.addr.2012.07.015

Leszczyńska, K., Namiot, A., Fein, D. E., Wen, Q., Namiot, Z., Savage, P. B., Horst, R. J., Nützel, H., Ignatowicz, L., & Bucki, R. (2009). Bactericidal activities of the cationic steroid CSA-13 and the cathelicidin peptide LL-37 against Helicobacter pylori in simulated gastric juice. BMC Microbiology, 9(1), 1-10. https://doi.org/10.1186/1471-2180-9-187

Leszczyńska, K., Namiot, D., Byfield, F. J., Cruz, K., Żendzian-Piotrowska, M., Fein, D. E., Namiot, A., Wen, Q., Savage, P. B., and Bucki, R. (2013). Antibacterial activity of the human host defense peptide LL-37 and selected synthetic cationic lipids against bacteria associated with oral and upper respiratory tract infections. Journal of Antimicrobial Chemotherapy, 68(3), 610-618. https://doi.org/10.1093/jac/dks434

Li, J., Chen, J., & Kirsner, R. (2007). Pathophysiology of acute wound healing. Clinics in dermatology, 25(1), 9-18. https://doi.org/10.1016/j.clindermatol.2006.09.007

Li, S., Dong, S., Xu, W., Tu, S., Yan, L., Zhao, C., ... & Chen, X. (2018). Antibacterial hydrogels. *Advanced science*, *5*(5), 1700527. https://doi.org/10.1002/advs.201700527

Li, S., Wang, X., Wang, Y., Zhao, Q., Zhang, L., Yang, X., Liu, S., Li, X., Li, Y., & Pan, W. (2015). A novel osmotic pump-based controlled delivery system consisting of pH-modulated solid dispersion for poorly soluble drug flurbiprofen: in vitro and in vivo evaluation. Drug Development and Industrial Pharmacy, 41(12), 2089-2099. https://doi.org/10.3109/03639045.2015.1078348.

Li, X., Li, A., Feng, F., Jiang, Q., Sun, H., Chai, Y., Guo, Y., Sun, Z., and Li, R. (2019). Effect of the hyaluronic acid-poloxamer hydrogel on skin-wound healing: In vitro and in vivo studies. Animal Models and Experimental Medicine, 2(2), 107-113. https://doi.org/10.1002/ame2.12067.

Lin, S. P., Lo, K. Y., Tseng, T. N., Liu, J. M., Shih, T. Y., & Cheng, K. C. (2019). Evaluation of PVA/dextran/chitosan hydrogel for wound dressing. Cellular Polymers, 38(1-2), 15-30. https://doi.org/10.1177/0262489319839211

Liu, D., Nikoo, M., Boran, G., Zhou, P., & Regenstein, J. M. (2015). Collagen and gelatin. Annual review of food science and technology, 6, 527-557. https://doi.org/10.1146/annurev-food-031414-111800

Liu, L., Huang, Y., Riduan, S. N., Gao, S., Yang, Y., Fan, W., & Zhang, Y. (2012). Main-chain imidazolium oligomer material as a selective biomimetic antimicrobial agent. Biomaterials, 33(33), 8625-8631. https://doi.org/10.1016/j.biomaterials.2012.08.006

Liu, S. J., Kau, Y. C., Chou, C. Y., Chen, J. K., Wu, R. C., & Yeh, W. L. (2010). Electrospun PLGA/collagen nanofibrous membrane as early-stage wound dressing. Journal of Membrane Science, 355(1-2), 53-59. https://doi.org/10.1016/j.memsci.2010.03.012.

Liu, X., Lin, T., Gao, Y., Xu, Z., Huang, C., Yao, G., Jiang L., Tang Y., & Wang, X. (2012). Antimicrobial electrospun nanofibers of cellulose acetate and polyester urethane composite for wound dressing. *Journal of Biomedical Materials Research Part B: Applied Biomaterials*, *100*(6), 1556-1565. https://doi.org/10.1002/jbm.b.32724

Luo, Xiaogang, Hao Zhang, Zhenni Cao, Ning Cai, Yanan Xue, and Faquan Yu. "A simple route to develop transparent doxorubicin-loaded nanodiamonds/cellulose nanocomposite membranes as potential wound dressings." *Carbohydrate polymers* 143 (2016): 231-238. https://doi.org/10.1016/j.carbpol.2016.01.076

Madaghiele, M., Demitri, C., Sannino, A., & Ambrosio, L. (2014). Polymeric hydrogels for burn wound care: Advanced skin wound dressings and regenerative templates. Burns & trauma, 2(4), 2321-3868. https://doi.org/10.4103/2321-3868.143616

Markova, A., & Mostow, E. N. (2012). US skin disease assessment: ulcer and wound care. Dermatologic clinics, 30(1), 107. http://doi.org/10.1111/j.1067-1927.2004.12601.x

Marler, J. J., Upton, J., Langer, R., & Vacanti, J. P. (1998). Transplantation of cells in matrices for tissue regeneration. Advanced drug delivery reviews, 33(1-2), 165-182. https://doi.org/10.1016/S0169-409X(98)00025-8

Marrella, A., Lagazzo, A., Dellacasa, E., Pasquini, C., Finocchio, E., Barberis, F., Inzitari, R., Poli, A., & Scaglione, S. (2018). 3D porous gelatin/PVA hydrogel as meniscus substitute using alginate micro-particles as porogens. Polymers, 10(4), 380. https://doi.org/10.3390/polym10040380

Maver, T., Hribernik, S., Mohan, T., Smrke, D. M., Maver, U., & Stana-Kleinschek, K. (2015). Functional wound dressing materials with highly tunable drug release properties. RSC advances, 5(95), 77873-77884. https://doi.org/10.1039/C5RA11972C

Miguel, S. P., Ribeiro, M. P., Brancal, H., Coutinho, P., & Correia, I. J. (2014). Thermoresponsive chitosan–agarose hydrogel for skin regeneration. Carbohydrate polymers, 111, 366-373. https://doi.org/10.1016/j.carbpol.2014.04.093

Montanari, E., D'arrigo, G., Di Meo, C., Virga, A., Coviello, T., Passariello, C., & Matricardi, P. (2014). Chasing bacteria within the cells using levofloxacin-loaded hyaluronic acid nanohydrogels. European Journal of Pharmaceutics and Biopharmaceutics, 87(3), 518-523. https://doi.org/10.1016/j.ejpb.2014.03.003

Morgado, P. I., Aguiar-Ricardo, A., & Correia, I. J. (2015). Asymmetric membranes as ideal wound dressings: An overview on production methods, structure, properties and

performance relationship. Journal of Membrane Science, 490, 139-151. https://doi.org/10.1016/j.memsci.2015.04.064

Morgado, P. I., Lisboa, P. F., Ribeiro, M. P., Miguel, S. P., Simões, P. C., Correia, I. J., & Aguiar-Ricardo, A. (2014). Poly (vinyl alcohol)/chitosan asymmetrical membranes: Highly controlled morphology toward the ideal wound dressing. Journal of membrane science, 469, 262-271. https://doi.org/10.1016/j.memsci.2014.06.035

Mtiaz, N., Niazi, M. B. K., Fasim, F., Khan, B. A., Bano, S. A., Shah, G. M., Khattak, S. U. K., Raza, A., & Uzair, B. (2019). Fabrication of an original transparent PVA/gelatin hydrogel: In vitro antimicrobial activity against skin pathogens. International Journal of Polymer Science, 2019, 1-9. https://doi.org/10.1155/2019/7651810.

Mühlstädt, M., Thomé, C., & Kunte, C. (2012). Rapid wound healing of scalp wounds devoid of periosteum with milling of the outer table and split-thickness skin grafting. British Journal of Dermatology, 167(2), 343-347. https://doi.org/10.1111/j.1365-2133.2012.10999.x

Naghshineh, N., Tahvildari, K., & Nozari, M. (2019). Preparation of chitosan, sodium alginate, gelatin and collagen biodegradable sponge composites and their application in wound healing and curcumin delivery. Journal of Polymers and the Environment, 27(12), 2819-2830. https://doi.org/10.1007/s10924-019-01559-z

Neibert, K., Gopishetty, V., Grigoryev, A., Tokarev, I., Al-Hajaj, N., Vorstenbosch, J., Kress, J. P., & Maysinger, D. (2012). Wound-healing with mechanically robust and biodegradable hydrogel fibers loaded with silver nanoparticles. Advanced Healthcare Materials, 1(5), 621-630. https://doi.org/10.1002/adhm.201200075

Norowski Jr, P. A., & Bumgardner, J. D. (2009). Biomaterial and antibiotic strategies for peri-implantitis: A review. Journal of Biomedical Materials Research Part B: Applied Biomaterials: An Official Journal of The Society for Biomaterials, The Japanese Society for Biomaterials, and The Australian Society for Biomaterials and the Korean Society for Biomaterials, 88(2), 530-543. https://doi.org/10.1002/jbm.b.31152

Nuutila, K., Grolman, J., Yang, L., Broomhead, M., Lipsitz, S., Onderdonk, A., Fudem, G., Mertz, P., Golinko, M., & Eriksson, E. (2020). Immediate treatment of burn wounds with high concentrations of topical antibiotics in an alginate hydrogel using a platform wound device. Advances in wound care, 9(2), 48-60. https://doi.org/10.1089/wound.2019.1018

Olekson, M. A., You, T., Savage, P. B., & Leung, K. P. (2017). Antimicrobial ceragenins inhibit biofilms and affect mammalian cell viability and migration in vitro. FEBS Open Bio, 7(7), 953-967. https://doi.org/10.1002/2211-5463.12235

Oliveira, R. N., McGuinness, G. B., Rouze, R., Quilty, B., Cahill, P., Soares, G. D., & Thiré, R. M. (2015). PVA hydrogels loaded with a Brazilian propolis for burn wound healing applications. *Journal of Applied Polymer Science*, *132*(25). https://doi.org/10.1002/app.42129

Oryan, A., Alemzadeh, E., & Moshiri, A. (2017). Burn wound healing: present concepts, treatment strategies and future directions. Journal of wound care, 26(1), 5-19. https://doi.org/10.12968/jowc.2017.26.1.5

Paarakh, M. P., Jose, P. A., Setty, C. M., & Christoper, G. P. (2018). Release kinetics–concepts and applications. Int. J. Pharm. Res. Technol, 8(1), 12-20.

Pakolpakçıl, A., Osman, B., Özer, E. T., Şahan, Y., Becerir, B., Göktalay, G., & Karaca, E. (2020). Halochromic composite nanofibrous mat for wound healing monitoring. Materials Research Express, 6(12), 1250c3. http://dx.doi.org/10.1088/2053-1591/ab5dc1

Pandima Devi, M., Sekar, M., Chamundeswari, M., Moorthy, A., Krithiga, G., Murugan, N. S., & Sastry, T. P. (2012). A novel wound dressing material—fibrin–chitosan–sodium

alginate composite sheet. Bulletin of Materials Science, 35(7), 1157-1163. https://doi.org/10.1007/s12034-012-0404-5

Parrett, B. M., Pomahac, B., Demling, R. H., & Orgill, D. P. (2006). Fourth-degree burns to the lower extremity with exposed tendon and bone: a ten-year experience. Journal of burn care & research, 27(1), 34-39. https://doi.org/10.1097/01.bcr.0000192265.20514.c5

Paul, W. (2015). Advances in wound healing materials. Smithers Rapra.

Peppas, N. A., Hilt, J. Z., Khademhosseini, A., & Langer, R. (2006). Hydrogels in biology and medicine: from molecular principles to bionanotechnology. Advanced materials, 18(11), 1345-1360. https://doi.org/10.1002/adma.200501612

Pogoda, K., Piktel, E., Deptuła, P., Savage, P. B., Lekka, M., & Bucki, R. (2017). Stiffening of bacteria cells as a first manifestation of bactericidal attack. Micron, 101, 95-102. https://doi.org/10.1016/j.micron.2017.06.011

Polat, Z. A., Cetin, A., & Savage, P. B. (2016). Evaluation of the in vitro activity of ceragenins against Trichomonas vaginalis. Acta parasitologica, 61(2), 376-381. https://doi.org/10.1515/ap-2016-0049

Pu, J., Yuan, F., Li, S., & Komvopoulos, K. (2015). Electrospun bilayer fibrous scaffolds for enhanced cell infiltration and vascularization in vivo. *Acta biomaterialia*, *13*, 131-141. https://doi.org/10.1016/j.actbio.2014.11.014

Queen, D., Orsted, H., Sanada, H., & Sussman, G. (2004). A dressing history. International wound journal, 1(1), 59-77. https://doi.org/10.1111/j.1742-4801.2004.0009.x

Rezaei, N., Hamidabadi, H. G., Khosravimelal, S., Zahiri, M., Ahovan, Z. A., Bojnordi, M. N., Shokrgozar, M. A., Dinarvand, R., & Gholipourmalekabadi, M. (2020). Antimicrobial peptides-loaded smart chitosan hydrogel: Release behavior and antibacterial potential against antibiotic resistant clinical isolates. International Journal of Biological Macromolecules, 164, 855-862. https://doi.org/10.1016/j.ijbiomac.2020.07.011

Rezvani Ghomi, E., Khalili, S., Nouri Khorasani, S., Esmaeely Neisiany, R., & Ramakrishna, S. (2019). Wound dressings: Current advances and future directions. *Journal of Applied Polymer Science*, *136*(27), 47738. https://doi.org/10.1002/app.47738

Rnjak, J., Wise, S. G., Mithieux, S. M., & Weiss, A. S. (2011). Severe burn injuries and the role of elastin in the design of dermal substitutes. Tissue Engineering Part B: Reviews, 17(2), 81-91. https://doi.org/10.1089/ten.teb.2010.0452

Rodriguez, G., Ortegon, M., Camargo, D., & Orozco, L. C. (1997). Iatrogenic Mycobacterium abscessus infection: histopathology of 71 patients. British Journal of Dermatology, 137(2), 214-218. https://doi.org/10.1046/j.1365-2133.1997.18081891.x

Roh, D. H., Kang, S. Y., Kim, J. Y., Kwon, Y. B., Kweon, H. Y., Lee, K. G., Park Y. H.,

Roy, D. C., Tomblyn, S., Isaac, K. M., Kowalczewski, C. J., Burmeister, D. M., Burnett, L. R., & Christy, R. J. (2016). Ciprofloxacin-loaded keratin hydrogels reduce infection and support healing in a porcine partial-thickness thermal burn. Wound Repair and Regeneration, 24(4), 657-668. https://doi.org/10.1111/wrr.12449

Saberian, M., Seyedjafari, E., Zargar, S. J., Mahdavi, F. S., & Sanaei-rad, P. (2021). Fabrication and characterization of alginate/chitosan hydrogel combined with honey and aloe vera for wound dressing applications. Journal of Applied Polymer Science, 138(47), 51398. https://doi.org/10.1002/app.51398

Saleem, M., Nazir, M., Ali, M. S., Hussain, H., Lee, Y. S., Riaz, N., & Jabbar, A. (2010). Antimicrobial natural products: an update on future antibiotic drug candidates. Natural product reports, 27(2), 238-254. https://doi.org/10.1039/b916096e

Salouti, M., & Ahangari, A. (2014). Nanoparticle based drug delivery systems for treatment of infectious diseases (Vol. 552). London, UK: InTech. http://dx.doi.org/10.5772/58423

Sanvicens, N., & Marco, M. P. (2008). Multifunctional nanoparticles–properties and prospects for their use in human medicine. Trends in biotechnology, 26(8), 425-433. https://doi.org/10.1016/j.tibtech.2008.04.005

Sapalidis, A. A. (2020). Porous Polyvinyl alcohol membranes: Preparation methods and applications. Symmetry, 12(6), 960. http://dx.doi.org/10.3390/sym12060960

Sarheed, O., Ahmed, A., Shouqair, D., & Boateng, J. (2016). Antimicrobial dressings for improving wound healing. Wound Healing-New Insights into Ancient Challenges. InTech, 373-398. http://dx.doi.org/10.5772/63961

Savage, P. B. (2001). Multidrug-resistant bacteria: overcoming antibiotic permeability barriers of gram-negative bacteria. Annals of medicine, 33(3), 167-171. https://doi.org/10.3109/07853890109002073

Savage, P. B. (2002). Cationic steroid antibiotics. Current Medicinal Chemistry-Anti-Infective Agents, 1(3), 293-304. https://doi.org/10.2174/1568012023354776

Savage, P. B. (2020). 846 Effects of Ceragenins on Pseudomonas Aeruginosa biofilm formation in burn wounds in a porcine model. *Journal of Burn Care & Research*, *41*(Supplement_1), S262-S263. https://doi.org/10.1093/jbcr/iraa024.418

Savage, P. B., Li, C., Taotafa, U., Ding, B., & Guan, Q. (2002). Antibacterial properties of cationic steroid antibiotics. *FEMS microbiology letters*, *217*(1), 1-7. https://doi.org/10.1111/j.1574-6968.2002.tb11448.x

Schindeler, A., Nicole, Y. C., Cheng, T. L., Sullivan, K., Mikulec, K., Peacock, L., Ahmadi, A. J., Cook, R. J., & Little, D. G. (2015). Local delivery of the cationic steroid antibiotic CSA-90 enables osseous union in a rat open fracture model of Staphylococcus aureus infection. Journal of Bone and Joint Surgery, 97(4), 302-309. https://doi.org/10.2106/JBJS.N.00840

Schmidt, E. J., Boswell, J. S., Walsh, J. P., Schellenberg, M. M., Winter, T. W., Li, C., Brogden, K. A., McElhaney, R. N., Miller, L. G., Andes, D., Craig, W. A., & Savage, P. B. (2001). Activities of cholic acid-derived antimicrobial agents against multidrug-resistant bacteria. Journal of Antimicrobial Chemotherapy, 47(5), 671-674. https://doi.org/10.1093/jac/47.5.671

Scott, A. J., Oyler, B. L., Goodlett, D. R., & Ernst, R. K. (2017). Lipid A structural modifications in extreme conditions and identification of unique modifying enzymes to define the Toll-like receptor 4 structure-activity relationship. Biochimica et Biophysica Acta (BBA)-Molecular and Cell Biology of Lipids, 1862(11), 1439-1450. https://doi.org/10.1016%2Fj.bbalip.2017.01.004

Shah, J. B. (2011). The history of wound care. *The Journal of the American College of Certified Wound Specialists*, *3*(3), 65-66. https://doi.org/10.1016/j.jcws.2012.04.002

Shamloo, A., Aghababaie, Z., Afjoul, H., Jami, M., Bidgoli, M. R., Vossoughi, M., Noghrekar, S. H., & Kamyabhesari, K. (2021). Fabrication and evaluation of chitosan/gelatin/PVA hydrogel incorporating honey for wound healing applications: An in vitro and in vivo study. International Journal of Pharmaceutics, 592, 120068. https://doi.org/10.1016/j.ijpharm.2020.120068

Sharma, K., Kaith, B. S., Kumar, V., Kalia, S., Kumar, V., & Swart, H. C. (2014). Water retention and dye adsorption behavior of Gg-cl-poly (acrylic acid-aniline) based conductive hydrogels. Geoderma, 232, 45-55. https://doi.org/10.1016/j.geoderma.2014.04.035

Simões, D., Miguel, S. P., Ribeiro, M. P., Coutinho, P., Mendonça, A. G., & Correia, I. J. (2018). Recent advances on antimicrobial wound dressing: A review. European Journal of Pharmaceutics and Biopharmaceutics, 127, 130-141. https://doi.org/10.1016/j.ejpb.2018.02.022

Singh, B., Varshney, L., & Sharma, V. (2014). Design of sterile mucoadhesive hydrogels for use in drug delivery: Effect of radiation on network structure. Colloids and Surfaces B: Biointerfaces, 121, 230-237. https://doi.org/10.1016/j.colsurfb.2014.06.020

Slaughter, B. V., Khurshid, S. S., Fisher, O. Z., Khademhosseini, A., & Peppas, N. A. (2009). Hydrogels in regenerative medicine. Advanced materials, 21(32-33), 3307-3329. https://doi.org/10.1002/adma.200802106

Smidsrød, O., & Skja, G. (1990). Alginate as immobilization matrix for cells. Trends in biotechnology, 8, 71-78. https://doi.org/10.1016/0167-7799(90)90139-O

Sørensen, L. T., Hørby, J., Friis, E., Pilsgaard, B., & Jørgensen, T. (2002). Smoking as a risk factor for wound healing and infection in breast cancer surgery. European Journal of Surgical Oncology (EJSO), 28(8), 815-820. https://doi.org/10.1053/ejso.2002.1308

Stoica, A. E., Chircov, C., & Grumezescu, A. M. (2020). Hydrogel dressings for the treatment of burn wounds: an up-to-date overview. Materials, 13(12), 2853. https://doi.org/10.3390/ma13122853

Stojadinovic, O., Brem, H., Vouthounis, C., Lee, B., Fallon, J., Stallcup, M., Merchant, Stubbe, B., Mignon, A., Declercq, H., Van Vlierberghe, S., & Dubruel, P. (2019). Development of gelatin-alginate hydrogels for burn wound treatment. Macromolecular bioscience, 19(8), 1900123. https://doi.org/10.1002/mabi.201900123

Suarato, G., Bertorelli, R., & Athanassiou, A. (2018). Borrowing from nature: Biopolymers and biocomposites as smart wound care materials. Front Bioeng Biotechnol 6 (Oct): 1–11. https://doi.org/10.3389/fbioe.2018.00137

Subrahmanyam, M. (1998). A prospective randomised clinical and histological study of superficial burn wound healing with honey and silver sulfadiazine. Burns, 24(2), 157-161. https://doi.org/10.1016/S0305-4179(97)00113-7

Sultanova, Z., Kaleli, G., Kabay, G., & Mutlu, M. (2016). Controlled release of a hydrophilic drug from coaxially electrospun polycaprolactone nanofibers. International journal of pharmaceutics, 505(1-2), 133-138. https://doi.org/10.1016/j.ijpharm.2016.03.032

Sundaramurthi, D., Krishnan, U. M., & Sethuraman, S. (2014). Electrospun nanofibers as scaffolds for skin tissue engineering. Polymer Reviews, 54(2), 348-376. https://doi.org/10.1080/15583724.2014.881374

Surel, U., Niemirowicz, K., Marzec, M., Savage, P. B., & Bucki, R. (2014). Ceragenins–a new weapon to fight multidrug resistant bacterial infections. Medical Studies/Studia Medyczne, 30(3), 207-213. https://doi.org/10.5114/ms.2014.45428

Szczotka-Flynn, L. B., Pearlman, E., & Ghannoum, M. (2010). Microbial contamination of contact lenses, lens care solutions, and their accessories: a literature review. Eye & contact lens, 36(2), 116. https://doi.org/10.1097%2FICL.0b013e3181d20cae

Tamahkar, E. (2021). Bacterial cellulose/poly vinyl alcohol based wound dressings with sustained antibiotic delivery. *Chemical Papers*, *75*(8), 3979-3987. https://doi.org/10.1007/s11696-021-01631-w

Tamahkar, E., Özkahraman, B., Süloğlu, A. K., İdil, N., & Perçin, I. (2020). A novel multilayer hydrogel wound dressing for antibiotic release. Journal of Drug Delivery Science and Technology, 58, 101536. https://doi.org/10.1016/j.jddst.2020.101536

Tandi, A., Kaur, T., Ebinesan, P. R., Thirugnanama, A., & Mondal, A. K. (2015). Drug loaded poly (vinyl alcohol)-cellulose composite hydrogels for wound dressings.

Taotafa, U., McMullin, D. B., Lee, S. C., Hansen, L. D., & Savage, P. B. (2000). Anionic facial amphiphiles from cholic acid. Organic letters, 2(26), 4117-4120. https://doi.org/10.1021/ol0064056

Thiruvoth, F. M., Mohapatra, D. P., Kumar, D., Chittoria, S. R. K., & Nandhagopal, V. (2015). Current concepts in the physiology of adult wound healing. Plastic and Aesthetic Research, 2, 250-256. https://doi.org/10.4103/2347-9264.158851

Tubbs, R. K. (1966). Sequence distribution of partially hydrolyzed poly (vinyl acetate). Journal of Polymer Science Part A-1: Polymer Chemistry, 4(3), 623-629. https://doi.org/10.1002/pol.1966.150040316

Uppal, R., Ramaswamy, G. N., Arnold, C., Goodband, R., & Wang, Y. (2011). Hyaluronic acid nanofiber wound dressing—production, characterization, and in vivo behavior. *Journal of Biomedical Materials Research Part B: Applied Biomaterials*, *97*(1), 20-29. https://doi.org/10.1002/jbm.b.31776

Van Hoorick, D. (2003). Raes A, Keysers W, Mayeur E, Snyders DJ. Differential modulation of Kv4 kinetics by KCHIP1 splice variants. Mol Cell Neurosci, 24, 357-366. https://doi.org/10.1016/s1044-7431(03)00174-x

Varaprasad, K., Raghavendra, G. M., Jayaramudu, T., Yallapu, M. M., & Sadiku, R. (2017). A mini review on hydrogels classification and recent developments in miscellaneous applications. Materials Science and Engineering: C, 79, 958-971. https://doi.org/10.1016/j.msec.2017.05.096

Varguez-Catzim, P., Rodríguez-Fuentes, N., Borges-Argáez, R., Cáceres-Farfán, M., González-Díaz, A., Alonzo-Garcia, A., González-Hernández, A., Balderas-Quintana, V., & González-Díaz, M. O. (2021). Bilayer asymmetric PVA/PAMPS membranes with efficient antimicrobial surface and enhanced biocompatibility. Applied Surface Science, 565, 150544. https://doi.org/10.1016/j.apsusc.2021.150544

Vijaya Shanti, B., Mrudula, T. P. K. V., & Pavan Kumar, V. (2011). An imperative note on novel drug delivery systems. J Nanomed Nanotechnol, 2(7). https://doi.org/10.4172/2157-7439.1000125

Visavadia, B. G., Honeysett, J., & Danford, M. H. (2008). Manuka honey dressing: An effective treatment for chronic wound infections. British Journal of Oral and Maxillofacial Surgery, 46(1), 55-56. https://doi.org/10.1016/j.bjoms.2006.09.013

Wang, J., Ghali, S., Xu, C., Mussatto, C. C., Ortiz, C., Lee, E. C., & Song, Y. (2018). Ceragenin CSA13 reduces Clostridium difficile infection in mice by modulating the intestinal microbiome and metabolites. Gastroenterology, 154(6), 1737-1750. https://doi.org/10.1053/j.gastro.2018.01.026

Wang, X., & Kimble, R. M. (2010). A review on porcine burn and scar models and their relevance to humans. Wound Practice & Research: Journal of the Australian Wound Management Association, 18(1), 41-49. https://search.informit.org/doi/10.3316/informit.984516969708007

Wang, Y., Beekman, J., Hew, J., Jackson, S., Issler-Fisher, A. C., Parungao, R., Herndon, D. N., Suman, O. E., Desai, M. H., Kulp, G. A., Maitz, P. K., & the Working Group of the Defense Health Agency-Research and Development Office. (2018). Burn injury: Challenges and advances in burn wound healing, infection, pain, and scarring. Advanced Drug Delivery Reviews, 123, 3-17. https://doi.org/10.1016/j.addr.2017.09.018

Wen, Y., Yu, B., Zhu, Z., Yang, Z., & Shao, W. (2020). Synthesis of antibacterial gelatin/sodium alginate sponges and their antibacterial activity. Polymers, 12(9), 1926. https://doi.org/10.3390/polym12091926

Wichterle, O., & Lim, D. (1960). Hydrophilic gels for biological use. *Nature*, *185*(4706), 117-118. https://doi.org/10.1038/185117a0

Williams, D. L., Sinclair, K. D., Jeyapalina, S., & Bloebaum, R. D. (2013). Characterization of a novel active release coating to prevent biofilm implant-related infections. Journal of

Biomedical Materials Research Part B: Applied Biomaterials, 101(6), 1078-1089. https://doi.org/10.1016/j.biomaterials.2012.08.003

Wimley, W. C. (2010). Describing the mechanism of antimicrobial peptide action with the interfacial activity model. ACS chemical biology, 5(10), 905-917. https://doi.org/10.1021/cb1001558

Winter, G. D. (1962). Formation of the scab and the rate of epithelization of superficial wounds in the skin of the young domestic pig. Nature, 193(4812), 293-294.

Winter, G. D. (1995). Formation of the scab and the rate of epithelisation of superficial wounds in the skin of the young domestic pig. 1962. Journal of wound care, 4(8), 366-7. https://doi.org/10.1038/193293a0

Wnorowska, U., Niemirowicz, K., Myint, M., Diamond, S. L., Wróblewska, M., Savage, P. B., Górski, A., & Bucki, R. (2015). Bactericidal activities of cathelicidin LL-37 and select cationic lipids against the hypervirulent Pseudomonas aeruginosa strain LESB58. Antimicrobial Agents and Chemotherapy, 59(7), 3808-3815. https://doi.org/10.1128/AAC.00421-15

Yang, Y., & Hu, H. (2017). Spacer fabric-based exuding wound dressing–Part I: Structural design, fabrication and property evaluation of spacer fabrics. Textile Research Journal, 87(12), 1469-1480. https://doi.org/10.1177/0040517516654111

Yang, Y., Qin, Z., Zeng, W., Yang, T., Cao, Y., Mei, C., & Kuang, Y. (2017). Toxicity assessment of nanoparticles in various systems and organs. Nanotechnology Reviews, 6(3), 279-289. https://doi.org/10.1515/ntrev-2016-0047

Yannas, I. V., Gordon, P. L., Huang, C., Silver, F. H., & Burke, J. F. (1981). *U.S. Patent No. 4,280,954*. Washington, DC: U.S. Patent and Trademark Office.

Ye, S., Jiang, L., Su, C., Zhu, Z., Wen, Y., & Shao, W. (2019). Development of gelatin/bacterial cellulose composite sponges as potential natural wound dressings. International journal of biological macromolecules, 133, 148-155. https://doi.org/10.1016/j.ijbiomac.2019.04.095

Young, S. R., & Dyson, M. (1990). Effect of therapeutic ultrasound on the healing of full-thickness excised skin lesions. Ultrasonics, 28(3), 175-180. https://doi.org/10.1016/0041-624X(90)90082-Y

Yun, Y. H., Lee, B. K., & Park, K. (2015). Controlled drug delivery: historical perspective for the next generation. Journal of Controlled Release, 219, 2-7. https://doi.org/10.1016/j.jconrel.2015.10.005

Zhang, M., Chang, W., Shi, H., Li, Y., Zheng, S., Li, W., & Lou, H. (2018). Floricolin C elicits intracellular reactive oxygen species accumulation and disrupts mitochondria to exert fungicidal action. FEMS yeast research, 18(1), foy002. https://doi.org/10.1093/femsyr/foy002

Zhou, C., Li, P., Qi, X., Sharif, A. R. M., Poon, Y. F., Cao, Y., ... & Chan-Park, M. B. (2011). A photopolymerized antimicrobial hydrogel coating derived from epsilon-poly-L-lysine. *Biomaterials*, *32*(11), 2704-2712. https://doi.org/10.1016/j.biomaterials.2010.12.040

RESUME

Name Surname	:Nawal Y A ALJAYYOUSI
Place and Date of Birth	:Russia, 16/01/1998
Foreign Languages	:Arabic, English, Turkish and Russian
Education Status	
High School	:Jenin Secondary School for Girls
Bachelor's	:An-Najah National University/Chemistry
Master's	:Bursa Uludağ University/Chemistry department/Biochemistry field
Work Experience	:Completed 90 hours internship in Dana Pharmaceutical Company (Assurance Control)
Contact (e-mail)	:nawalaljayyousi@gmail.com
Projects	:Researcher in the ongoing project named 'Development of a three-layered synthetic skin substitute loaded with cationic steroid antibiotics'
Publications	:Suleiman, M., Alali, A., Aljayyousi, N., Alkanad, K., El-khatatneh, N., Almaqashah, M., ... & Abu-Rayyan, A. (2023). Sulfur Nanoparticle as an Effective HEK-293 Anticancer Agent. Moroccan Journal of Chemistry, 11(2), 11-2.